

Application of Nanomaterials in Asphalt Modification

by

Thomas Weaseh Johnson

A thesis submitted in partial fulfillment of the requirements for the degree of

Master of Science
in
Civil (cross-disciplinary)

Department of Civil and Environmental Engineering
University of Alberta

© Thomas Weaseh Johnson, 2020

Abstract

Canada has the 7th largest road network in the world with a total of 1.13 million kilometers (40% paved and 60% unpaved). Rise in traffic volumes, increased vehicle axle loading, extremely low air temperatures and seasonal freeze-thaw cycles have resulted in decreased performance of the asphalt layer and, consequently, pavement life. Modification of asphalt binder have been found to be a promising possibility for increasing the performance of asphalt pavements at extreme temperature ranges. Previous research suggests that the addition of nanoclay to asphalt binder can improve the rheological properties of asphalt cement and, consequently, affect its mechanical properties, such as tensile strain, flexural strength, and elasticity. Prior research also has shown that the addition of cellulose nanocrystals to asphalt binder can increase the shear modulus at high temperatures, increase asphalt cement toughness at low temperatures, and decrease thermal susceptibility.

The objective of this research is to investigate and compare the effects on the properties of PG 64-28 when each type of nanomaterial (i.e. bentonite nanoclay, halloysite nanoclay and cellulose nanocrystals) is added to it in 2 distinct proportions by weight of the binder (i.e. 3% and 6% for each of the nanoclays, and 0.5% and 1% for the cellulose nanocrystals). The research also investigated and compared the effects of the aforementioned modifications on the asphalt mixes produced therewith. The Superpave asphalt mixture design and analysis system was used and the properties evaluated were: (1) asphalt cement rheology at high and intermediate service temperatures using the dynamic shear rheometer (DSR) and at low service temperatures using the bending beam rheometer (BBR); (2) asphalt mix performance at high service temperatures using the Hamburg wheel tracker (HWT) permanent rutting test at 45°C; intermediate temperature fatigue resistance and cracking potential using the indirect tensile asphalt cracking test (IDEAL-CT); and low temperature cracking resistance using the indirect tensile strength (IDT) test and creep compliance at temperatures of 0, -10, and -20°C; (3) moisture sensitivity of asphalt mixes using the indirect tensile test (ITS) after

freeze/thaw conditioning of asphalt mix samples and determination of the inflection points of asphalt mixes after conducting HWT tests; and (4) mixing method used to disperse the nanomaterials in the asphalt binder matrix.

The results of the Superpave testing protocols for the asphalt binder and the asphalt mixes indicated that there was a 28% to 40% increase in the stiffness of the modified asphalt binders which had a 29% to 75% increase in the rutting resistance the asphalt mixes produced therewith, as well as 55% to 93% increase in the resistance to moisture sensitivity. Although the increase in the stiffness, along with an increase in the mixing and compaction temperatures of the modified asphalt binders, showed no increase in the high temperature performance grade (PG), an increase in the high temperature continuous PG grade was observed. At low temperature, the results show a 2% to 23% increase in fracture energy of the modified specimens. There was also a 10% to 79% increase in the CT index at intermediate temperature for the modified specimens. Moreover, preliminary cost estimates indicate CNC is the most reasonable option in terms of cost and benefit. Finally, the foregoing results show that the high shear mixer-hot plate combo could be an effective tool for dispersing the nanomaterials in the asphalt matrix without causing aging of the asphalt binder.

Preface

The research conducted for this thesis forms part of a broader research developing methods for preventing premature failure in asphalt pavements. Chapters 1 and 2 are the introduction and literature review conducted by me during this study. The analysis, summary and conclusions contained in chapter 7 and 8 were carried out by Dr. Hashemian and me.

Chapter 3 of this research has been published as T. W. Johnson, L. Hashemian, S. Patra and A. Shabani, "Application of Nanoclay Materials in Asphalt Pavements.," in *TAC 2019 Joint Conference and Exhibition: Innovations in Pavement Management, Engineering and Technologies (S)*, Halifax, 2019. Dr. L. Hashemian was responsible for the study conception and I was responsible for data collection. S. Patra and A. Shabani assisted with data collection. A Dr. L. Hashemian and I were responsible for the analysis and interpretation of results as well as the draft manuscript preparation. All authors reviewed the result and approved the final version of the manuscript.

Chapter 4 of this research has been accepted for publication as T. W. Johnson, L. Hashemian, S. Patra and A. Shabani, "Application of Nano-Sized Materials in Asphalt Pavements.," in the *CTAA 64th Annual Conference and Annual General Meeting to be held in Montréal, Québec*, at the Fairmont Queen Elizabeth Hotel. The program runs from Sunday, November 24 to Wednesday, November 27, 2019. Dr. L. Hashemian was responsible for the study conception and I was responsible for data collection. S. Patra and A. Shabani assisted with data collection. A Dr. L. Hashemian and I were responsible for the analysis and interpretation of results as well as the draft manuscript preparation. All authors reviewed the result and approved the final version of the manuscript.

Chapter 5 of this research has been submitted for publication as T. W. Johnson and L. Hashemian, "Laboratory Evaluation of Modified Hot Mix Asphalt Using Nanoclay and Nanocellulose.," in the *Journal of Testing and Evaluation*. Dr. L. Hashemian was responsible

for the study conception and design; T. Johnson was responsible for data collection; T. Johnson and L. Hashemian were responsible for analysis and interpretation of results and draft manuscript preparation. All authors reviewed the results and approved the final version of the manuscript.

Chapter 6 of this research has been submitted for publication as T. W. Johnson and L. Hashemian, "Laboratory Investigation of Permanent Deformation of Modified Asphalt Mixes using Nanocellulose.," in the *International Symposium on Bituminous Materials (ISBM Lyon 2020)*. Dr. L. Hashemian was responsible for the study conception and design; T. Johnson was responsible for data collection; T. Johnson and L. Hashemian were responsible for analysis and interpretation of results and draft manuscript preparation. All authors reviewed the results and approved the final version of the manuscript.

Chapters 7 and 8 contains original work (additional testing) for the completion of this research.

Dedicated to

*My wife and daughter, for the unwavering love and support
and the enthusiasm in moving forward with this level of
professional development.*

*My beloved mother, for setting the foundation for my
development.*

Acknowledgements

Thanks to God, my Father, the Giver of life and the Creator of possibilities.

My thanks and appreciation go to my supervisor, Dr. Leila Hashemian, for her time, guidance and steadfast support throughout the entire research.

My appreciation also goes to Dr. Alireza Bayat for providing me the opportunity to study at the University of Alberta.

I like to acknowledge and appreciate Dr. Farook Hamzeh, the Chair of the Examining Committee; Dr. Leila Hashemian, Supervisor; Dr. Alireza Bayat, Examiner; and Dr. Yaman Boluk, Examiner, professors who allotted time from their respective busy schedules to participate in the Examining Committee for this research.

I would also like to extend my thanks and appreciation to all who contributed the materials used in this research: Dr. Yaman Boluk and Mr. Geoff Clarke (TEC Edmonton) for providing the two samples of the cellulose nanocrystals (CNC); Husky Energy for providing the asphalt binder; and Lafarge Canada for providing the aggregates.

I would like to appreciate my colleagues, Vinicius Velasco for providing the knowledge for most of the laboratory equipment; Amirhossein Ghasemirad for his assistance with the PAV and BBR; Farshad Kamran for his assistance with the UTM; Sidharth Patra and Azar Shabani, as well as Caiyu Xu, Yiwen Zhang and Katrina Sha for their assistance with data collection; Luis Perca for his assistance during the research (laboratory and literature); and Roshan Rijal for his moral support.

I would like to also appreciate Lana Gutwin for her thorough review of my research work.

I would also acknowledge and appreciate Heena Dhasmana and Nura Bala who made valuable contributions to fine-tuning my defense presentation.

Table of Contents

1	Introduction	1
1.1	Objective	2
1.2	Methodology.....	3
1.3	Thesis Structure	3
2	Literature Review	5
2.1	Asphalt Binder	5
2.2	Mechanical Properties of the Asphalt Binder.....	5
2.3	Asphalt Binder Testing Protocols	6
2.3.1	Pre-construction Handling, Mixing and Compaction	6
2.3.2	Rutting Resistance (during construction).....	7
2.3.3	Fatigue and Thermal Cracking Resistance (post-construction).....	10
2.4	Asphalt Binder Modification	12
2.4.1	Polymer Modification of the Asphalt Binder	12
2.4.2	Nano Modification of the Asphalt Binder	13
2.5	Mechanical Properties of Asphalt Concrete.....	15
2.6	Asphalt Mix Testing Protocols	17
2.6.1	Rutting Resistance and Moisture Sensitivity.....	17
2.6.2	Fatigue Cracking Resistance	20
2.6.3	Thermal Cracking Resistance.....	22
3	Application of Nanoclay Materials in Asphalt Pavements	25
3.1	Abstract.....	25
3.2	Introduction and Background.....	25
3.3	Nanotechnology	26
3.4	Objectives and Scope	26
3.5	Materials.....	27
3.5.1	Asphalt.....	27
3.5.2	Halloysite Nanoclay	27
3.5.3	Nanoclay, Hydrophilic Bentonite.....	27
3.5.4	Preparing the modified asphalt sample	28
3.5.5	Qualitative Evaluation of Modified Asphalt Binder Samples	28
3.6	Rheology tests on the modified asphalt binder samples.....	29
3.6.1	Samples Modified with Halloysite Nanoclay.....	30

3.6.2	Samples Modified with Bentonite Nanoclay	31
3.7	Performance Tests	32
3.7.1	HMA Mix Design	32
3.7.2	Mixing and Compaction Temperatures	33
3.7.3	Rutting Test	34
3.7.4	Indirect Tensile (IDT) Creep and Strength Test.....	36
3.8	Conclusions and Future Steps	39
4	Application of Nanosized Materials in Asphalt Pavements.....	40
4.1	Abstract.....	40
4.2	Introduction	40
4.2.1	Nanotechnology	41
4.3	Objectives and Scope	41
4.4	Materials.....	42
4.4.1	Asphalt.....	42
4.4.2	Halloysite Nanoclay	42
4.4.3	Nanoclay, Hydrophilic Bentonite.....	43
4.4.4	Cellulose Nanocrystals (CNC)	43
4.5	Preparation of the Nanomodified Asphalt.....	44
4.5.1	Qualitative Evaluation of the Modified Asphalt Binder Sample	44
4.6	Laboratory testing.....	45
4.6.1	Dynamic Mechanical Analysis (DMA).....	45
4.6.2	Rotational Viscometer Testing	46
4.6.3	Mix Design	46
4.6.4	Hamburg Wheel Tracking Testing.....	47
4.6.5	Indirect Tensile (IDT) Creep and Strength Test.....	48
4.7	Results and Discussion	50
4.7.1	Dynamic Mechanical Analysis (DMA).....	50
4.7.2	Mixing and Compaction Temperatures	51
4.7.3	Performance Tests	52
4.8	Conclusions and Future Steps	55
5	Laboratory Evaluation of Nano-Modified Asphalt.....	57
5.1	Abstract.....	57
5.2	Introduction and Background.....	57
5.3	Objectives and Scope	59

5.4	Materials and Modified Asphalt Preparation.....	60
5.4.1	Asphalt Binder	60
5.4.2	Halloysite Nanoclay	60
5.4.3	Nanoclay, Hydrophilic Bentonite.....	61
5.4.4	Cellulose Nanocrystals	61
5.4.5	Preparation of the Nanomodified Asphalt	61
5.4.6	Qualitative Evaluation and Results of the Modified Asphalt Binder Sample	61
5.5	Laboratory Testing, Results and Discussion	62
5.5.1	Dynamic Mechanical Analysis	62
5.5.2	Rotational Viscometer Testing	64
5.5.3	Mix Design	65
5.5.4	Rutting and Moisture Susceptibility Testing	65
5.5.5	Indirect Tensile Creep and Strength Test	66
5.5.6	Wheel Tracking Tests	68
5.6	Cost Performance Analysis of Nanomodified Asphalt	71
5.7	Conclusion	71
6	Laboratory Investigation of Permanent Deformation of Modified Asphalt mixes using Nanocellulose	73
6.1	Abstract.....	73
6.2	Introduction	73
6.2.1	Objectives and Scope	74
6.3	Materials and Modification Method.....	74
6.3.1	Asphalt Binder	74
6.3.2	Cellulose Nanocrystals (CNC)	74
6.3.3	Preparation of the Nanomodified Asphalt	75
6.3.4	Qualitative Evaluation of the Modified Asphalt Binder Sample	75
6.4	Laboratory Testing	76
6.4.1	Rheological Testing (Asphalt Binder)	76
6.4.2	HWT Testing.....	76
6.4.3	3.3 Comparison of Rheology Test and HWD Test Results.....	78
6.5	Conclusions.....	79
7	Additional Testing	80
7.1	Asphalt Binder Performance Grading	80
7.1.1	High Temperature Performance Grading (Dynamic Shear Rheometer - DSR)	80

7.1.2	Low Temperature Performance Grading (Bending Beam Rheometer - BBR) ...	81
7.1.3	Intermediate Temperature Performance (Fatigue Resistance)	83
7.2	Indirect Tension Asphalt Cracking Test (IDEAL-CT) – Fatigue Resistance.....	84
7.3	Moistures Sensitivity (Stripping)	85
8	Summary and Conclusions	86
8.1	Summary.....	86
8.2	Conclusions.....	86
	References	89

List of Tables

Table 2-1: Performance Graded Asphalt Binder DSR specifications	9
TABLE 3-1: Amount of nanomaterial added to base asphalt binder (% by weight)	28
TABLE 3-2: Performance Graded Asphalt Binder DSR specifications (as summarized from Superpave Fundamentals (Federal Highway Authority/National Highway Institute, 2000)).	30
Table 3-3: Asphalt mix properties	33
Table 3-4: Aggregate grain size distribution.....	33
TABLE 3-5: HWTB Results (Mechanical Properties)	36
TABLE 3-6: Summary of IDT Test Results.....	39
TABLE 4-1: Unmodified Asphalt Binder Specification	42
TABLE 4-2: Amount of Nanomaterial Added to Base Asphalt Binder (% by weight of binder)	44
Table 4-3: Aggregate Grain Size Distribution	47
Table 4-4: Asphalt Mix Properties.....	47
Table 4-5: Mixing and Compaction Temperatures for Sample Preparation.....	52
Table 4-6: Hamburg Wheel Tracker Test Results (Mechanical Properties)	53
Table 4-7: Summary of Indirect Tensile Creep and Strength Test Results.....	55
Table 5-1: Asphalt Mix Properties.....	65
TABLE 5-2: Indirect Tensile Strength and Creep Test Results.....	70
TABLE 5-3: Added Cost Versus Performance Analysis Per Ton of HMA	71
Table 7-1: High Temperature PG Grade	80
Table 7-2: Low Temperature PG Grade	82
Table 7-3: Fatigue Performance of Modified/Unmodified Asphalt Binders	83
Table 7-4: Results for the IDEAL-CT	84
Table 7-5: Indirect Tensile Strength (ITS) Results	85

List of Figures

Figure 2-1: Rotational viscometer	7
Figure 2-2 (a) DSR spindles (b) DSR molds	8
Figure 2-3: (a) RTFO (b) rotating rack and air flow system (c) Empty bottle (d) Loaded bottle (e) Bottle after ageing	9
Figure 2-4: (a) Pressure aging vessel (b) Vacuum oven (c) PAV pan and holder	10
Figure 2-5: (a) Bending beam rheometer (b) BBR mold (c) BBR asphalt beam sample	11
Figure 2-6: Cylindrical specimen mounting system	18
Figure 2-7: ITS test (a) Samples for freezing (b) 60°C for 34 hours and 25°C for 2 hours conditioning (c) Dry/conditioned specimen testing	20
Figure 2-8: (a) Equipment setup (b) Load vs displacement curve	21
Figure 2-9: Model illustration for 75% post peak point (PPP ₇₅) and modulus (m ₇₅)	22
Figure 3-1: High shear mixer with a hot plate beneath: setup for preparing binders modified with nanoclay.	28
Figure 3-2: (a) SEM equipment and (b) Image of modified binder using 6% by weight halloysite clay	29
Figure 3-3: DSR test (a) sample, (b) testing equipment	30
Figure 3-4: Halloysite modified binder at 20°C – (a) Complex Modulus and (b) Rutting Parameter	31
Figure 3-5: Bentonite modified binder at 20°C – (a)Complex Modulus and (b) Rutting Parameter	32
Figure 3-6: Aggregate Gradation Curve.....	33
Figure 3-7: Viscosity-temperature curves for modified and unmodified binders	34
Figure 3-8: HWTD Cylindrical specimens (saw-cut) in HDPE moulds before (left) and after (right) test	35
Figure 4-1: Scanning Electron Microscope (SEM) Images of Modified Binder	45
Figure 4-2: Halloysite-Modified Binder at 20°C – (a) Complex Modulus and (b) Phase Angle	50
Figure 4-3: Bentonite-Modified Binder at 20°C – (a) Complex Modulus and (b) Phase Angle	51
Figure 4-4: CNC-Modified Binder at 20°C – (a) Complex Modulus and (b) Phase Angle	51
Figure 4-5: Viscosity-temperature curves for unmodified and nanomodified binders	52
Figure 4-6: Samples after Hamburg Wheel Tracker Test.....	53
Figure 5-1: Scanning electron microscope images of modified binders: (a) 3% halloysite; (b) 1% CNC.....	62

Figure 5-2: Rutting parameter vs angular frequency: (a) Halloysite (3% & 6%); (b) Bentonite (3% & 6%); (c) CNC (0.5% & 1%)	63
Figure 5-3: Viscosity-temperature curves for neat and modified binders.....	64
Figure 5-4: Mix design aggregate gradation curve	65
Figure 5-5: (a) HWT Results (b) Rutting improvement comparison of rheology test and wheel tracking test.....	69
Figure 5-6: Moisture sensitivity: (a) Stripping inflection point; (b) Improvement in moisture resistance	70
Figure 6-1: FESEM image of CNC-modified binder	75
Figure 6-2: Comparison of rutting parameter vs angular frequency for the neat and CNC-modified asphalt binders	76
Figure 6-3: Results of HWT for HMA samples made with neat and CNC-modified asphalt binders	77
Fig. 6-4: (a) SIP for neat and CNC-modified asphalt binders (b) Improvement in moisture resistance	78
Fig. 6-5: Correlation between rutting improvement results for both DSR testing and HWT testing	78
Figure 7-1: Continuous high PG grade	81
Figure 7-2: Continuous low PG grade.....	83
Figure 7-3: CT index of modified/unmodified asphalt mixes	84

1 Introduction

Flexible pavements are the predominantly used pavement type the world over due to its comparatively low initial investment costs, good temperature variation resistance, ease of maintenance works, and ease of locating underground utilities [1]. Flexible pavements not only account for nearly eighty-five percent of the world's consumption of asphalt, but also over ninety percent of the pavement infrastructures of the two world's largest economies (i.e. China and USA) [2]. Contributing significantly to pavement performance, the asphalt binder accounts for about thirty percent of the asphalt mix rutting resistance, more than fifty percent of its fatigue resistance and up to ninety percent of its thermal crack resistance [3]. It is a viscoelastic material that exhibits a time-dependent strain response to applied stresses at intermediate temperatures; and a thermoplastic material that displays glass-like elasticity (brittleness) at very low temperatures and acts as a fluid at very high temperatures [4]. With the advent of climate change phenomenon, rapid increase in vehicle axle load intensity and frequency in recent years, the failure rates of the undesirable pavement distresses are exacerbated, causing decreased serviceability and consequent increase lifecycle and vehicle operation costs [5]. Adapting to these new design thresholds may require modification of the asphalt binder. Furthermore, depending on the environmental elements, loading conditions and the structural requirement of the pavement, the appropriate modifier should be introduced to achieve the desired improvement [6].

Polymer modification of the asphalt binder have been extensively used over the decades to provide increased binder stiffness at high, improved thermal cracking resistance, lower moisture sensitivity or increased fatigue life. Although it was officially announced as an asphalt modifier in 1972, its early usage in North America dates back to the 1950s. While these improvements are evident, polymer modified asphalts (PMB) are generally expensive, have low ageing resistance and poor storage stability [7]; thus, hindering continuous development of asphalt-polymer modification [8]. Researchers have identified the application of nanotechnology to asphalt binders as one of the ways to remove these shortcomings [5].

Nanotechnology makes use of ultra-small, functional structures with at least one dimension under 100 nm to remarkably alter the macro properties of the materials to which it is added. The quantum effect comes into play as a result of the high aspect ratio of nanomaterials, and enables the design of systems that have high surface density, are resistant to the aggressive effects of environmental elements, have enhanced shear resistance and increased strength [9], have excellent stability [10], are cost effective and appear to be promising in the design and construction of flexible pavements [11]. Previous research show that nano modification

of asphalt binder not only enhances the mechanical and rheological properties, as well as the storage stability, of the binder, but also improves the rutting resistance, tensile strength and resilient modulus of the asphalt mix produced therewith [12]. Moreover, preliminary cost analysis demonstrates a 22%-33% cost reduction for nano-modified asphalt binder compared with its polymer-modified equivalent [13]. Further developments and innovations that trigger market growth are expected to drive the costs of nano-modified asphalt binder lower, and make the margin more significant [6]. However, to achieve the expected improvement, it cannot be overemphasized that good dispersion of the nanomaterial at the nanoscopic level is critical [14].

In nanotechnology, different types of materials are characterized according to their respective morphology, including nanoparticles, nanotubes, nanowires, nanoplatelets, nanorods and nanoporous [15]. Before large scale applications for a novel technology are attempted, laboratory testing is usually required to provide valuable information to reliably predict field performance [4]. The nanomaterials of interest in this research are bentonite nanoclay (plate-like morphology), halloysite nanoclay (tube-like morphology) and cellulose nanocrystals (CNC) with a rod-like morphology, and the system of interest to evaluate their respective effects on the asphalt binder, and consequently the asphalt mix, is the Superpave asphalt mixture design and analysis system.

The Superpave asphalt mixture design and analysis system was developed by the Strategic Highway Research Program (SHRP) to provide an "improved, performance-based system for specifying asphalt binders and mineral aggregates, performing asphalt mixture design, and analyzing pavement performance." With the introduction of this system which includes new specifications and physical property tests for the asphalt binder and aggregates, a design and analysis system for hot mix asphalt (HMA), and the integration of the system components using computer software, temperatures and aging conditions faced by pavements in service can be reproduced during laboratory testing [16].

1.1 Objective

The objective of this research is to investigate and compare the effects of modification of asphalt binders with three different nanomaterials (bentonite nanoclay, halloysite nanoclay, and cellulose nanocrystals) and the resulting properties of the corresponding asphalt cement at various temperatures (high, intermediate, and low). This will be done by using various testing methods, as indicated below:

- asphalt cement rheology, by using dynamic mechanical analysis (DMA) and conducting Superpave performance grading (PG) tests at high, intermediate and low service temperatures;
- asphalt mixes performance at low temperatures using the indirect tensile strength (IDT) test and creep compliance at 0, -10, and -20°C temperatures; at intermediate temperature conducting indirect tensile strength test (ITS) at 25°C; and high temperatures using permanent rutting test at 45°C;
- moisture sensitivity of asphalt mixes using ITS test results after freeze/thaw conditioning of asphalt mix samples and the inflection points as determined from wheel tracking tests;
- permanent deformation of asphalt mixes containing different nanomodified binders based on the correlation of the results of asphalt cement rheology tests and wheel tracking tests; and
- cracking potential and fatigue resistance of asphalt mixes based on IDEAL-CT test results.

1.2 Methodology

Unless otherwise stated, the asphalt binder used in this research shall be identified by and referred to as performance grade PG 58-31 in accordance with the manufacturer's specifications. However, upon verification, the standard performance grade determined was PG 64-28.

The original (unaged) asphalt, with performance grade of PG 58-31, was mixed with hydrophilic bentonite nanoclay (3% and 6% by weight of the binder), halloysite nanoclay (3% and 6% by weight of the binder) and CNC (0.5% and 1% by weight of the binder) using a high shear mixer to produce six types of nano modified binders. Scanning electron microscopy (SEM) was used to investigate the dispersion of nanomaterial in the base asphalt after mixing. Subsequently, the binders and their respective asphalt mixes were evaluated using the Superpave testing protocols for the asphalt binders and asphalt mixes.

1.3 Thesis Structure

The thesis has the following organization:

Chapter 1 – Introduction: In this chapter, the background and motivations of the research are outlined, along with the objectives, methodology, and thesis structure.

Chapter 2 – Literature Review: In this chapter, the materials used in this study are reviewed extensively. The applicable procedures, advantages/disadvantages, and prior work in the literature are discussed and appropriately cited. Relevant case studies are also presented.

Chapter 3 – Application of Nanoclay Materials in Asphalt Pavements: In this chapter, the results of performance testing of nanoclay-modified asphalt binders are presented and compared with the results of the same tests conducted using the original, unmodified binder. Test results presented include rheology, rutting, indirect tensile creep and strength tests.

Chapter 4 – Application of Nanosized Materials in Asphalt Pavements: In this chapter, nanoclay-modified asphalt binders and cellulose nanocrystals modified asphalt binder were prepared, performance evaluated and compared with the original binder's performance. Tests performed included rheology, rutting, indirect tensile creep and strength tests.

Chapter 5 – Laboratory Evaluation of Modified Hot Mix Asphalt Using Nanoclay and Nanocellulose: In this chapter, nanoclay-modified asphalt binders and cellulose nanocrystals modified asphalt binder were prepared, performance evaluated and compared with the original binder's performance. Tests performed included rheology, rutting, indirect tensile creep and strength tests. Cost analysis was also performed

Chapter 6 – Laboratory Investigation of Permanent Deformation of Modified Asphalt mixes using Nanocellulose: In this chapter, 3 concentrations of cellulose nanocrystals (0.5%, 1% and 3% by weight of the asphalt binder) were added to PG 58-31 performance grade asphalt binder and evaluated for rutting resistance and moisture susceptibility. The improvement in the materials' performance are summarized and explained.

Chapter 7 – Additional Testing: This chapter contains the results of additional tests that were conducted but not yet published. These include the performance grading (high/low temperature) of the modified/unmodified asphalt binders, as well as fatigue resistance; separation of the asphalt into its 4 major constituents (SARA); indirect tensile asphalt cracking test (IDEAL-CT) on asphalt mixes to evaluate fatigue resistance; and moisture susceptibility using the indirect tensile strength (ITS).

Chapter 8 – Summary and Conclusions: The effects of nanomodification using bentonite nanoclay (3% and 6%), halloysite nanoclay (3% and 6%) and cellulose nanocrystals (0.5% and 1%) on asphalt rheology and, consequently, the performance of the mix produced therewith are summarized and explained.

2 Literature Review

2.1 Asphalt Binder

Asphalt is a viscoelastic material derived from the fractional distillation of crude oil. It is totally soluble in toluene, essentially non-volatile and temperature susceptible. Carbon (80% to 88% by weight) forms a large fraction of its contents, followed by hydrogen (8% to 11% by weight), along with, sulfur (0 to 2% by weight), nitrogen (0 to 2% by weight), oxygen (0 to 2% by weight), vanadium (2000 ppm) and nickel (200 ppm). This complex mixture of about 300 to 2000 chemical compounds allows only four principal constituents to be identified as SARA: Saturates, Aromatic, Resin and Asphaltene.

Asphaltenes are amorphous brown/black solids at room temperature with dimensions varying between 5 to 30 μm and completely soluble in n-heptane [17]. They contain the heavy metals, are negatively charged and makeup 5 to 25% by weight of the asphalt.

The saturates are the lightest fraction of the asphalt and accounts for 0 to 15% by weight of the overall material. Any change in the concentration of the saturates affects the rheological parameters of complex shear modulus and phase angle [18].

Resins are similar to the asphaltenes in structure and content but have lower molecular mass. They appear as a dark brown solid (or semi-solid) with particle sizes varying between 1-5 nanometers. Resins make up 30 to 45% by weight and are responsible for dispersing the asphaltenes and oils within the matrix [18]. The resins-asphaltene ratio contributes significantly to the asphalt properties [17].

The lightweight aromatic compounds are within the aromatic oils. Aromatic oils are dark brown viscous liquids with molar mass ranging between 300 and 2000 grams/mole. They occupy 40 to 65% of the asphalt and they work with the saturates to plasticize the matrix.

2.2 Mechanical Properties of the Asphalt Binder

Viscoelasticity defines the behavior of the asphalt binder when it is subjected to stress. Because of the temperature susceptibility characteristics of the asphalt, it behaves as an elastic solid at very low temperatures and a Newtonian fluid at very high temperatures. At intermediate temperatures, the kind that exists during field operating conditions, it exhibits a time-dependent relationship between the applied stress and the resultant strain – viscoelasticity. When the applied stress is released, the elastic strain is fully recovered while the viscous strain remains. For engineering applications, an applied stress must be

accompanied by a linearly predictable strain, and the quantities that make this alignment possible is temperature and time.

Airey defined asphalt rheology as the fundamental measurements (i.e. complex shear modulus and phase angle) associated with the flow and deformation characteristics of bitumen [4]. Sandwiching an asphalt samples between two parallel plates and using the strain-controlled oscillatory type testing in dynamic mechanical analysis (DMA), the rheology of the binder can be measured over a wide range of temperature and loading times and represented as [4]:

- Isochronal plots (i.e. constant frequency)
- Isothermal plots (i.e. constant temperature)
- Master curves – a type of isotherm where curves at different temperatures are shifted to form one continuous curve at a reference temperature. A smooth curve is indicative of thermo-rheological simplicity. An unsmooth curve may be indicative of structural changes with temperature, high wax content and GEL type asphalt
- Black diagrams – used to check time-temperature equivalency, presence of high wax content, high asphaltene structured asphalt or a highly polymer modified binder
- Cole-Cole diagrams – used to represent viscoelastic balance in the binder

2.3 Asphalt Binder Testing Protocols

The Superpave binder classification system is represented by PG 58-28. The “PG” stands for “Performance Grade”. The high PG grade is represented by “58”, which indicates the average 7-day maximum pavement temperature (in °C), while the low performance grade, “-28”, represents the minimum pavement temperature (in °C). Standard PG grading requires that a new grade is defined at $\pm 6^\circ\text{C}$ increments. The system also requires that the asphalt binders resistance to rutting, fatigue and thermal cracking be evaluated in relatively typical stages of (1) transportation, storage and handling; (2) mix production and construction; and (3) after long periods of service in a pavement [16].

2.3.1 Pre-construction Handling, Mixing and Compaction

During the pre-construction phase, rotational viscometer (RV) was used to evaluate the handling (pumpability) of the binder at high temperatures, as well as the workability of the asphalt binder during mixing and compaction of the asphalt mix. In accordance with AASHTO T316-13, the torque required to maintain a cylindrical spindle was submerged in a preheated asphalt binder sample and rotated at a constant rotational speed of 20 revolutions per minute (rpm) was determined, converted to viscosity automatically and displayed by the equipment.

The test continued at 10°C increments in temperature until viscosity measurements between 0.15 mPa·s and 0.31 mPa·s at were acquired. Viscosity versus temperature plots were prepared to determine the mixing and compaction temperatures of asphalt mixes prepared with such binder (Figure 2-1).

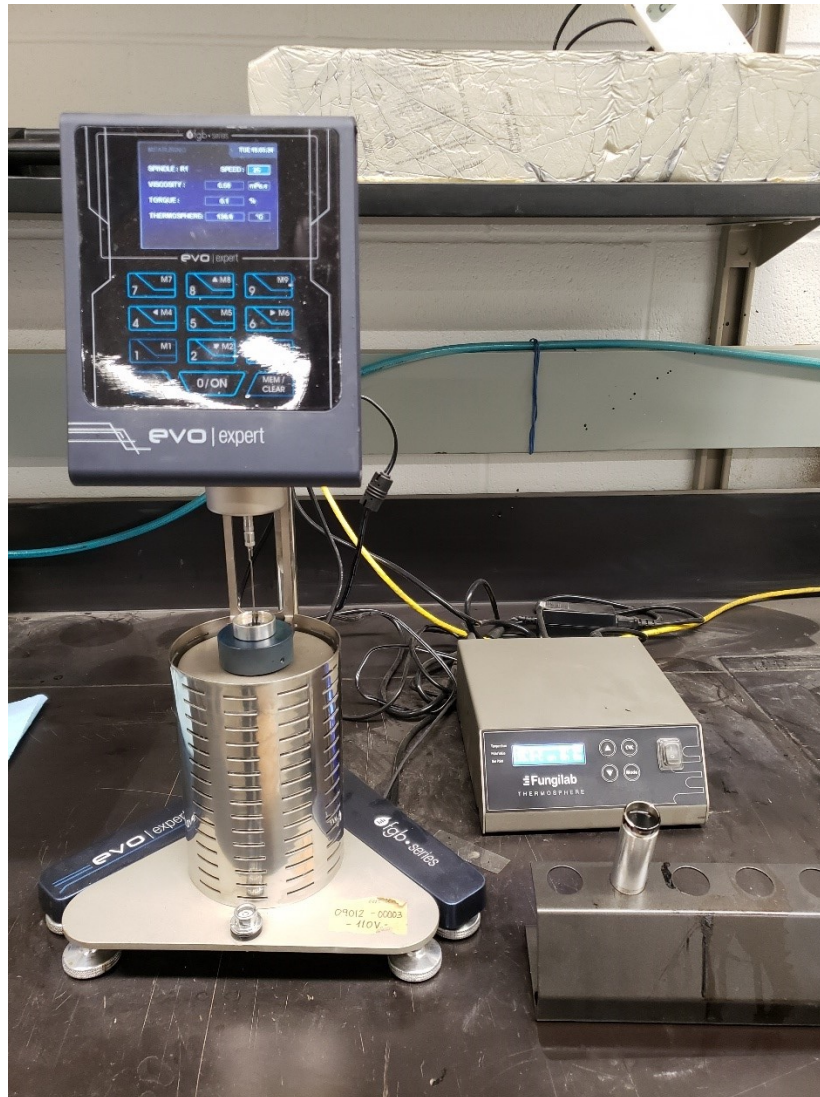


Figure 2-1: Rotational viscometer

2.3.2 Rutting Resistance (during construction)

To understand the high temperature properties of modified/unmodified binders during construction, 14 specimens were prepared (i.e. 7 rolling thin film oven-aged and 7 unaged). A dynamic shear rheometer (DSR), using a strain rate of 0.5%, an angular frequency of 10 rad/s and a 25 mm diameter spindle-plate geometry with a 1-mm gap (Figure 2-2), was used to perform rheological tests in accordance with the Superpave test method [16] and AASHTO

T315. For the unaged asphalt binders, the complex modulus (G^*), which is a measure of the binder's resistance to shear deformation (stiffness), and the phase angle (δ), an indication of the binder's response (viscous/elastic) to shear deformation, were determined at the initial temperature of 58°C and then in 6°C increments until the temperature at which the ratio, $G^*/\sin \delta$, was less than 1 kPa (Table 2-1).

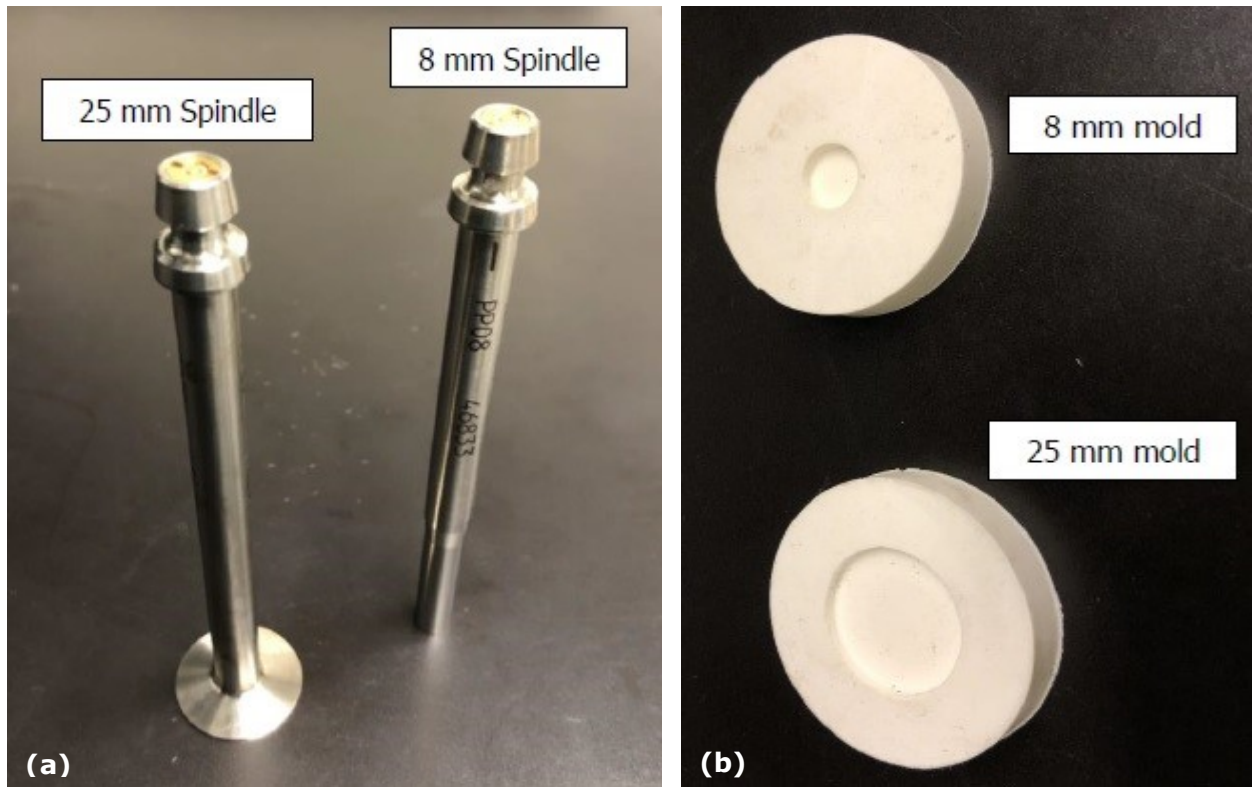


Figure 2-2 (a) DSR spindles (b) DSR molds

The rolling thin film oven (RTFO) was used to prepare the RTFO-aged modified/unmodified binders in accordance with AASHTO T240-13 (Figure 2-3). This process simulates the effect of the conventional batch plant mixing on the asphalt binder viscosity and other rheological measurements. To achieve this, each of the eight glass bottles was filled with 35 ± 0.5 grams of a binder type and allowed to cool between one to three hours in a horizontal position. The bottles were then placed in a preheated oven on a rotating rack and exposed to a temperature of 163°C and airflow of 4 ± 0.3 litres/minute for 85 minutes (Figure 2-3). The rheology of the recovered RTFO-aged sample was evaluated with the DSR using a strain rate of 0.5%, angular frequency of 10 rad/s and a 25 mm diameter spindle-plate geometry with a 1-mm gap (Figure 2-2). For this aged sample, G^* and δ were determined at the initial temperature of 58°C and in 6°C increments until the temperature at which the ratio, $G^*/\sin \delta$, was less than 2.2 kPa (Table 2-1).

The failure temperatures of the unaged and the RTFO-aged specimens were then compared, and the lower failure temperature was considered the “continuous high PG grade” (meaning the temperature at which either, or both, of the specimens failed). The standard high PG grade became the highest standard temperature both specimens passed.

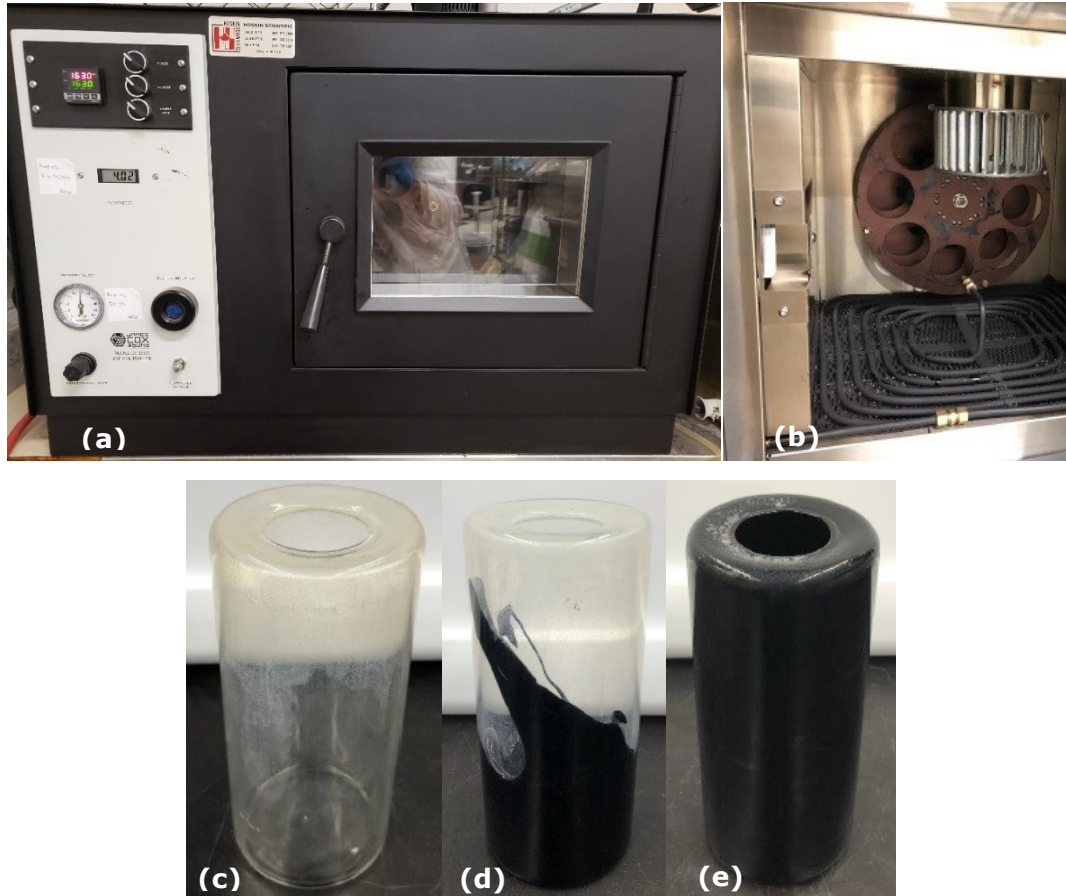


Figure 2-3: (a) RTFO (b) rotating rack and air flow system (c) Empty bottle (d) Loaded bottle (e) Bottle after ageing

Table 2-1: Performance Graded Asphalt Binder DSR specifications¹

Material	Quantity	Specification	HMA Distress of Concern
Unaged binder	$G^*/\sin(\delta)$	$\geq 1.0 \text{ kPa (0.145 psi)}$	Rutting
RTFO residue	$G^*/\sin(\delta)$	$\geq 2.2 \text{ kPa (0.319 psi)}$	Rutting
PAV Residue	$G^* \cdot \sin(\delta)$	$\geq 5,000 \text{ kPa (725 psi)}$	Fatigue Cracking

¹ AASHTO T315

2.3.3 Fatigue and Thermal Cracking Resistance (post-construction)

Fatigue and thermal cracking usually initiate, or become more severe, in asphalt pavements after 7 to 10 years in service (post- construction) [19]. During mixing and placement, elevated temperatures age the binder not only through the loss of the asphalt binder lighter components, but also through higher exposure to oxidation – short term (RTFO-ageing). In service, the asphalt layer gradually ages (oxidative) through continuous interaction with the environment – long term (PAV-ageing). In accordance with AASHTO R28, approximately 50 grams of preheated RTFO-aged asphalt binder’s residue was poured into each preheated PAV pan (a total of 4 pans @ 50 grams per pan) and placed on the pan holder. The pan holder was then placed into the preheated PAV to the desired temperature of 100°C. At 100°C, a pressure of 2.07 MPa (300 psi) was applied and maintained for 20 hours. At the end of the aging period and depressurizing the sample(s), the residue in the pans were scraped into a single container and placed in a vacuum oven at 170°C for 30 minutes to degas the sample. The residue collected was used for intermediate and low temperature testing (Figure 2-4).



Figure 2-4: (a) Pressure aging vessel (b) Vacuum oven (c) PAV pan and holder

A dynamic shear rheometer (DSR), using a strain rate of 0.5%, angular frequency of 10 rad/s and an 8-mm diameter spindle-plate geometry with a 2-mm gap (Figure 2-2), was used to perform rheological tests on the PAV-aged specimen in accordance with the Superpave test method [16] and AASHTO T315. For this aged sample, G^* and δ were determined at the initial temperature of 25°C, and then in -3°C increments until the temperature at which the product, $G^* \sin \delta$, was greater than 5,000 kPa (Table 2-1).

The bending beam rheometer (BBR) was used to determine the asphalt binder low temperature PG grade. By measuring the low temperature stiffness and relaxation properties,

the asphalt binder's ability to resist thermal cracking at low service temperatures was determined. The test was performed in accordance with AASHTO T313 (standard BBR test) and AASHTO PP 42 (Superpave PG binder specification for BBR). BBR specimens were prepared from an asphalt binder that was first RTFO-aged and then Pressure Ageing Vessel (PAV)-aged.

To prepare the specimens for BBR testing, the residue of the preheated PAV-aged asphalt binder was poured into an aluminum mold to achieve a beam with dimensions measuring 6.25 x 12.5 x 127 mm and allowed to cool in the mold at room temperature for about an hour. In the meantime, the BBR was calibrated and set to -18°C (i.e. 10°C higher than the expected low temperature PG grade) prior to the beam placement. The beam was then trimmed with a hot spatula to flush with the mold, demolded and placed into the BBR and conditioned for 1 hour. The specimen was then placed on a 102-mm span simple support and loaded with 0.98 N force and the beam deflection was measured at 8, 15, 30, 60, 120 and 240 seconds. The beam (or creep) stiffness and the m-value were measured at these times and a stiffness master curve was plotted. 2 replicates were tested for each asphalt binder type. The maximum temperature at which both the m-value and creep stiffness conditions were satisfied was considered the "continuous low PG grading" (or failure temperature). The highest standard temperature at which both creep stiffness and m-value were satisfied is considered the low temperature PG grade of the asphalt binder (Figure 2-5).

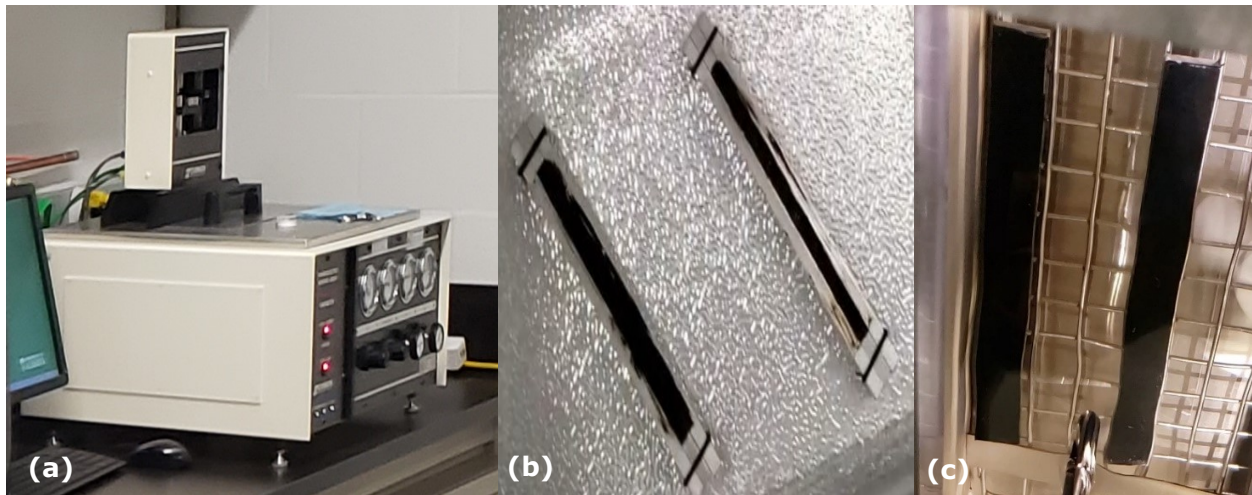


Figure 2-5: (a) Bending beam rheometer (b) BBR mold (c) BBR asphalt beam sample

2.4 Asphalt Binder Modification

2.4.1 Polymer Modification of the Asphalt Binder

Polymers have traditionally been used to provide considerable improvement [20] to the temperature susceptibility of asphalt by increasing binder stiffness at high service temperatures to resist rutting, crack reduction at low service temperatures through softer matrix, obtain viscosity reduction at layout temperatures, improve stability and strength of the matrix, enhance fatigue resistance, boost abrasion resistance, augment oxidation and ageing resistance, reduction in life-cycle costs [21]. Polymers are long chain macromolecules produced through the chemical synthesis of smaller molecules called monomers. The chemical structure and arrangement of the monomers in the polymer chain dictate the physical properties of the resulting polymer. Among the broad range of polymers used in asphalt modification, the types most frequently used in pavement applications are plastomeric (or plastomer) and elastomeric (or elastomer) modifiers. Polymer can form a simple mixture with the asphalt binder as a filler through mechanical mixing, or a complex mixture through chemical reaction. [22]. It should be noted that the degree of modification dependent on the choice of polymer and the quantities introduced, the nature of the asphalt binder and the type of mixture required [4].

Pareek *et al* evaluated the performance of conventional penetration grade asphalt (60/70) and polymer modified asphalt (PMB-70) and concluded that the PMB showed significantly high elastic recovery, better age resistance than the 60/70, enhanced Marshall stability, higher indirect tensile strength and increased resilient modulus. They also suggested that these performance-related benefits can be achieved without altering its chemical nature of the original binder [23].

While polymer modification of the asphalt binder for pavement applications reports some advantages, some drawbacks are evident. Rodrigues and Hanumanthgari reported that SBS, a popular elastomer used in bitumen modification [5], competes for the maltenes in the PMB and facilitates formulation of two separate domains: polymer swollen with maltenes and asphaltenes, giving rise to thermodynamic instability and resulting phase separation [24]. Airey evaluated the effects of modifying two sources of penetration graded asphalt binders with the elastomer styrene-butadiene-styrene (SBS). Though the results show that the degree of the SBS modification is function of the bitumen source, asphalt-polymer compatibility and polymer concentration in asphalts with high aromatic content to produce a high elastic network, increased viscosity and elastic response at high service temperatures, it still showed reduction in the molecular size and decreased elastic response [25]. On the other hand,

Masson et al showed that a 70-80% aromatic content in the asphalt can cause an increase in the glass transition temperature, thereby compromising the low temperature capacity of the asphalt binder [26].

Plastomer, another major category of polymer used in asphalt binder modification for pavement applications, emerged as a result of the high cost and polymer-binder instability. Polyethylene (PE) and Ethylene-vinyl-acetate (EVA)/Ethylene-methacrylate (EMA) are relatively inexpensive and more stable [24]. Punith and Veeraragavan investigated the effects of reclaimed PE, obtained from domestic waste carry bags, as an additive to 80/100 penetration grade asphalt binder and concluded that the PE-modified asphalt binder exhibited high shear and resilient moduli, higher resistance to thermal cracking, increased rutting resistance and lower moisture susceptibility [27]. Then again, the non-polar nature of the PE, as well as their tendency to crystallize, results in compatibility issues [8]. To improve compatibility and crystallization issues, EVA and EMA have been introduced. Despite the disruption of the closely packed crystalline structure and increasing polarity, elastic recovery remains a problem [21].

In summary, the issues of poor storage stability, high costs and relatively weak ageing resistance of the PMB still exist, and have caused PMB investigations to be divided into two areas: (1) Investigation into the mechanism of PMB and its failures and (2) Attempting to overcome the disadvantages of some PMBs [8]. Researchers with interest in the second area of PMB investigations have considered the application of nanotechnology.

2.4.2 Nano Modification of the Asphalt Binder

Applications of nanotechnology in PMBs have resulted in some improvement though limited it may be. Previous studies suggest that the exclusive use of nanotechnology, without the inclusion of polymer, have exhibited improved rheological and mechanical properties, as well as storage stability, of the binder in addition to the rutting resistance, tensile strength and resilient modulus improvement of the asphalt mix produced therewith [12]. Moreover, preliminary cost analysis show that these improvements come with a 67%-78% of the cost of the polymer-modified equivalent [13].

Nanoclay

Clays are inorganic, fine-grained, hydrophilic layered silicates that can be broadly categorized into three classes: kaolinite (halloysite), illite and montmorillonite (bentonite). Kaolinite clay consist of repeating layers of a silica sheet with either a gibbsite, or brucite, sheet held together by hydrogen bonding and Van der Waals forces. Each sheet is about 0.72 nm thick.

The combination of these two sheets form the kaolinite clay particle, or platelet, with lateral dimensions of about 100-2000 nm (1,000-20,000 Å), and a thickness of 0.1-100 nm (100-1,000 Å). Illite and montmorillonite (bentonite) clay particles have a 2:1 layered structure with the alumina sheet sandwiched between two silica sheets [28]. While potassium ions bond the illite layers together, they are absent in the montmorillonite and a large amount of water is attracted to the interlayer spacing. The illite particle has lateral dimensions of 100-500 nm and 5-50 nm in thickness. The montmorillonite platelet is also 100-500 nm in lateral dimensions but 1-5 nm in thickness. A complete separation of these particles into individual sheets results in nanoclay and facilitates its interaction with the asphalt binder [14] in order to achieve the "seemingly magic effects" [29].

Morgan reported the use of polyimide-6, a polymer nanocomposite (PNC) produced from exfoliation of montmorillonite (MMT) platelets (2% by weight of polymer) in polypropylene, for flame retardant applications. Compared with the non-nanocomposite flame retardant product, the PNC provided a lighter weight, lower cost and better balance of properties [30].

Jahromi and Khodaii investigated the effects of modifying 60/70 penetration grade binder (AC-10) with two types of montmorillonite nanoclays: nanofil-15 and cloisite-15A (contents: 2%, 4% and 7% by weight of the binder). Though nanofil-15 had no significant effect on the unmodified binder, cloisite-15A reported a reduction in penetration (from 63 to 45) and increase in penetration (from 54 to 61) with increasing nanoclay concentrations.

Crucho et al conducted a study to evaluate the durability of asphalt mixtures modified with three types of nanomaterials (i.e. nanosilica, nanoiron and nanoclay). Each nanomaterial constituted 4% of their respective final binder (35/50 penetration grade binder (AC-14))-nanomaterial matrix. The TEAGE method was used to age the compacted samples in the lab and the binders of each of the compacted specimens were recovered for further testing. The results show that the modifications containing nanosilica and nanoclay increased the ageing resistance of the binder [31].

Motivated by recent developments in the nanotechnological applications in asphalt pavements, Ashish et al assessed the rutting, fatigue and moisture damage of asphalt mixtures produced with AC-10 viscosity grade asphalt binder modified with Cloisite 30B (CL-30B) in 2%, 4% and 6% by weight of the asphalt binder using surface free energy (SFE) approach. Although the study recorded significant improvement in rutting (even 1 PG and 2 PG grade bumps after the addition of 4% and 6% CL-30B), fatigue resistance and resistance to moisture damage, Ashish et al mentioned, however, that the behavior of the nanomodified

binder may not only change with proper selection of the nanoclay [32] but also with the type, mode of production and chemical composition of the base binder [33].

Halloysite nanoclays have a tube-like morphology owing to the strain caused by the lattice mismatch between adjacent silica tetrahedral and alumina octahedral platelets [34]. Considered as a leader in green nanotechnology, halloysite nanotubes (HNT) provide several cross-industry applications including cosmetics, electronics, pharmaceuticals and polymer. With respect to cytotoxicity and cytocompatibility, the material is natural, non-toxic, biocompatible and chemically stable [35]. However, it has not been extensively used in asphalt modification.

Cellulose Nanocrystals (CNC)

Cellulose Nanocrystals (CNCs) is the most abundant organic biopolymer that is odourless, flavourless hydrophilic and insoluble in most solvents. They have a rod-like morphology with a rectangular cross-section. It is a derivative of plant and animal matter and is composed of carbon, hydrogen, and oxygen bioengineered as a linear homopolysaccharide chain with cellobiose as the recurrent building block. The cellulose molecules are held together by many hydrogen bonds that maintain the strong lateral association of the chain-like linear cellulose molecules [36]. However, with an interruption of these crystalline (i.e. strong, highly oriented) regions with amorphous (i.e. weak, poorly oriented) regions, the nanosized cellulose-based crystals (or CNCs) can be isolated by acid hydrolysis [37].

With high aspect ratio (i.e. 5-20 nm lateral dimensions by 100-200 nm longitudinal), recent discoveries reveal that CNC provides tensile strengths theoretically stronger than steel and comparable to Kevlar fibres, thus making it an excellent reinforcing material for natural or synthetic matrix polymers [38]. CNC is also considered to be gas-impermeable and can therefore be used to protect materials sensitive to air and oxidation [39].

2.5 Mechanical Properties of Asphalt Concrete

Flexible pavement performance is significantly influenced by the mechanical properties and durability characteristics of the asphalt mix. Though the volumetric composition of the aggregate, asphalt binder (as well as binder properties) and air contributes significantly to the mechanical properties and serves as a first screening of the asphalt mix formulation, the evaluation of pavement performance is incomplete without the evaluation of the mechanical properties (i.e. stiffness and resistance to rutting, thermal cracking and fatigue). Moreover, the mix must be able to endure field operating conditions during its service life without compromising these mechanical properties. [4].

Two main aspects of the material properties that influence the design of pavements are: response to stress (load-deformation characteristics) and the modes of failure. The elastic stiffness provides indication of the load spreading capabilities of the mix to redistribute the wheel loads throughout the pavement while at the same time providing an impervious cover for the underlying unbounded aggregate and/or soil pavement layers [4]. It should be noted that the temperature susceptibility characteristics of the bituminous mix – frequency of loading (i.e. high versus low vehicle speeds) and temperature conditions (low versus high service temperatures) – affect its stiffness and influence its response (elastic – high load frequency at low/moderate service temperatures; or viscous – low load frequency at high service temperatures) to traffic loading and characteristic deformation (permanent/temporary) [40].

The three major distresses associated with the performance of flexible pavements in field-operating conditions identified by the Strategic Highway Research Program (SHRP) are rutting, fatigue cracking and thermal cracking [41]. Rutting is associated with permanent, or non-recoverable, deformation of the surface bituminous layer, which may reflect in the sublayers, and represented as channelized depression in wheel tracks in the direction of traffic. It is caused by shear displacement or densification of poorly compacted bituminous layer under repeated high vehicle axle load under high field operating temperature conditions [42]. The use of leaner, but stiffer, mixtures may reduce rutting; however, susceptibility to fatigue failure may result [4].

Fatigue failure refers to the number of load cycles a bituminous layer can tolerate in service before cracking develops [43]. In relatively thin pavements, this structural distress initiates deep within the pavement, where the horizontal tensile strains at the bottom of the pavement structure and the vertical compressive stresses/strains at the top of the subgrade exceed the design threshold, and progressively propagates to the surface as a result of repeated loading. Water accessibility through the cracks reduces the strength of the lower pavement layers thereby accelerating deterioration [44]. In relatively thicker pavements where these horizontal tensile and vertical compressive strains are kept within acceptable design limits, ultraviolet, as well as oxidative, aging of the bituminous surface together with repeated traffic loading, cracks initiate at the surface and propagates downward [45] leading to surface disintegration.

Thermal cracking is a major pavement distress mode in cold climate regions. At extremely low temperatures when thermally induced tensile stresses exceed the design limits, cracks develop in the transverse direction (i.e. perpendicular to the road centerline) and provide

access to the intrusion of water and consequent degradation of the pavement structure [46]. Although the mechanical properties of the asphalt binder and the environmental conditions to which the pavement is subjected play a major role in the initiation and propagation of thermal cracking, the single most important contributor to the degree of the thermal cracking is the temperature-susceptibility characteristics of the asphalt binder [4].

Bituminous mixtures exhibiting these mechanical capabilities pass the first set of requirements for application in flexible pavements. However, its long-term performance is of utmost importance. Durability, though not a mechanical property, require that not only the individual components of the mix (the properties of the binder, aggregates and air) and their volumetric composition, but also the quality of workmanship, will produce a complementary composite to resist the aggressive effects of the environment while in service [47].

2.6 Asphalt Mix Testing Protocols

The Superpave specifications requires that the appropriate asphalt binder grade selected is based on geographical location, pavement temperature and air temperature of the area in which the pavement will serve. With the appropriate binder performance grade selected, the asphalt mix is prepared and subjected to the Superpave testing protocol for asphalt mix to evaluate its resistance to rutting, fatigue and thermal cracking [16].

2.6.1 Rutting Resistance and Moisture Sensitivity

Hamburg Wheel Tracking Test

The Hamburg Wheel Tracking Device (HWTDD) was used to evaluate the rutting potential of the cylindrical asphalt mix samples. In accordance with AASHTO T324-16, the device cyclically tracks a 705 ± 4.5 N, 47 mm-wide steel wheel (at a frequency of 52 ± 2 passes per minute and a maximum speed of 0.305 m/s at midpoint) an approximate distance of 230 mm across a submerged HMA sample (cylindrical or slab) compacted to 7.0 ± 0.5 percent or 7.0 ± 1.0 percent air voids using a Superpave gyratory compactor or linear kneading compactor, respectively. The machine tracks for 20,000 passes or until a 12-mm rut depth is achieved (whichever is earlier) at a predefined temperature. A graph of rut depth versus number of passes is plotted to provide valuable information about the asphalt concrete mixes' rutting potential as well as their susceptibility to moisture damage. The graph also shows the Stripping Inflection Point (SIP), which marks the point at which moisture damage begins to take effect and accelerates the rut depth. An HMA with SIP occurring at a number of load cycles less than 10,000 passes may be susceptible to moisture damage [48]. The device has been observed to have reproducible results for asphalt mixtures produced with different

aggregates as well as test specimens made by different compacting devices. Furthermore, cylindrical samples compacted with the superpave gyratory compactor (SGC) could also be used for comparative moisture evaluation of materials [49].

In this study, the Superpave gyratory compactor was used to prepare all HMA samples in accordance with AASHTO T324-16. The cooled samples were then saw-cut along a secant line such that, when joined together in the high-density polyethylene molds, a gap of no greater than 7.5 mm was achieved between the molds (Figure 2-6). The samples were then tested for 20,000 passes (or until 12-mm rut depth was achieved, whichever was earlier) at 45°C.

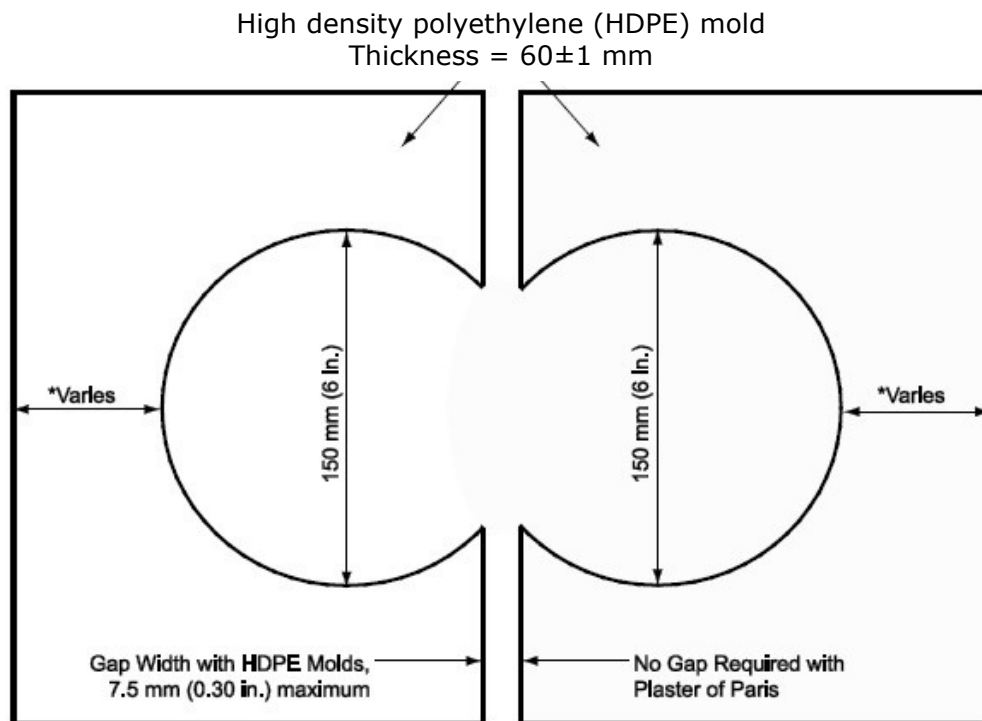


Figure 2-6: Cylindrical specimen mounting system

Indirect Tensile Strength (ITS)

Stripping is a failure phenomenon associated with the loss of strength or modulus of the asphalt pavement which was initially considered to be the separation of the asphalt binder from the surface of the aggregates (i.e. loss of adhesion) as a probable result of the properties of the aggregates (coarse/fine), properties of the asphalt binder, mix design, construction conditions, environmental factors and traffic [50]. Since strength or modulus loss can be attributed to the loss of cohesion/adhesion of the constituents of the asphalt mix, it is logical to assume that stripping is the consequence thereof. Parker and Gharaybeh conducted indirect tensile strength (ITS) test on asphalt mixtures with 6-8% air voids content as recommended

by Texas DOT [51] and concluded that stripping is dependent on the asphalt cement content and the type of mix (dense-graded or gag-graded) and not the stripping potential of the aggregate sources, types and blends. Furthermore, the NCHRP Report 673 [52] suggests the 70% to 80% tensile strength ratio (TSR) criteria to determine the susceptibility of an asphalt mix to stripping in order to predict stripping in the field. He discovered that stripping is not only a function of environmental conditioning, but also traffic intensity and ageing of the asphalt layer.

The indirect tensile strength evaluates the effects of saturation and accelerated water conditioning, along with freeze-thaw cycle, of compacted asphalt mixtures. 7 sets of 3 dry, along with 7 sets 3 conditioned, replicates were prepared and conditioned as appropriate from 7 binder types in accordance with AASHTO T 283-14 (the Lottman procedure). The dry specimen sets were tested immediately at 25°C and a loading rate of 50 mm/min. The maximum load was recorded, and the indirect tensile strength calculated according to equation 2-1.

The specimens for preconditioning were saturated, plastic wrapped and frozen at -18°C for approximately 16 hours, placed in the 60°C water bath, immediately removed the plastic wrap and thawed at 60°C for 24±1 hour. The specimens were then transferred to another water bath set to 25±0.5°C and conditioned for 2 hours ±10 minutes and tested afterwards (Figure 2-7). The tensile strengths were calculated using equation 2-1 and the TSRs were calculated using equation 2-2.



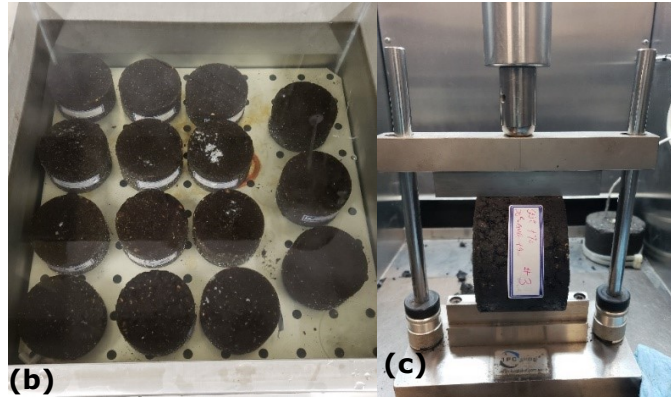


Figure 2-7: ITS test (a) Samples for freezing (b) 60°C for 34 hours and 25°C for 2 hours conditioning (c) Dry/conditioned specimen testing

$$S_t = \frac{2000P}{\pi tD} \quad (2-1)$$

where: S_t = tensile strength, kPa
 P = maximum load, N
 t = specimen thickness, mm
 D = specimen diameter, mm.

$$TSR = \frac{S_2}{S_1} \quad (2-2)$$

where: TSR = tensile strength ratio
 S_1 = average tensile strength of the dry subset, kPa; and
 S_2 = average tensile strength of the conditioned subset, kPa.

2.6.2 Fatigue Cracking Resistance

Indirect Tension Asphalt Cracking Test (IDEAL-CT)

In efforts to reduce rutting and initial investment cost during the turn of the twentieth century, the asphalt industry experimented various measures including the individual use, or combination thereof, of polymer modified binders, coarser aggregated gradations, lower asphalt contents, reclaimed asphalt pavement (RAP), recycled asphalt shingles (RAS), polyphosphoric acid and recycled engine oil. While the rutting problem was solved and resources apparently conserved, a new problem of premature cracking emerged [53].

Cracking of asphalt pavement has become a major problem faced by transportation agencies across North America. Though many cracking tests have been developed in the past, no single test is simple, practical, repeatable, efficient, cost less than ten thousand United States dollars, sensitive to asphalt mix composition [54]. The Indirect Tension Asphalt Cracking Test (IDEAL-CT) has been developed as the ideal cracking test to be used by contractors, departments of transportation and researchers for routine mix design and QA/QC.

Similar to the traditional indirect tensile strength test, the IDEAL-CT is run without instrumentation at 50 mm/min and at room temperature with field cores or laboratory Marshall (100 mm or 4 in diameter) or Superpave (150 mm or 6 in) samples with various thicknesses (38, 50, 62, 75 mm, etc.). Laboratory prepared specimens usually have 7 ± 0.5 percent air voids. Figure 2-8 shows the equipment setup and typical test results. The CT index is a quantity derived from the load-displacement curve and indicates the asphalt mix resistance to fatigue cracking (Figure 2-9 and equation 2-3); hence, the higher the CT index, the higher the fatigue resistance.

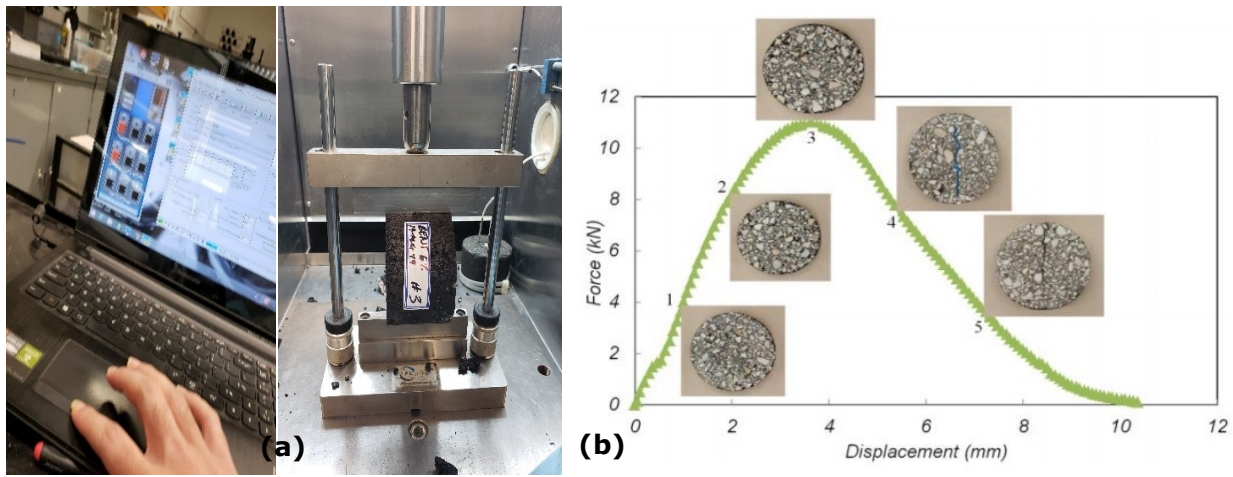


Figure 2-8: (a) Equipment setup (b) Load vs displacement curve
 Source: (Zhou, 2019)

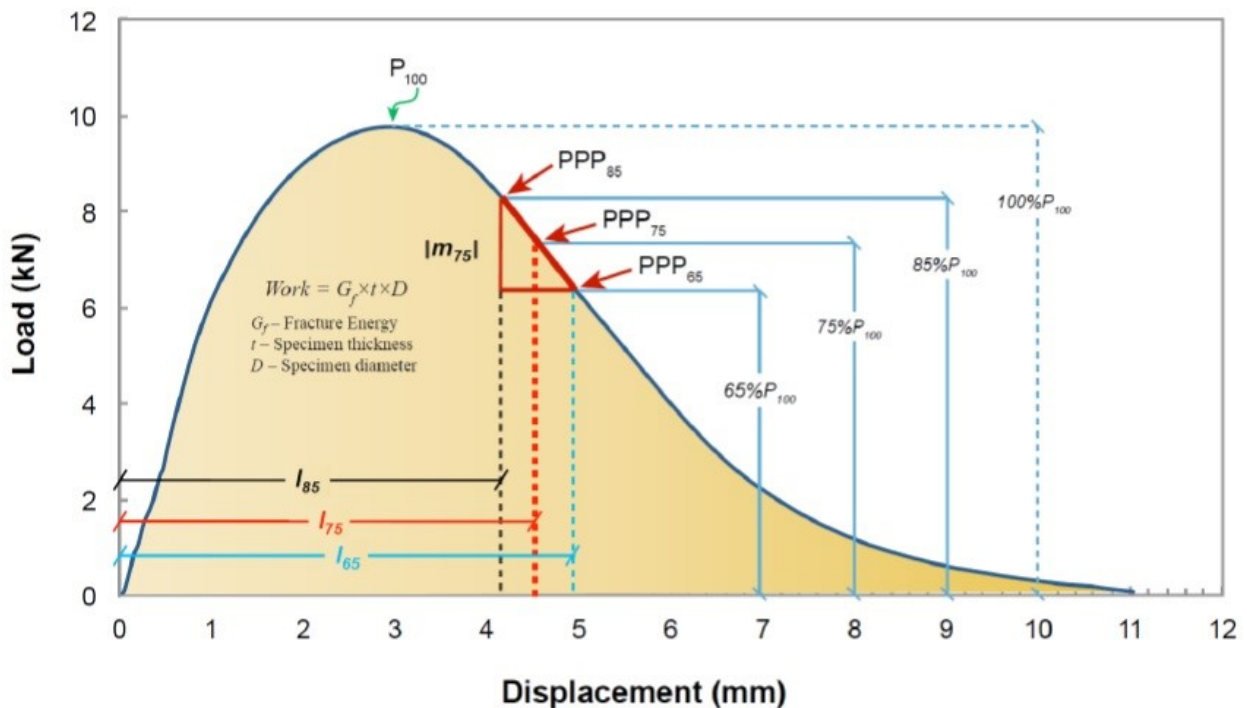


Figure 2-9: Model illustration for 75% post peak point (PPP₇₅) and modulus (m₇₅)
 Source: (Zhou, 2019)

$$CT_{Index} = \frac{t}{62} \times \frac{G_f}{P/l} \times \frac{l}{D} \quad (2-3)$$

where: t = thickness of specimen
 G_f = fracture energy
 l = vertical deformation
 $\frac{P}{l}$ = slope of the load-displacement curve (or modulus) at 75% peak load
 $\frac{l}{D}$ = strain tolerance at 75% peak load

The fatigue performance is a function of the ability of the asphalt mix to resist crack initiation and propagation. Therefore, the higher the modulus (P/l), the stiffer the mix, the faster the crack growth, the higher the load reduction resulting in a low cracking resistance. On the other hand, the larger the tolerable strain, the slower the crack growth and load reduction and, consequently, higher cracking resistance [55].

The IDEAL-CT is not only simple and practical, it can also be completed under a minute and the results are quite reproduceable with a coefficient of variation less than 20% with other established laboratory tests as well as field cracking performance. The CT index is influenced by binder type and content, presence and content of recycled materials, and age of the mix. The higher the CT index the higher the binder's resistance to fatigue cracking [55].

2.6.3 Thermal Cracking Resistance

Indirect Tensile Creep and Strength Test

The indirect Tensile strength and creep (IDT) test is applicable to asphalt concrete since its ultimate compressive strength is greater than three times its ultimate tensile strength at low temperatures [56], and these tests have become the most promising method for predicting the low-temperature performance of asphalt concrete mixtures [57] [58]. Considering an air void content between 4%-8%, as recommended by Richardson *et al* [59], a total of 9 specimens (i.e. 3 replicates for each of the test temperatures of -20°C, -10°C and 0°C) were prepared at a minimum air void content of 6% for each of the binder types (PG 58-31, 3% bentonite, 6% bentonite, 3% halloysite, 6% halloysite, 0.5% CNC and 1% CNC). Having cut the faces of the specimens in accordance with AASHTO T322-07, the samples were conditioned in the environmental chamber of the IPC Global Universal Testing Machine (UTM-100) [60]. Linear variable differential transducers (LVDTs) mounted on brass gauge points with a gauge length of 25 mm on each face of the specimens measured horizontal and vertical strain deformations when loaded with a target creep load of 1 kN for 100 seconds. The

strength test was conducted at a loading rate of 12.5 mm/min. The creep compliance [D(t)], tensile strength and fracture energy were calculated for each asphalt mix as explained below.

Creep Compliance

Creep compliance was calculated as a function of horizontal and vertical deformation, gauge length over which the deformation is measured, dimensions of the test specimen, and magnitude of the static load. It is given by the formula:

$$D(t) = \frac{\Delta X_{tm,t} \times D_{avg} \times b_{avg}}{P_{avg} \times GL} \times C_{cmpl} \quad (2-4)$$

where:

D(t) = creep compliance at time t (kPa)⁻¹

GL = gauge length (m)

D_{avg} = average diameter of all specimens (m)

b_{avg} = average thickness of all specimens (m)

P_{avg} = average creep load (kN)

X_{tm,t} = trimmed mean of the normalized, horizontal deformations of all specimen faces at time t (m)

The parameter C_{cmpl} is a correction factor and is given by

$$C_{cmpl} = \text{correction factor} = 0.6354 \times \left(\frac{x}{y}\right)^{-1} - 0.332 \quad (2-5)$$

where:

$\frac{x}{y}$ = absolute value of the ratio of the normalized, trimmed mean of horizontal deformation to the normalized, trimmed mean of vertical deformation at a time corresponding to half the total creep test time (typically 50 seconds) for all specimen faces.

Tensile Strength

Based on the recommendation of the NCHRP Report 530, the tensile strength, S_{t,n}, was calculated as a function of the maximum load and then corrected to its true tensile strength [58]. The tensile strength is given by the formula below:

$$S_{t,n} = \frac{2 \times P_{f,n}}{\pi \times b_n \times D_n} \quad (2-6)$$

Tensile strength = (0.78 × S_{t,n}) + 38 (for psi)

Tensile strength = (0.78 × S_{t,n}) + 0.262 (for MPa)

where:

S_{t,n} = "uncorrected" tensile strength of specimen, (MPa)

P_{f,n} = maximum load observed for specimen, (MN)

b_n = thickness of specimen, (m)

D_n = diameter of specimen, (m)

Fracture Energy

In accordance with the principles of fracture mechanics, an object's resistance to crack growth, or toughness, is dependent on the energy absorbed as the crack advances. This energy, called the fracture energy, is associated with plastic flow and concentrated at the crack tip, a plastic zone where the material's yield stress is present [61]. The fracture energy provides an indication of the propagation of cracks within asphalt pavement at low service temperatures. In this study, it was determined by calculating the area under the curve of the IDT strength test using the trapezoidal method and dividing by the crack cross-section (ASTM D8225-19).

3 Application of Nanoclay Materials in Asphalt Pavements

3.1 Abstract

Heavy vehicle loads and seasonal temperature changes can influence the rheological and mechanical properties of asphalt mixtures in flexible pavements. Pavements designed and constructed for heavy-duty traffic under extreme weather conditions generally require engineered asphalt cement modification. Depending on the required type of improvement, proper modifier(s) should be introduced to improve the properties of the asphalt cement. Recently, nanomaterials with sizes of 1 to 100 nm have been introduced as potential asphalt modifiers. These particles, with their high surface area to volume ratio, possess unique bulk, surface, and colloidal properties. Based on previous studies, the addition of nanoclay, nanocarbon, and nanosilica can improve the rheological properties of asphalt cement and, consequently, also affect its mechanical properties, such as tensile strain, flexural strength, and elasticity.

Previous studies suggest that nano-clays, although not widely used as asphalt additives, has the potential to enhance the low-temperature properties and performance of asphalt cement. This research focused on the modification of the rheological properties of asphalt cement using two different nanoclays. The mechanical performance of hot mix asphalt (HMA) containing nanoclay-modified binders at different temperatures was also compared with that of unmodified asphalt mixes.

3.2 Introduction and Background

Low-temperature cracking (or thermal cracking) in hot mix asphalt (HMA) is a critical issue for many transportation agencies across North America. To address this type of cracking, the Strategic Highway Research Program (SHRP) in the US developed the Superpave mix design method, which provides the criteria for selection of the appropriate performance grade (PG) asphalt binder [58]. To avoid thermal cracking in cold regions such as Canada, there is a tendency to use softer binders with lower PG for HMA layers; however, flexible pavements can also undergo severe rutting failure during the summer [11].

In flexible pavements, both heavy vehicle loads and variation in seasonal temperatures can sway the temperature susceptibility characteristics (rheology) of asphalt binders. Consequently, the mechanical properties and long-term performance of asphalt mixtures will be affected [14]. Pavements designed and constructed for heavy-duty traffic under extreme weather conditions generally require engineered asphalt cement modification. Depending on the characteristics required, proper modifier(s) should be introduced to improve such

properties [62]. Recently, nanomaterials with at least one dimension between 1-100 nm have been introduced as potential asphalt modifiers. These particles, with their high surface area to volume ratio, possess unique bulk, surface, and colloidal properties. Based on previous studies, the addition of nanoclay, nanocarbon, or nanosilica can improve the rheological properties of asphalt cement and, consequently, its mechanical properties, such as tensile strain, flexural strength and elasticity [63]. This research focused on the rheological properties of asphalt cement modified using two different nanoclays, bentonite and halloysite.

Since the early 1970s, synthetic polymers [with the most common being the elastomer, styrene butadiene styrene (SBS)] have been employed to modify the performance of bituminous binders, resulting in decreased temperature susceptibility, increased cohesion and modified rheological characteristics [64]. However, current trends in the industry have involved investigating the application of nanotechnology for modification of HMA pavements. Though limited studies of nanotechnology application in HMA pavements have been conducted, a preliminary cost analysis revealed that nano-modification of asphalt binder is 22 – 33% cheaper than its polymer-modified equivalent [65].

3.3 Nanotechnology

Nano (1 billionth) is derived from a Greek word which means dwarf, is approximately 1/80000 the diameter of the human hair [66] and is used to refer to dimensions in the range of 0.1 to 100 nm. Due to their high surface area to volume ratio and small dimensions, nanomaterials have been observed to significantly alter properties at the macro level, since quantum effects come into play. As a leading technology the world over, nanotechnology provides an opportunity to create new structures with enhanced functional properties which are more cost-effective and efficient in almost all areas of technology [11].

3.4 Objectives and Scope

The objective of this paper is to investigate and compare the effects of nanoclays on asphalt rheology and HMA performance. For this purpose, asphalt samples were mixed using one of two different nanoclays – hydrophilic bentonite nanoclay and halloysite nanotubes – using a high shear mixer. Scanning electron microscopy (SEM) was used to investigate the dispersion of the nanoclay in the base asphalt after mixing. Frequency sweeps were performed between 4°C and 40°C and master curves were plotted at 20°C to evaluate complex modulus (G^*) and phase angle (δ) of the modified and non-modified asphalt samples using a dynamic shear rheometer (DSR). Viscosity measurements were taken to verify and determine the mixing and compaction temperatures of the control and nanoclay-modified asphalt mix specimens,

respectively. Hamburg wheel tracker tests were conducted on hot-mix asphalt samples prepared from the normal asphalt binder, as well as the nanoclay-modified asphalt binder, to evaluate and compare the resistance of the samples to rutting and susceptibility to moisture. Indirect tensile (IDT) tests were also performed to evaluate the cracking potential of asphalt mixes at low temperatures.

3.5 Materials

3.5.1 Asphalt

The asphalt binder used in this study was PG 58-31 (provided by Husky Energy), meaning it met performance criteria for a 7-day average maximum pavement temperature of 58°C and at a minimum pavement temperature of -31°C [16].

3.5.2 Halloysite Nanoclay

For this research, halloysite nanoclay (kaolin) with a formula of $H_4Al_2O_9Si_2 \cdot 2H_2O$, with a molecular weight of 294.19 g/mol, and density of 2.53 g/cm³, in the form of a nanopowder was used. It has a tube-like morphology, with diameters ranging between 30-70 nm and lengths of 1-3 μm. It appears as a white to tan powder, has a pore volume of 1.26 – 1.34 mL/g, specific gravity of 2.53, and surface area of 64 m²/g [67]. Although it exhibits low electrical and thermal conductivity, it possesses strong hydrogen interactions due to its inner hydroxyl groups. The application of halloysite nanoclay as a reinforcement in nanocomposites has yielded improvements in thermal and mechanical properties, likely due to its characteristic tube-like morphology and high aspect ratio [68].

3.5.3 Nanoclay, Hydrophilic Bentonite

Bentonite is an absorbent aluminum phyllosilicate clay, which consists mainly of montmorillonite, a subclass of smectite. It is composed of two tetrahedral silicon oxide layers sandwiching an octahedral aluminum oxide layer, with a chemical formula of $H_2Al_2O_6Si$ and a molecular weight of 180.1 g/mol. It exists in powder form with a particle size less than or equal to 25μm [69]. Although clay platelets have negatively charged surfaces, the replacement of aluminum atoms in the octahedral layer with other cations (sitting on top of the tetrahedral silicon layer) tends to balance the charge in the octahedral layer, which creates a charging defect. The ability of bentonite to readily trade these surface cations in exchange for hydratable, as well as organic, cations makes the normally hydrophilic montmorillonite hydrophobic (or generates organically treated clays); consequently, making it dispersible in polymer matrices [30].

3.5.4 Preparing the modified asphalt sample

Modified asphalt samples were prepared by adding the nanoclays to the base asphalt binder (PG 58-31) in the proportions shown in Table 3-1. To prepare the modified binder sample, 500 g of PG 58-31 asphalt binder was poured in a cylindrical tin container and heated to a temperature around 140°C on a hot plate to maintain this temperature while a high shear mixer was used (Figure 3-1). Using this arrangement of mixer and hot plate, the nanomaterial was added to the asphalt binder and mixed at a shear rate of 5500 – 6000 rpm for 4.5 hours.

TABLE 3-1: Amount of nanomaterial added to base asphalt binder (% by weight)

Nanomaterial	Amount added to base asphalt binder (% by weight)
Halloysite Nanoclay	3 and 6
Nanoclay, Hydrophilic Bentonite	3 and 6



Figure 3-1: High shear mixer with a hot plate beneath: setup for preparing binders modified with nanoclay.

3.5.5 Qualitative Evaluation of Modified Asphalt Binder Samples

A Zeiss Sigma Field Emission Scanning Electron Microscope (FESEM) was used to evaluate the dispersion of nanoclay in the asphalt binder qualitatively. Asphalt samples were first sputter-coated with gold using Denton Vacuum gold coating equipment to improve their conductivity. This coating increases the number of secondary electrons that can be detected from the surface of the specimen in the SEM. For SEM, the sputtered films typically have a thickness range of 2 to 20 nm [70]. Figure 3-2 shows the SEM equipment (3-2(a)) and also an example of the dispersion of the nanoclay in the binder. As Figure 3-2(b) shows, the

dispersion of nanoclay samples in the binder seems to be consistent after 4.5 hours of mixing at a rate of 5500-6000 rpm.

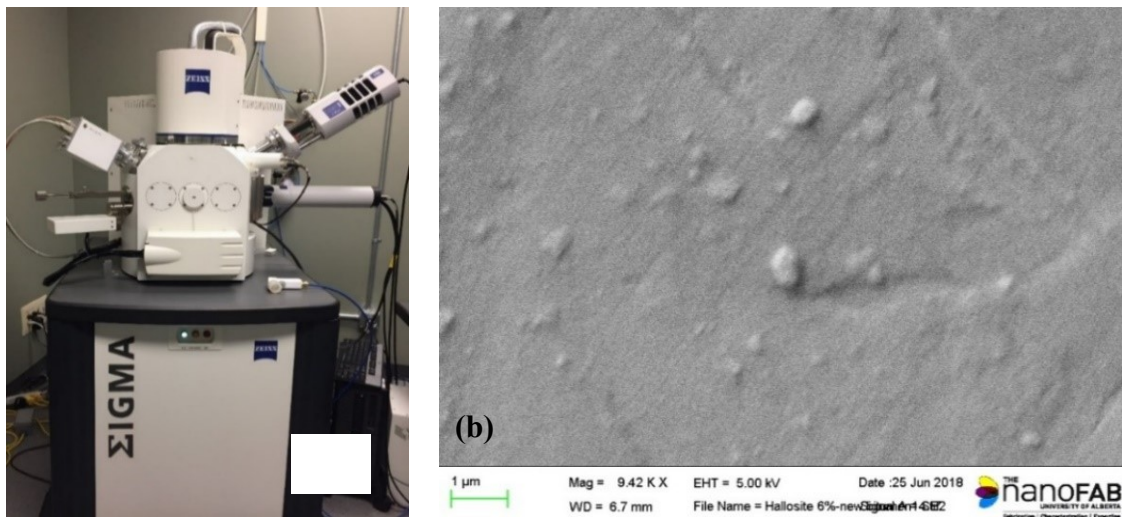


Figure 3-2: (a) SEM equipment and (b) Image of modified binder using 6% by weight halloysite clay

3.6 Rheology tests on the modified asphalt binder samples

To investigate the performance of modified binders at different temperatures and loading frequencies, rheological tests were performed. About 20 to 30 g of the prepared sample was heated in an oven in a small aluminum tray at 140°C. When the sample was sufficiently fluid, it was poured into an 8-mm diameter silicone mold (Figure 3-3(a)). Rheological measurements were carried out using a Smartpave 102 Dynamic Shear Rheometer (DSR) from Anton Paar (Figure 3-3(b)). Using an 8-mm diameter parallel plate, a gap of 2 mm and an angular frequency range of 0.3 to 300 rad/s, frequency sweep tests were performed on the samples through loop temperatures of 40°C, 30°C, 20°C, 10°C and 4°C. The parameters calculated were the complex modulus (G^*), phase angle (δ) and rutting parameter ($G^*/\sin(\delta)$).

A minimum of four tests were conducted for each of the modified samples, as well as the base asphalt binder. The average of the results for each sample was used to determine the effect of modification on the asphalt binder. Data measurements were then taken for the target temperature of 20°C and a broader frequency range using the time-temperature superposition principle and the Williams-Landel-Ferry (WLF) equation. This was performed using Rheoplus software (Anton Paar).

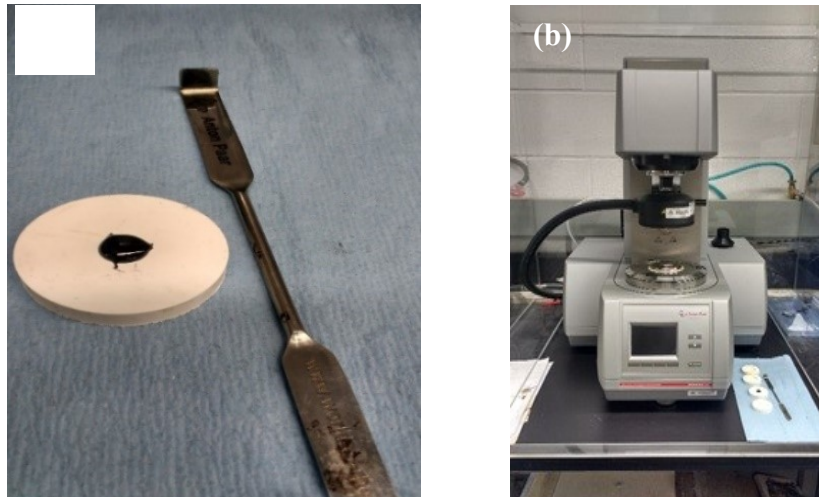


Figure 3-3: DSR test (a) sample, (b) testing equipment

The base asphalt PG 58-31 was modified with halloysite nanoclay in two different proportions (3% and 6% by weight). Complex modulus (G^*) versus angular frequency curves, as well as phase angle (δ) versus angular frequency curves, at the target temperature of 20°C were analysed for the base asphalt specimens, as well as those of the modified asphalt, and their values were compared. An increase in the value of complex modulus leads to improvement in the rutting parameter ($G^*/\sin(\delta)$). $G^*/\sin(\delta)$ is a quantity to determine the susceptibility of HMA (prepared with a specified performance grade asphalt binder) to rutting (Table 3-2) [16].

TABLE 3-2: Performance Graded Asphalt Binder DSR specifications (as summarized from Superpave Fundamentals (Federal Highway Authority/National Highway Institute, 2000))

Material	Quantity	Specification	HMA Distress of Concern
Unaged binder	$G^*/\sin(\delta)$	≥ 1.0 kPa (0.145 psi)	Rutting
RTFO residue	$G^*/\sin(\delta)$	≥ 2.2 kPa (0.319 psi)	Rutting
PAV Residue	$G^* \cdot \sin(\delta)$	$\geq 5,000$ kPa (725 psi)	Fatigue Cracking

3.6.1 Samples Modified with Halloysite Nanoclay

Figure 3-4(a) shows that asphalt samples modified using halloysite showed an improvement in the complex modulus (increase) at low frequencies, with little or no change at high frequencies. There was a greater increase in the G^* value for the binder containing 6% by weight halloysite than for the binder containing 3% halloysite. Rutting parameter ($G^*/\sin(\delta)$) versus angular frequency was also plotted, and the results compared (Figure 3-4(b)). As there

was not a significant reduction in phase angle due to halloysite modification, there was an improvement in the rutting parameter similar to G^* (Figure 3-5).

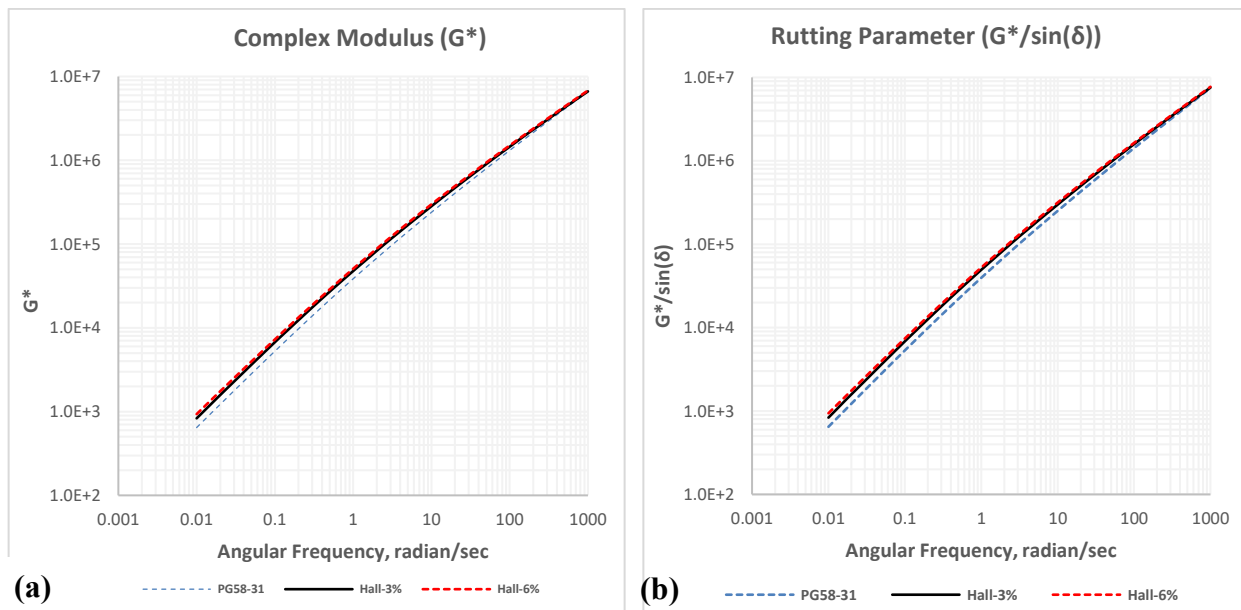


Figure 3-4: Halloysite modified binder at 20°C – (a) Complex Modulus and (b) Rutting Parameter

3.6.2 Samples Modified with Bentonite Nanoclay

Like halloysite nanoclay, the asphalt samples modified using bentonite nanoclay showed an improvement (increase) in the complex modulus at low frequencies with little or no change at high frequencies (Figure 3-5(a)). Using 6% of the bentonite nanoclay by weight in the binder increased the G^* value compared to the mixture containing 3% by weight. The rutting parameter ($G^*/\sin(\delta)$) was also plotted with against angular frequency and the results were compared for the different mixtures (3%, 6% and control) (Figure 3-5(b)). As Figure 3-5(b) shows, the addition of more halloysite nanoclay led to a higher rutting resistance.

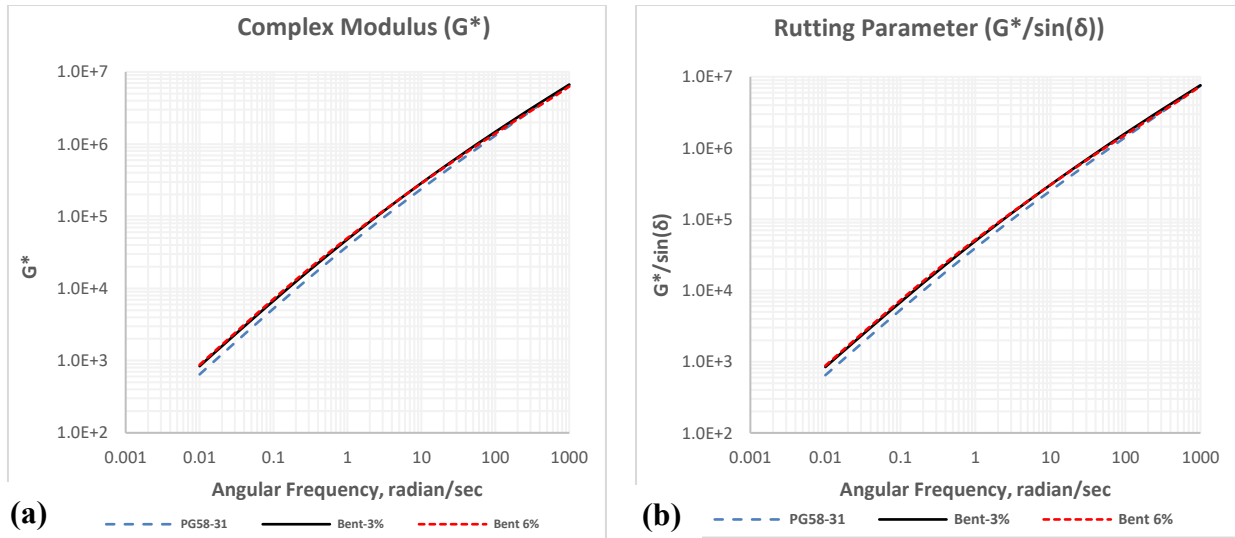


Figure 3-5: Bentonite modified binder at 20°C – (a)Complex Modulus and (b) Rutting Parameter

3.7 Performance Tests

3.7.1 HMA Mix Design

The HMA mix design used for this research was based on the Superpave mix design procedure for a 10 mm – High Traffic (HT) asphalt layer. The grain size distribution and asphalt mix properties of the aggregates summarized in Tables 3-3 and 3-4 below were provided by Lafarge, Canada in consonance with Table 3.53.2.2A of the Standard Specification for Highway Construction [71]. The same mix design was used for preparing all modified and unmodified asphalt samples. Figure 3-6 shows the aggregate gradation curve with respect to the upper and lower limits.

Table 3-3: Asphalt mix properties

Properties	Actual	Specifications
Number of gyrations	100	100
A.C. % of Total Mix	5.5	-
Gmm (kg/m ³)	2431	-
Gmb (kg/m ³)	2337	-
Air voids (%)	3.9	3.6 – 4.4
VMA (%)	14.9	13 min
VFA (%)	73.8	70 – 80
% Gmm @ Nmax	96.8	98.0 max
Dust/AC	1.0	-

Table 3-4: Aggregate grain size distribution

Sieve Size (mm)	% Passing
12.5	100
10	98.3
8	88.5
6.3	75.4
5	64.8
2.5	49.0
1.25	39.5
0.63	32.7
0.315	20.2
0.16	10.3
0.08	5.1

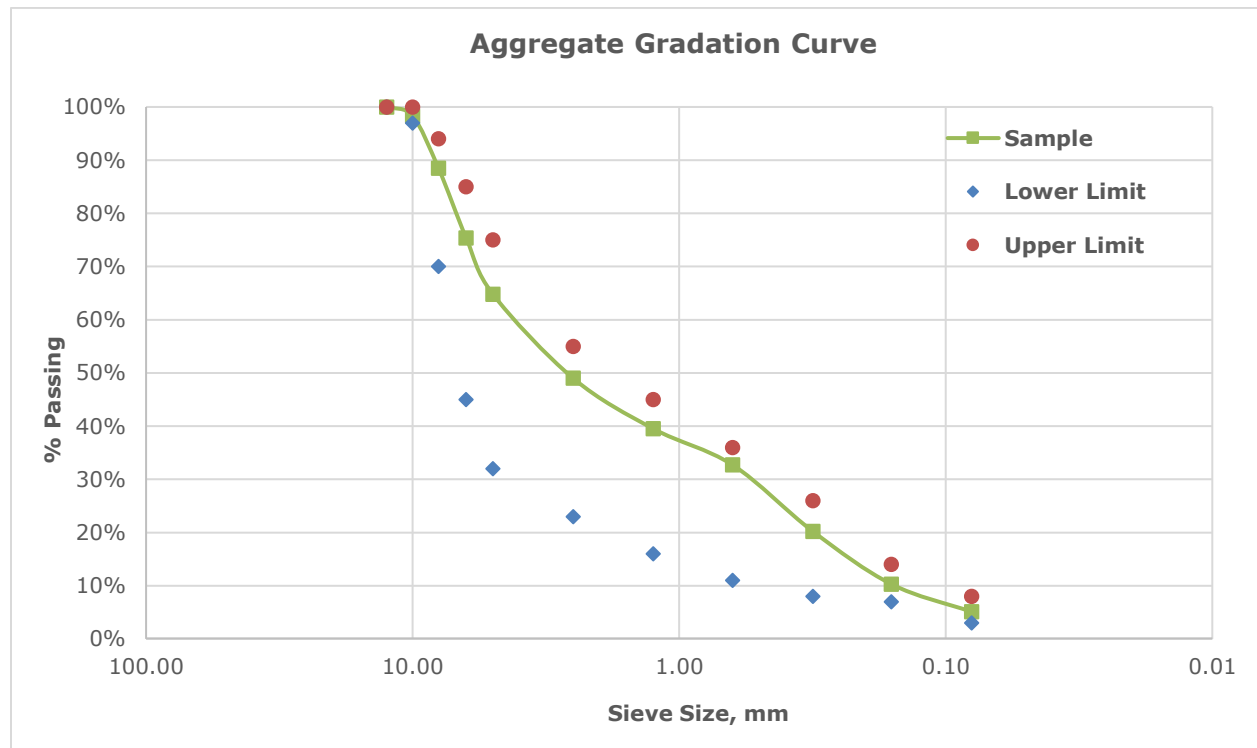


Figure 3-6: Aggregate Gradation Curve

3.7.2 Mixing and Compaction Temperatures

To select the appropriate mixing and compaction temperatures for each modified and unmodified asphalt sample, a Fungilab EVO Expert Rotational Viscometer (RV) was used. In

this measurement, the torque required to maintain a cylindrical spindle submerged in an asphalt binder sample at a constant rotational speed of 20 revolutions per minute (RPM) at constant temperature is determined. This torque is converted to viscosity and displayed automatically by the equipment.

Figure 3-7 shows the viscosity curves for the neat asphalt binder, along with the four nanomodified binders. Based on these results, the mixing and compaction temperatures used for sample preparation were:

- PG 58-31 (Mixing = 145°C; Compaction = 135°C)
- 3% Halloysite-modified PG 58-31 (Mixing = 150°C; Compaction = 140°C)
- 6% Halloysite-modified PG 58-31 (Mixing = 155°C; Compaction = 144°C)
- 3% Bentonite-modified PG 58-31 (Mixing = 150°C; Compaction = 140°C)
- 6% Bentonite-modified PG 58-31 (Mixing = 155°C; Compaction = 144°C)

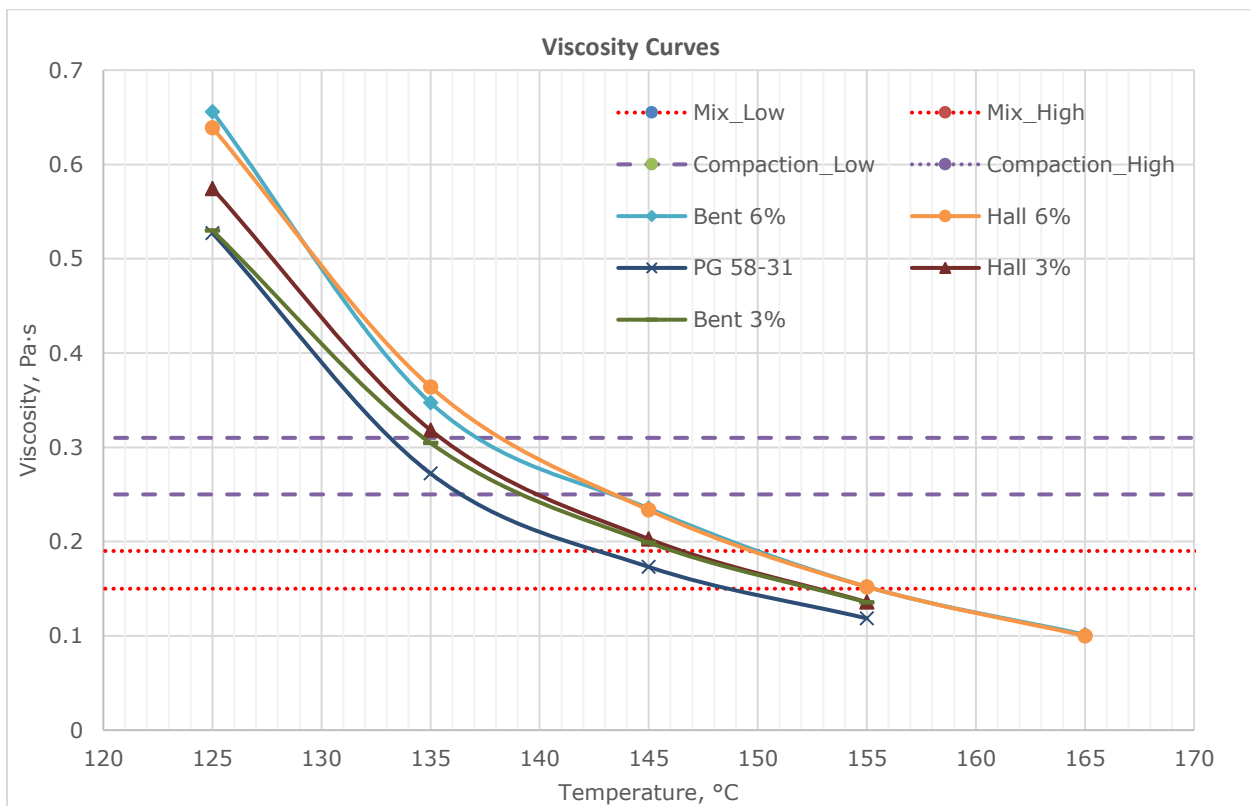


Figure 3-7: Viscosity-temperature curves for modified and unmodified binders

3.7.3 Rutting Test

A Hamburg Wheel Tracker (HWT) was used to evaluate the rutting potential of the HMA samples. Based on AASHTO T324-16, this device tracks a 705±4.5N, 47mm-wide steel wheel

(at a frequency of 52 ± 2 passes per minute and a maximum speed of 0.305m/s at midpoint) cyclically across a submerged HMA sample (cylindrical or slab), compacted to $7.0 \pm 0.5\%$ or $7.0 \pm 1.0\%$ using a Superpave gyratory compactor or linear kneading compactor, respectively. This is continued for 20,000 passes or until a rut depth of 12mm is achieved, whichever is first, for a predefined temperature. A graph of rut depth vs. number of passes can provide valuable information about the rutting potential of asphalt concrete mixes, as well as their susceptibility to moisture damage [72].

3.7.3.1 Sample Preparation

Using the same mix design and the mixing and compaction temperatures listed above, five sets of asphalt mixes, including unmodified binder, binder modified using 3% and 6% (by weight) bentonite nanoclay and binder modified using 3% and 6% of halloysite nanoclay, with air voids of 6-8% were prepared. The cooled samples were saw-cut along a secant line, such that when joined together in the high-density polyethylene molds, a gap of no greater than 7.5 mm was achieved between the molds (Figure 3-8).



Figure 3-8: HWT D Cylindrical specimens (saw-cut) in HDPE molds before (left) and after (right) test

A total of five (5) types of samples were prepared and tested, and the results are tabulated below (Table 3-5). It was observed that neat asphalt (PG 58-31) showed a rut depth of 11.6 mm at 20,000 passes. Results from the halloysite- and bentonite-modified asphalt concrete specimens resulted in significant reductions of rut depth after 20,000 passes – approximately 30% reduction in rut depth for the 3% bentonite and halloysite and approximately 80% reduction in rut depth for the 6% bentonite and halloysite. Comparison of the two nanoclays,

bentonite and halloysite, show a similar effect in terms of rutting resistance on the asphalt binder.

A comparison of the increase in the number of passes at the stripping inflection points for the nanoclay-modified samples and the neat binder samples shows that the addition of 3% halloysite and bentonite increased the number of passes by 80% and 55%, respectively; while the addition of 6% halloysite and bentonite increased the number of passes by 96% and 92%, respectively. These results indicate a significant improvement in the resistance of modified mixes to moisture damage with the addition of nanoclay to the binder.

TABLE 3-5: HWTD Results (Mechanical Properties)

S/No	Sample ID	Description	Test Temperature (°C)	Post Compaction Consolidation (mm)	Stripping Inflection Point (# of Passes/mm)	Rut Depth (mm)
1	A & B	PG 58-31	45	1.74	9179 / 3.86	11.60
2	A & B	PG 58-31 + Hall 3%	45	1.32	16529 / 4.69	7.83
3	A & B	PG 58-31 + Hall 6%	45	0.67	18022 / 2.12	2.29
4	A & B	PG 58-31 + Bent 3%	45	1.43	14260 / 3.95	7.84
5	A & B	PG 58-31 + Bent 6%	45	0.89	17693 / 2.97	3.21

3.7.4 Indirect Tensile (IDT) Creep and Strength Test

The indirect tensile creep and strength tests were developed to evaluate the resistance of hot mix asphalt (HMA) to thermal cracking, and these tests have become the most promising method for predicting the low-temperature performance of asphalt concrete mixtures [57], [73]. Creep compliance is defined as the rate at which the strain increases for a constant application of stress, that is, the time-dependent strain per unit stress, while indirect tensile strength gives the strength of HMA when subjected to tension.

To compare the low-temperature properties of samples modified with nanoclay, specimens were prepared for each of the modified and unmodified binder types. All specimens were conditioned and tested using an IPC Global Universal Testing Machine (UTM-100) in

accordance with AASHTO T322-07. Specimen deformations were measured using horizontal and vertical linear variable differential transducers (LVDTs) mounted on brass gauge points with a gauge length of 25 mm on each face of the specimen. Each specimen was loaded to a target creep load of 1 kN for 100 seconds, after which the strength test was conducted at a loading rate of 12.5 mm/min. The creep compliance [D(t)], tensile strength and fracture energy were calculated for each asphalt mix as explained below.

Creep Compliance

Creep compliance was calculated as a function of horizontal and vertical deformation, gauge length over which the deformation is measured, dimensions of the test specimen, and magnitude of the static load, and is tabulated (Table 3-6) below. It is given by the formula:

$$D(t) = \frac{\Delta X_{tm,t} \times D_{avg} \times b_{avg}}{P_{avg} \times GL} \times C_{cmpl} \quad (3-1)$$

where: D(t) = creep compliance at time t (kPa)⁻¹

GL = gauge length (m)

D_{avg} = average diameter of all specimens (m)

b_{avg} = average thickness of all specimens (m)

P_{avg} = average creep load (kN)

X_{tm,t} = trimmed mean of the normalized, horizontal deformations of all specimen faces at time t (m)

The parameter C_{cmpl} is a correction factor and is given by

$$C_{cmpl} = \text{correction factor} = 0.6354 \times \left(\frac{x}{y}\right)^{-1} - 0.332 \quad (3-2)$$

where: $\frac{x}{y}$ = absolute value of the ratio of the normalized, trimmed mean of horizontal deformation to the normalized, trimmed mean of vertical deformation at a time corresponding to half the total creep test time (typically 50 seconds) for all specimen faces.

Tensile Strength

Based on the recommendation of the NCHRP Report 530, the tensile strength, S_{t,n}, was calculated as a function of the maximum load and then "corrected" to its "true" tensile strength [58]. The tensile strength is given by equation 3-3 below, and tabulated in (Table 3-6) below:

$$S_{t,n} = \frac{2 \times P_{f,n}}{\pi \times b_n \times D_n} \quad (3-3)$$

$$\text{Tensile strength} = (0.78 \times S_{t,n}) + 38 \quad (\text{for psi})$$

$$\text{Tensile strength} = (0.78 \times S_{t,n}) + 0.262 \quad (\text{for MPa})$$

where: $S_{t,n}$ = "uncorrected" tensile strength of specimen, (MPa)

$P_{f,n}$ = maximum load observed for specimen, (MN)

b_n = thickness of specimen, (m)

D_n = diameter of specimen, (m)

Fracture Energy

An object's resistance to crack growth, or toughness, is dependent on the energy absorbed as the crack advances. This energy, called the fracture energy, is associated with plastic flow and concentrated at the crack tip, a plastic zone where the material's yield stress is present [61]. The fracture energy provides an indication of the propagation of cracks within asphalt pavement at low service temperatures. In this study, it was determined by calculating the area under the curve of the IDT tensile strength test using the trapezoidal method and dividing by the crack cross-section (ASTM D8225-19).

Table 3-6 summarizes the results of the IDT test for neat asphalt binder (PG 58-31) and the four nanoclay-modified samples (3% and 6% halloysite by weight and 3% and 6% bentonite by weight). Based on the results shown in the table, 6% bentonite and halloysite added to the base binder slightly reduced the tensile strength of the mix by approximately 1% and 3%, respectively, but increased the fracture energy by 20% and 2%, respectively. The table also shows that there is no significant effect on the creep compliance for 3% nanoclay in the base binder; however, the addition of 6% nanoclay causes a 12% to 69% reduction in the creep compliance when compared to the control mix.

TABLE 3-6: Summary of IDT Test Results

Parameters	PG 58-31	3% Bentonite-modified	6% Bentonite-modified	3% Halloysite-modified	6% Halloysite-modified
Creep compliance [D(t)], 1/GPa (-20°C)	0.0032	0.0032	0.0010	0.0035	0.0028
Poisson Ratio (-20°C)	0.054	0.167	0.239	0.070	0.210
Tensile strength ($S_{t,n}$), MPa (-10°C)	3.72	3.73	3.67	4.15	3.62
Fracture Energy, kJ/m ² (-10°C)	4.057	4.994	4.873	4.574	4.166

3.8 Conclusions and Future Steps

- Dynamic Shear Rheometer (DSR) results show that the modification of PG 58-31 with nanomaterials (hydrophilic bentonite nanoclay and halloysite nanoclay) results in an increase in the complex modulus (or stiffness) of the matrix, as well as an increase in the binder's resistance to rutting. The increase in stiffness is proportional to the concentration of the nanoclay.
- Rotational viscometer (RV) measurements confirmed this increase in stiffness and showed that the addition of nanoclay increased the viscosity of the modified binder and, consequently, the mixing and compaction temperatures.
- Permanent deformation test results using a Hamburg Wheel Tracker showed that the addition of either nanoclay significantly improved both the rutting resistance and moisture sensitivity of the modified mixes.
- HMA produced with a 3% nanoclay-modified binder provides a significant improvement in performance at low service temperatures. Moreover, although the 6%-nanoclay modification resulted in a slight reduction of the tensile strength of the mix, once a crack was initiated, its propagation seemed to be slower than that for HMA produced with the neat binder.
- The rheology of the asphalt binder and its nanoclay-modified equivalents provides a useful indication of the expected performance of the HMA produced at high, intermediate and low temperatures

4 Application of Nanosized Materials in Asphalt Pavements

4.1 Abstract

Researchers and engineers have explored the potential of enhancing asphalt cement properties using nanomaterials for many years, however, to date these materials have not been widely used for asphalt mix modification. Previous studies suggest that nanoclay has the potential to enhance the high-temperature properties and performance of asphalt cement. Nanocellulose is another material of interest for asphalt cement modification and, in recent years, it has been successfully applied to increase the fracture energy of concrete material. Literature shows that a small amount of nanocellulose in asphalt cement (1 percent by weight of asphalt cement) can increase shear modulus at high temperatures, increase asphalt cement toughness at low temperatures, and decrease thermal susceptibility.

This research focuses on the rheological properties of asphalt cement modified using nanoclay and nanocellulose at various temperatures. Microscopic research techniques were used to investigate appropriate dispersion of nanomaterials in the asphalt cement. The mechanical performance of asphalt mixes containing nanoclay and nanocellulose, including permanent deformation at high temperature, indirect tensile strength, and creep compliances at low temperature, was evaluated and compared with unmodified asphalt mixes.

4.2 Introduction

Hot Mix Asphalt (HMA) is a complex material with two basic constituents: aggregates and asphalt binder. In addition to being workable during construction and providing a good, skid resistant surface during service, it must resist the five major distresses in HMA flexible pavements [74]:

- plastic deformation at high service temperatures (asphalt-related);
- fatigue cracking at intermediate service temperatures (asphalt-related);
- thermal cracking at low service temperatures (asphalt-related);
- premature aging (environmental conditioning); and
- moisture damage (environmental conditioning and aggregate-related).

It is evident from the literature that the performance of HMA is significantly dependent on the appropriate selection of asphalt binder. Conventional paving-grade asphalts possess, to a satisfactory extent, the mechanical properties for most of the traffic and environmental conditions encountered in North America. However, the advent of climate change, an increase in axle loads and the ongoing demand for cost savings have pushed their performance to the

limit [75], thereby causing premature failure, higher vehicle operating costs and higher life-cycle costs. Hence, pavements designed and constructed for heavy-duty traffic under extreme weather conditions generally require engineered asphalt cement modification. Depending on the required types of improvement, proper modifier(s) should be introduced to improve properties [62].

In recent years, nanomaterials with small sizes of 1-100 nm have been introduced as potential asphalt modifiers. With their high surface area, these particles reveal unique bulk, surface, and colloidal properties. Recent studies suggest that the addition of nanoclay, nanocarbon, and nanosilica can improve the rheological properties of the asphalt binder and consequently, mechanical properties such as tensile strain, flexural strength and elasticity [63].

Synthetic polymers have been employed extensively since the early 1970s to modify the performance of bituminous binders, resulting in decreased temperature susceptibility, increased cohesion, and modified rheological characteristics [64]. However, current trends in the industry have investigated the application of nanotechnology in the modification of asphalt pavements. Though limited studies of nanotechnology application in asphalt pavements have been conducted, a preliminary cost analysis revealed that nanomodification of asphalt binder is 22 to 33 percent cheaper than its polymer-modified equivalent [13].

4.2.1 Nanotechnology

Nanotechnology is the study and application of ultra-small, functional structures with at least one dimension not greater than 100 nm [76]. Nano (1 billionth), derived from a Greek word which means dwarf, is approximately 1/80,000 the diameter of the human hair [66]. Nanotechnology works with materials sized in the range of 0.1-100 nm. Studies show that its principles apply to the modification of material properties at the atomic level, thereby remarkably altering macro-properties and bringing the quantum effect into play. This effect is seen due to the high surface area to volume ratio and small dimensions. As one of the leading technologies the world over, nanotechnology provides an opportunity to create new structures with enhanced functional properties which are more cost-effective and more efficient in almost all areas of technology. Nanotechnology also appears to be promising in the design, construction and infrastructure of road pavements [11].

4.3 Objectives and Scope

The objective of this paper is to investigate and compare the effects of the application of nanoclays and nanocellulose crystals on asphalt rheology and asphalt mix performance. For this purpose, asphalt samples were mixed with hydrophilic bentonite nanoclay, halloysite

nanotubes and cellulose nanocrystals using a high shear mixer. Scanning Electron Microscopy (SEM) was used to investigate the dispersion of nanomaterial in the base asphalt after mixing. Dynamic Mechanical Analyses (DMA) were performed on the modified/unmodified asphalt binder using the Dynamic Shear Rheometer (DSR) and the outputs evaluated at target temperatures and reduced frequencies. Viscosity measurements were taken to verify the mixing and compaction temperatures of the nanomodified asphalt mix specimens. Hamburg wheel tracker tests were conducted on the HMA samples prepared from the normal asphalt binder, as well as the nanomodified asphalt binders, to evaluate and compare the resistance to rutting and susceptibility to moisture. An Indirect Tensile test (IDT) test was also performed to evaluate the cracking potential of asphalt mixes at low service temperatures.

4.4 Materials

4.4.1 Asphalt

The asphalt binder used in this study was unaged PG 58-31, meaning it met performance criteria at an average 7 days maximum pavement temperature of 58°C and at a minimum pavement temperature of -31°C [16]. The asphalt properties are summarized in Table 4-1.

TABLE 4-1: Unmodified Asphalt Binder Specification

Properties	Description
Appearance	Black viscous material
Color	Black
Odor	Asphalt
Physical State	Liquid
Melting Point/Freezing Point	> 31°C (87.8°F)
Boiling Range	> 228°C (442.4°F) (1 atm)
Flash Point	> 243°C (469.4°F) (COC)
Relative Density	1.020 to 1.040 (Water = 1) at 15°C (59°F) (1 atm)
Viscosity	0.100 tot 0.800 Pa·s at 135°C (275°F)

4.4.2 Halloysite Nanoclay

For this research, halloysite nanoclay (Kaolin clay) with a formula of $Al_2Si_2O_5(OH)_4 \cdot 2H_2O$, molecular weight of 294.19 g/mol, density of 2.53 g/cm³, and which appears in the form of nanopowder was used. It has a tube-like morphology with diameters ranging between 30 and 70 nm and lengths of 1-3 µm. It appears as a white to tan powder, has a pore volume of

1.26-1.34 ml/g, specific gravity of 2.53, and surface area of 64 m²/g [67]. Although it exhibits low electrical and thermal conductivity, it possesses strong hydrogen interaction due to its inner hydroxyl groups. Its application as reinforcement in nanocomposites has yielded improvements in thermal and mechanical properties, likely due to its characteristic tube-like morphology and high aspect ratio [68].

4.4.3 Nanoclay, Hydrophilic Bentonite

Bentonite is an absorbent aluminum phyllosilicate clay which consists mainly of montmorillonite, from the smectite group. It is composed of two tetrahedral silicon oxide layers sandwiching an octahedral aluminum oxide layer. Its chemical formula is $H_2Al_2O_6Si$ and its molecular weight is 180.1 g/mol. It exists in powder form with a particle size $\leq 25 \mu m$ [69]. Although clay platelets have negatively charged surfaces, the replacement of aluminum atoms in the octahedral layer (which sits on top of the tetrahedral silicon layer) with other cations tends to balance the charge in the octahedral layer and creates a charging defect. The ability of the bentonite to readily trade off these surface-lying cations in exchange for hydratable and organic cations makes the hydrophilic montmorillonite hydrophobic (or generates organically treated clays) and, consequently, dispersible in polymer matrices [30].

4.4.4 Cellulose Nanocrystals (CNC)

Cellulose Nanocrystals (CNCs) are a derivative of cellulose, the most important and naturally abundant organic biopolymer in the sphere of earth's living organisms. Constituting between 40 to 90 percent of plants and/or their associated derivatives [36], [37], it is composed of carbon, hydrogen, and oxygen bioengineered as a linear homopolysaccharide chain with cellobiose as the recurrent building block. The cellulose molecules are held together by many hydrogen bonds that maintain the strong lateral association of the chain-like linear cellulose molecules [36]. However, with an interruption of these crystalline (i.e. strong, highly oriented) regions with amorphous (i.e. weak, poorly oriented) regions, the nanosized cellulose-based crystals (or CNCs) can be isolated by acid hydrolysis [37].

With a rod-like morphology, rectangular cross section and high aspect ratio (i.e. 5-20 nm lateral by 100-200 nm longitudinal), recent studies suggest that CNC provides tensile strengths comparable to Kevlar fibres, thus making it an excellent reinforcing material for natural or synthetic matrix polymers. CNC is also considered to be gas-impermeable and can therefore be used to protect materials sensitive to air and oxidation [39] or used as filler in polymer matrices to produce materials with superior thermal and mechanical properties [77], [78].

4.5 Preparation of the Nanomodified Asphalt

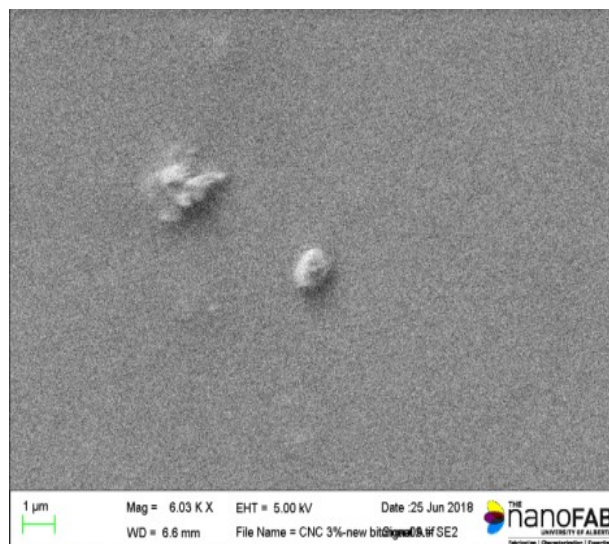
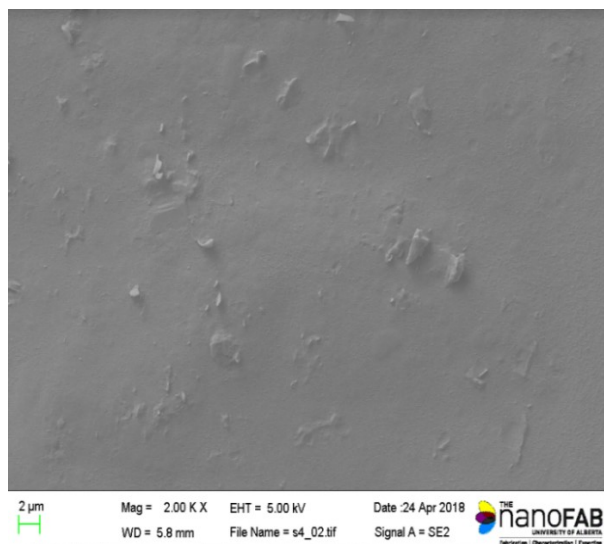
The modified asphalt samples were prepared by adding the nanomaterials to the unaged base asphalt binder (PG 58-31) in proportions shown in Table 4-2. Maintaining a temperature around 140°C on a hot plate under a high shear mixer, the nanomaterial material was added to 500 g of asphalt binder and mixed at a shear rate of 5500-6000 rpm for 4.5 hours.

TABLE 4-2: Amount of Nanomaterial Added to Base Asphalt Binder (% by weight of binder)

Nanomaterial	% Addition in Base Asphalt Binder
Halloysite nanoclay	3% and 6 %
Nanoclay, Hydrophilic Bentonite	3% and 6%
Cellulose Nanocrystals (CNC)	0.5% and 1%

4.5.1 Qualitative Evaluation of the Modified Asphalt Binder Sample

A Zeiss Sigma Field Emission Scanning Electron Microscope (FESEM) was used to qualitatively evaluate the dispersion of nanomaterials added to the asphalt binder. To improve conductivity, the asphalt samples were first sputter-coated with gold using Denton Vacuum gold coating equipment. This coating increased the number of secondary electrons that could be detected from the surface of the specimen in the SEM. Sputtered films for SEM typically have a thickness range of 2–20 nm [70]. Figure 4-1(a) shows the SEM equipment and an example of the dispersion of nanoclay in the binder. As Figure 4-1(b) shows, dispersion of nanoclay samples in the binder seems to be consistent after 4.5 hours of mixing with the rate of 5500-6000 rpm. However, it seems there is still some agglomeration of nanomaterial at some spots that could be improved by surface modification [79].



(a) Halloysite – 3% **(b) Cellulose Nanocrystals (CNC) – 1%**
Figure 4-1: Scanning Electron Microscope (SEM) Images of Modified Binder

4.6 Laboratory testing

4.6.1 Dynamic Mechanical Analysis (DMA)

To investigate the performance of modified binders at different temperatures and loading frequencies, rheological tests were performed. A specimen of about 20-30 g of the sample was taken in a small aluminum tray and oven heated at 140°C until sufficiently fluid for pouring into an 8-mm diameter silicone mold. The rheological measurements were carried out using a Smartpave 102 DSR from Anton Paar. Using an 8-mm diameter parallel plate, a gap of 2 mm, and an angular frequency range between 0.3 and 300 rad/s, frequency sweep tests were performed on the samples through loop temperatures of 40, 30, 20, 10 and 4°C.

A minimum of four tests were conducted for each of the modified samples, as well as the base asphalt binder, and the average of the results was used to compare the effect of modification on the asphalt binder. Master curves of complex modulus (G^*) and phase angle (δ) were then plotted at the target temperature of 20°C and a broader frequency range using the time-temperature superposition principle and the Williams-Landel-Ferry (WLF) equation were performed by the Rheoplus software (by Anton Paar).

A viscoelastic material, such as paving grade asphalt used in HMA, must be capable of resisting the traffic load at high or intermediate service temperatures. Shear modulus, or G^* , which indicates the stiffness (or resistance to deformation) of the asphalt, has two components: the loss (or viscous) modulus and the storage (or elastic) modulus. The phase

angle, or δ , defines the three types of responses to deformation [80]: purely elastic ($\delta = 0$), purely viscous ($\delta = 90$) and viscoelastic response ($0 \leq \delta \leq 90$).

The master curve is one of the primary analytical techniques used in DMA. It uses the interrelationship between temperature and frequency to produce a smooth and continuous curve, termed "thermo-rheologically simple," at a reduced frequency or time scale (the time-temperature superposition principle). A viscoelastic material like asphalt is considered "thermo-rheologically simple" provided it undergoes no structural change during the transition (e.g. glass transition) at a constant increase in temperature [81]. Conventional unmodified asphalt binders, consistent with the Superpave Binder Specification, exhibit this thermo-rheological simplicity; hence, characterization by DMA is appropriate [80].

4.6.2 Rotational Viscometer Testing

To select the appropriate mixing and compaction temperatures for each modified or unmodified sample, the Fungilab EVO Expert Rotational Viscometer (RV) was used. The RV measures the torque required to maintain a constant rotational speed of 20 Revolutions Per Minute (RPM) of a cylindrical spindle submerged in an asphalt binder sample at constant temperatures. This torque is converted to viscosity and displayed automatically by the equipment [82].

4.6.3 Mix Design

The HMA mix design used in this research was based on the Superpave mix design procedure for the 10 mm – High Traffic (HT) asphalt layer. Aggregate grain size distribution and mix properties are summarized in Tables 4-3 and 4-4, respectively. The same mix design was used for preparing all modified and unmodified asphalt samples.

Table 4-3: Aggregate Grain Size Distribution

Sieve Size (mm)	% Passing	Upper Limit	Lower Limit
12.5	100	100	100
10	98.3	97	100
8	88.5	70	94
6.3	75.4	45	85
5	64.8	32	75
2.5	49	23	55
1.25	39.5	16	45
0.63	32.7	11	36
0.315	20.2	8	26
0.16	10.3	7	14
0.08	5.1	3	8

Table 4-4: Asphalt Mix Properties

Properties	Actual	Specifications
Number of Gyration	100	100
Asphalt Cement (AC) % of Total Mix	5.5	-
Theoretical Maximum Specific Gravity, G_{mm} (kg/m ³)	2431	-
Bulk Specific Gravity, G_{mb} (kg/m ³)	2337	-
Air Voids (%)	3.9	3.6 – 4.4
Voids in the Mineral Aggregate, VMA (%)	14.9	13 min
Voids Filled with Asphalt, VFA (%)	73.8	70 – 80
% G_{mm} @ Maximum No. of Gyration, N_{max}	96.8	98.0 max
Dust/AC	1.0	-

4.6.4 Hamburg Wheel Tracking Testing

The Hamburg Wheel Tracking Device (HWTDD) was used to evaluate the rutting potential of the cylindrical asphalt mix samples. Based on AASHTO T324-16, the device cyclically tracks a 705 ± 4.5 N, 47 mm-wide steel wheel (at a frequency of 52 ± 2 passes per minute and a maximum speed of 0.305 m/s at midpoint) across a submerged HMA sample (cylindrical or slab) compacted to 7.0 ± 0.5 percent or 7.0 ± 1.0 percent air voids using a Superpave

gyratory compactor or linear kneading compactor, respectively. The machine tracks for 20,000 passes or until a 12-mm rut depth is achieved (whichever is earlier) at a predefined temperature. A graph of rut depth versus number of passes is plotted to provide valuable information about the asphalt concrete mixes' rutting potential as well as their susceptibility to moisture damage. The graph also shows the Stripping Inflection Point (SIP), which marks the point at which moisture damage begins to take effect and accelerates the rut depth. An HMA with SIP occurring at a number of load cycles less than 10,000 passes may be susceptible to moisture damage [48].

The HMA samples used in this study were compacted to 6.0 ± 0.5 percent air voids using a Superpave gyratory compactor. The cooled samples were saw-cut along a secant line such that, when joined together in the high-density polyethylene molds, a gap of no greater than 7.5 mm was achieved between the molds. The samples were then tested for 20,000 passes (or until 12-mm rut depth was achieved, whichever was earlier) at 45°C.

4.6.5 Indirect Tensile (IDT) Creep and Strength Test

The IDT creep and strength tests were developed to evaluate the resistance of HMA to thermal cracking and have become the most promising method for predicting the low-temperature performance for asphalt concrete mixtures [58]. Creep compliance is defined as the rate at which strain increases for a constant application of stress time-dependent strain per unit stress, while indirect tensile strength is the strength of the HMA when subjected to tension [83].

To compare the low-temperature properties of samples modified with nanomaterials, specimens were prepared for each of the modified and unmodified binder types. All specimens were conditioned and tested using the IPC Global Universal Testing Machine (UTM-100) in accordance with AASHTO T322-07. Specimen deformations were measured using horizontal and vertical Linear Variable Differential Transducers (LVDTs) mounted on brass gauge points with a gauge length of 75 mm on each face of the specimen. Each specimen was loaded to a target creep load of 1,000 N (1 kN) for 100 seconds, after which strength test was conducted at the loading rate of 12.5 mm/min. Creep compliance $[D(t)]$, tensile strength and fracture energy were calculated for each asphalt mix.

Creep Compliance

The creep compliance was calculated as a function of the horizontal and vertical deformations, the gauge length over which these deformations are measured, the dimensions of the test specimen and the magnitude of the static load. Creep compliance is given by Equation 4-1.

$$D(t) = \frac{\Delta X_{tm,t} \times D_{avg} \times b_{avg}}{P_{avg} \times GL} \times C_{cmpl} \quad (4-1)$$

Where: D(t) is the creep compliance at time t (kPa)⁻¹;
 GL is the Gauge Length in metres;
 D_{avg} is the average Diameter of all specimens;
 b_{avg} is the average thickness of all specimens;
 P_{avg} is the average creep load;
 X_{tm,t} is the trimmed mean of the normalized, horizontal deformations of all specimen faces at time t; and
 C_{cmpl} is a correction factor as per Equation 2.

$$C_{cmpl} = \text{correction factor} = 0.6354 \times \left(\frac{x}{y}\right)^{-1} - 0.332 \quad (4-2)$$

Where: $\frac{x}{y}$ is the absolute value of the ratio of the normalized, trimmed mean of horizontal deformations to the normalized, trimmed mean of vertical deformations at time corresponding to half the total creep test time (typically 50 seconds) for all specimen faces.

Tensile Strength

Based on the recommendation of the NCHRP Report 530, the tensile strength is calculated as a function of the maximum load and then “corrected” to its “true” tensile strength [58], given by Equation 4-3.

$$S_{t,n} = \frac{2 \times P_{f,n}}{\pi \times b_n \times D_n} \quad (4-3)$$

$$\text{Tensile strength} = (0.78 \times S_{t,n}) + 38 \quad (\text{for psi})$$

$$\text{Tensile strength} = (0.78 \times S_{t,n}) + 0.262 \quad (\text{for MPa})$$

Where: S_{t,n} is the “uncorrected” tensile strength of specimen n;
 P_{f,n} is the maximum load observed for specimen n;
 b_n is the thickness of specimen n; and
 D_n is the diameter of specimen n.

Fracture Energy

An object’s resistance to crack growth, or toughness, is dependent on the energy absorbed as the crack advances. This energy, called fracture energy, is associated with plastic flow and is concentrated at the crack tip, a plastic zone where the material’s yield stress is present. Fracture energy provides an indication of the crack’s propagation within the asphalt pavement at low service temperatures. It is determined by calculating the area under the curve of the

indirect tensile strength test using the trapezoidal method and dividing by the crack cross-section [84].

4.7 Results and Discussion

4.7.1 Dynamic Mechanical Analysis (DMA)

Figures 4-2(a), 4-3(a) and 4-4(a) show that the complex modulus (shear stiffness) increased for all of the nanomodified asphalt samples and the difference is more significant at lower frequencies.

For the nanoclay modified samples, the G^* values were greater for modified asphalt using 6 percent nanoclay compared to those using 3 percent nanoclay. For nanocellulose-modified asphalt samples, the G^* values for modified asphalt using 1 percent CNC were slightly greater than 0.5 percent. Figures 4-2(b), 4-3(b) and 4-4(b) show a relative reduction in δ for the nanomodified samples that indicates an increase in the elasticity, or increase in recoverable strains, of nanomodified asphalt samples.

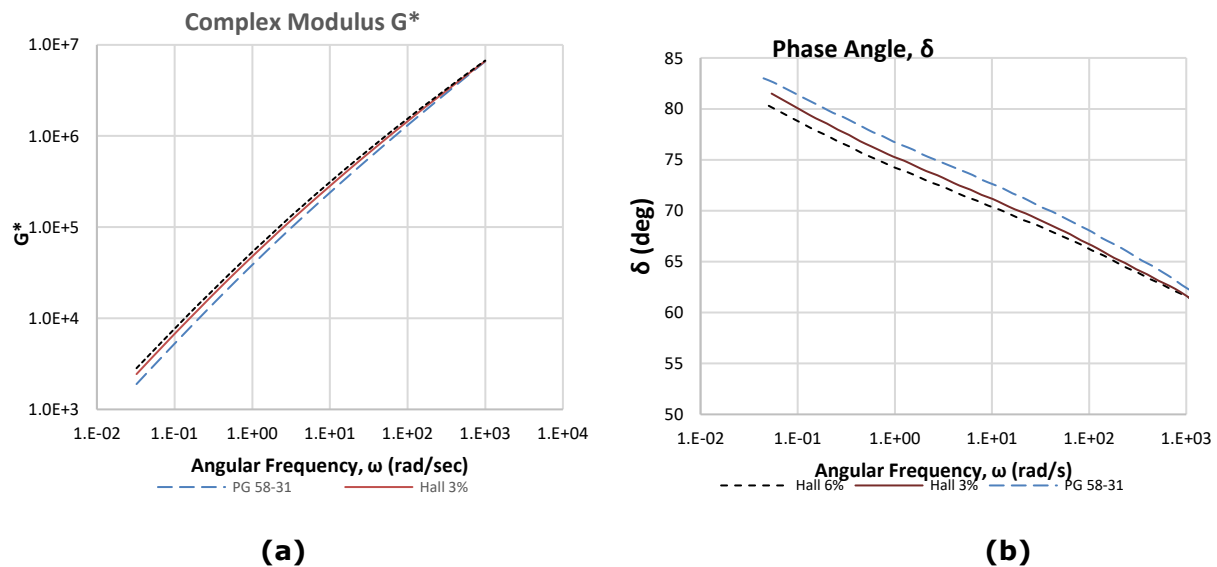
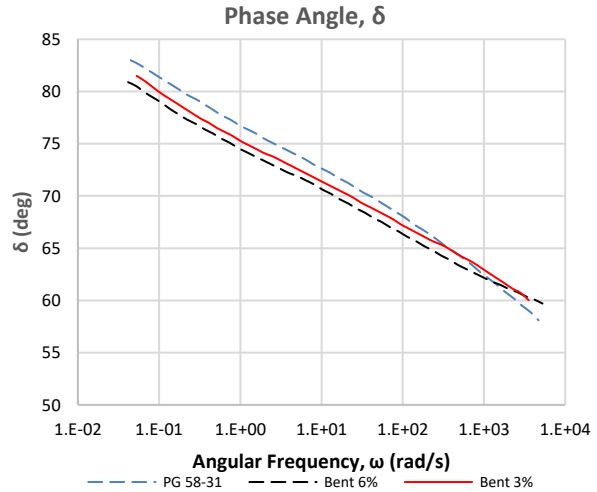
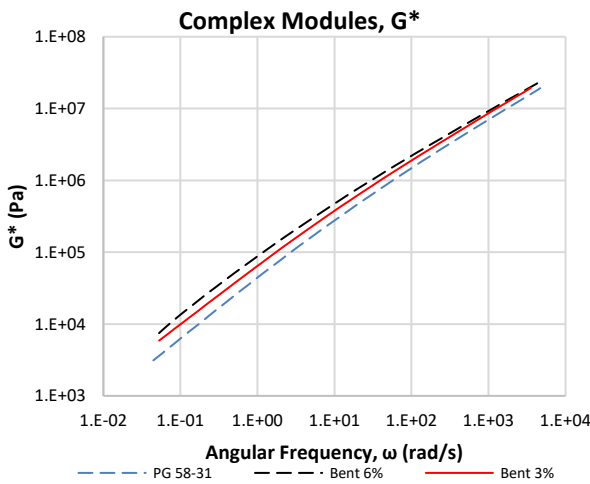
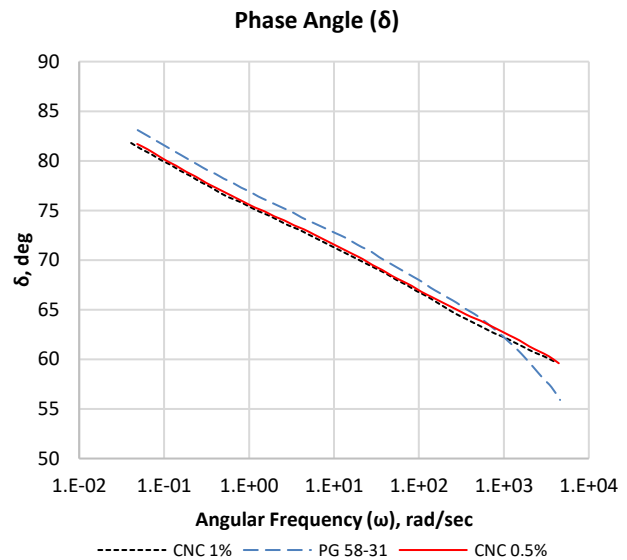
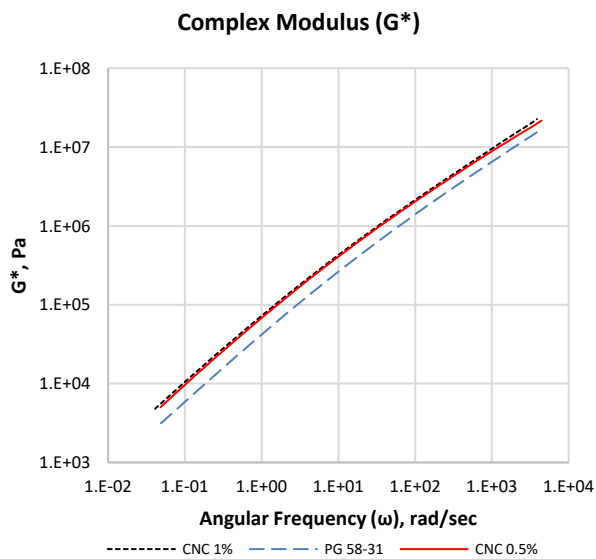


Figure 4-2: Halloysite-Modified Binder at 20°C – (a) Complex Modulus and (b) Phase Angle



(a) (b)
Figure 4-3: Bentonite-Modified Binder at 20°C – (a) Complex Modulus and (b) Phase Angle



(a) (b)
Figure 4-4: CNC-Modified Binder at 20°C – (a) Complex Modulus and (b) Phase Angle

4.7.2 Mixing and Compaction Temperatures

Figure 4-5 summarizes the viscosities of the neat asphalt binder along with its nanomodified replicates, as well as the mixing and compaction temperatures used for sample preparation. As the figure shows, every 3 percent increase in nanoclay material leads to a 5°C increase in the modified binder mixing compaction and temperature. The addition of 1 percent nanocellulose also increases the mixing and compaction temperature by 5°C. However, the addition of 0.5 percent nanocellulose does not change the binder viscosity significantly.

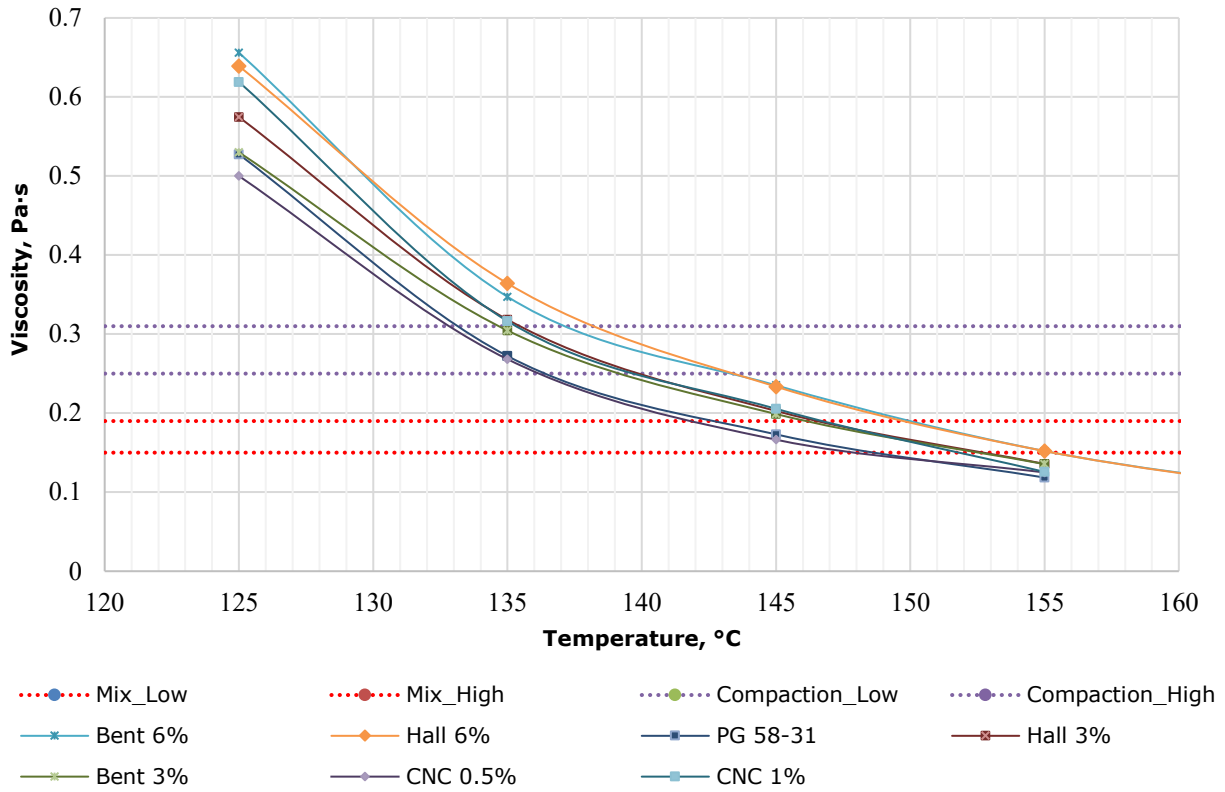


Figure 4-5: Viscosity-temperature curves for unmodified and nanomodified binders

Table 4-5: Mixing and Compaction Temperatures for Sample Preparation

Binder Type	Mixing Temperature (°C)	Compaction Temperature (°C)
PG 58-31	145	135
3% Bentonite-modified	150	140
6% Bentonite-modified	155	145
3% Halloysite-modified	150	140
6% Halloysite-modified	155	145
0.5% CNC-modified	145	135
1% CNC-modified	150	140

4.7.3 Performance Tests

4.7.3.1 Hamburg Wheel Tracking Device Test

A total of seven kinds of samples were prepared and tested with the results provided in Table 4-6. The overall rutting and moisture susceptibility performances of the various mixtures are shown in Figure 4-6. It was observed that the neat asphalt (PG 58-31) achieved a rut depth

of 11.6 mm at 20,000 passes. Results from the halloysite-, bentonite- and CNC-modified asphalt concrete specimens reported significant reductions of between 30 and 80 percent in rut depth for modified mixes. The two nanoclay types were observed to have a similar effect on asphalt binder in term of rutting resistance with respect to the amount of added nanoclay materials.

Table 4-6: Hamburg Wheel Tracker Test Results (Mechanical Properties)

S/NO	Description	Test Temperature (°C)	Post Compaction Consolidation (mm)	Stripping Inflection Point (# of passes/mm)	Rut Depth (mm)
1	PG 58-31	45	1.74	9179 / 3.86	11.60
2	PG 58-31 + Hall 3%	45	1.32	16529 / 4.69	7.83
3	PG 58-31 + Hall 6%	45	0.67	18022 / 2.12	2.85
4	PG 58-31 + Bent 3%	45	1.43	14260 / 3.95	7.84
5	PG 58-31 + Bent 6%	45	0.89	17693 / 2.97	3.21
6	PG 58-31 + CNC 0.5%	45	2.38	14856 / 5.77	8.20
7	PG 58-31 + CNC 1%	45	1.36	15771 / 4.63	6.48

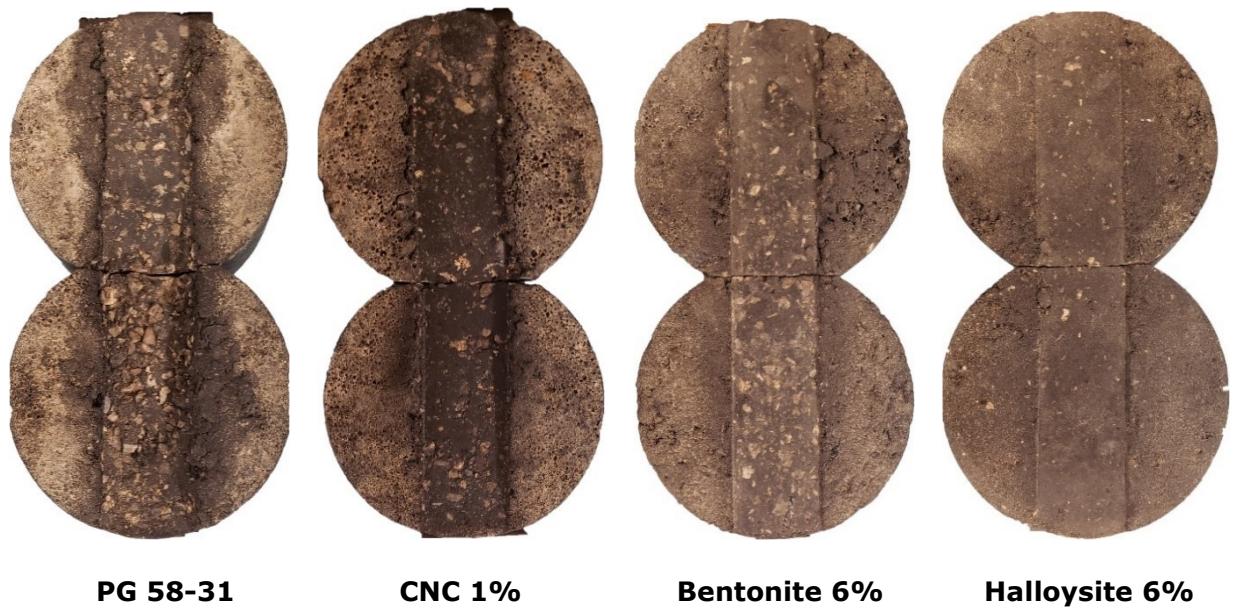


Figure 4-6: Samples after Hamburg Wheel Tracker Test

After comparing the increase in the number of passes at the stripping inflection points for the nanomodified samples with the neat binder samples, it was concluded that the addition of the nanomaterials increased the number of passes by between 55 and 95 percent. These indicate a significant improvement in the resistance of modified mixes to moisture damage with the application of the nanomaterials. Of the modified asphalt mixes, the lowest permanent deformation and moisture susceptibility results were obtained for the modified samples using 6 percent halloysite nanoclay and the highest ones for the modified samples with 0.5 percent nanocellulose.

After comparing the permanent deformation and moisture sensitivity of nanomodified samples, it was concluded that the performance of asphalt mixes modified using 1% nanocellulose is comparable with that of modified samples using 3 percent nanoclay materials.

4.7.3.2 Indirect Tensile (IDT) Creep and Strength Test

Table 4-7 summarizes the results of the IDT for the asphalt mixes composed of neat asphalt binder (PG 58-31) and nanomodified binders (halloysite, bentonite and CNC). Comparing the tensile strength of modified asphalt mixes to the control sample, it was observed that the addition of nanomaterial increases the tensile strength of the asphalt mixes. Comparing the fracture energy values of nanomodified asphalt samples with the control samples, it was concluded that the addition of nano material to the asphalt mix affects the mix toughness and makes it less flexible. Creep compliance values of nanomodified samples also confirm that the addition of nanomaterial would reduce the relaxation modulus $[D(t)]$ of the HMA and, consequently, reduced the HMA's ability to deform plastically (or cause to be more brittle) at low service temperatures.

Table 4-7: Summary of Indirect Tensile Creep and Strength Test Results

Parameters	PG 58-31	3% Bentonite -modified	6% Bentonite -modified	3% Halloysite -modified	6% Halloysite -modified	0.5% CNC- modified	1% CNC- modified
Creep compliance [D(t)], 1/GPa (- 20°C)	0.0032	0.0032	0.0010	0.0035	0.0028	0.0054	0.0046
Tensile strength ($S_{t,n}$), MPa (- 10°C)	3.72	3.73	3.67	4.15	3.62	3.61	3.80
Fracture Energy, kJ/m ² (-10°C)	4.057	4.994	4.873	4.574	4.166	4.783	4.951

4.8 Conclusions and Future Steps

- The scanning electron microscope (SEM) results showed that using a high shear mixer could be effective for dispersion of nanomaterial inside the asphalt binder. However, the dispersion still could be improved by using other methods such as surface modification of nanomaterial.
- The dynamic shear rheometer (DSR) results show that modification of PG 58-31 with nanomaterials (hydrophilic bentonite nanoclay, halloysite nanoclay and CNC) increased the complex modulus (or shear stiffness) of the matrix, which is proportional to the concentration of the nanomaterials.
- The phase angle results indicate an increase in the recoverable strains (higher binder elasticity) of the binder as a result of the nanomodification
- Rotational viscometer (RV) tests confirmed an increase in the viscosity of nanomodified binders and, consequently, increases in mixing and compaction temperatures of nanomodified asphalt mixes.
- Permanent deformation test results using a Hamburg Wheel Tracker showed that the addition of nanomaterials significantly improved both rutting resistance and moisture sensitivity of the mixes.

- Although there appears to be no significant difference in the tensile strengths, Hot Mix Asphalt (HMA) produced with nanomodified binders had higher fracture energies and relaxation modulus; thereby, rendering the nano-modified mixes more resistant to crack propagation at lower temperatures.
- In all rheological and performance tests, both nanoclay materials (bentonite and halloysite) affected asphalt properties similarly. When comparing the rutting and Indirect Tensile (IDT) test results, the asphalt mixes composed of 1% CNC and 3% nanoclay material had similar performance properties.

The objective of this study was to understand the low-temperature behaviour of asphalt mixes modified with nanomaterial. Experiments were limited to IDT tests at -20°C . To better understand the low and intermediate temperature behaviour of the mixes, further steps would involve conducting rheological testing on modified binders at low temperature (bending beam rheometer), indirect tensile strength (ITS) tests before and after freeze-and-thaw conditioning, and conducting of IDT tests at different temperatures (-10 and 0°C), as well as dynamic modulus tests at a range of temperatures and frequencies.

5 Laboratory Evaluation of Nano-Modified Asphalt

5.1 Abstract

Physical properties and thermal susceptibility of asphalt binder can significantly influence the performance of hot mix asphalt (HMA). The increase in loading conditions and frequency of application, as well as increase in maximum pavement temperatures, result in decreased performance of the asphalt layer and, consequently, pavement life. One promising possibility for increasing the performance of asphalt pavements at extreme temperature ranges is modification of the asphalt to enhance the properties of the asphalt mix. Polymer modification has been used extensively to improve the performance of asphalt mixes but have experienced drawbacks in the areas of incompatibility with the binder, poor ageing resistance, cost and operational difficulties. In the last few years, there has been a remarkable increase in the interest in nanotechnology applications in the HMA pavement. Nanomaterial has a high surface area to volume ratio and unique bulk, surface, and colloidal properties. Past research suggests that the addition of nanoclay, nanocarbon, and nanosilica to base binders can improve the rheological properties of asphalt cement and, consequently, affect its mechanical properties, such as tensile strain, flexural strength, and elasticity.

This research focused on the changes in rheological properties of the neat asphalt binder when modified with unmodified/untreated nanoclays (bentonite or halloysite) or crystalized nanocellulose (CNC), and the effects of the modification on the mechanical performance of HMA produced therewith in comparison with control HMA. Finally, a material cost-versus-performance analysis was conducted to provide reliable data for selecting suitable materials to fulfill modification requirements. The research results show that pronounced improvements were observed in the rheological properties of the modified binder, as well as the performance of the HMA produced with the modified binder.

5.2 Introduction and Background

The appropriate selection of asphalt binder is critical to the performance of hot mix asphalt (HMA) [3]. To avoid low-temperature cracking, one of the major problems in cold climates, low-performance grade (or softer) binders are usually used for the HMA layers. However, these flexible pavements undergo severe rutting failure during the summer. As the effects of climate change, increased axle loads and the ongoing demand for cost savings push the performance of conventional paving grade asphalts beyond the limit [75], the design and construction of pavements to accommodate these new critical limits may require asphalt

binder modification. Hence, depending on the required type of improvement, the appropriate modifier(s) should be introduced to enhance these rheological properties [85].

Nanotechnology involves the design, construction, and use of ultra-small, functional structures with at least one dimension not more than 100 nm [76]. The application of nanotechnology principles to the modification of material properties at the nano level remarkably alters macro properties and brings the quantum effect into play due to a high surface area to volume ratio and small dimensions. With attributes that are directly or indirectly the outcome of the small dimensions of the particles, nanotechnology facilitates the design of systems with high functional density, high sensitivity, special surface effects (including high water repellency), high strain resistance and catalytic effects [86]. These systems have enhanced structures, greater cost-effectiveness, more efficient functional properties, and appear to be promising in the design, construction of road pavements [11].

With the introduction of nanomaterials as potential asphalt modifiers, other researches suggest that the addition of nanoclay to polymer matrices increases the thermal stability [87] and chemical resistance of asphalts [88]. Currently, the combination of small amounts of nanoclays (less than 10% by weight) and polymers form nanocomposites with increased strength, mechanical modulus, and toughness, as well as improved barrier and flame retardant properties [89], [90]. Golestani et al. conducted a laboratory investigation on the effects of asphalt binder modified with nanocomposites (i.e. nanoclays and polymers) and discovered enhanced physical and rheological properties and storage stability of the binder, and that the asphalt concrete specimens produced therewith displayed increased tensile strength and resilient modulus, as well as improved rutting resistance [12]. Van de ven et al investigated two types of montmorillonite nanoclay additives in asphalt binder. One of the nanoclays (up to 6% of the binder by mass) significantly improved both the short-term and long-term aging, with no change to the neat binder viscosity, while the other nanoclay showed a substantial increase in the binder's viscosity. The former applies to porous asphalt concrete while the latter has possible applications in the prevention of binder drainage during transportation [91]. Jahromi and Khodaii conducted a comparative rheological evaluation of unmodified and two types of modified asphalt binders and found that the improvement to the binder's rheological properties is dependent on the dispersion of the nanomaterial at the nanoscopic level [92]. Zare-Shahabade et al. used two types of bentonite nanoclay to modify a neat binder by melt processing under sonication and shearing stresses. In addition to the improved rutting resistance exhibited by the modified asphalts, low-temperature properties were also notably improved, as was resistance to cracking [93]. Care should be taken in the

selection of nanoclay to ensure effective penetration of the base material into the nanoclay's interlayer spacing, to yield an exfoliated or intercalated product [94].

Synthetic polymers have been employed extensively since the early 1970s to modify the performance of bituminous binders to decrease temperature susceptibility, increase cohesion, and modify rheological characteristics [95] but have, however, experienced drawbacks in the areas of incompatibility with the binder [96], poor ageing resistance, cost and operational difficulties. Current trends, though limited in the industry, have begun investigating the application of nanotechnology in the modification of asphalt pavements, and a preliminary cost analysis revealed that nanoclay modification of asphalt binder is 22%-33% cheaper than its polymer-modified equivalent [13].

Cellulose nanocrystals (CNC) are a low-density nanomaterial with a versatile range of applications. In the food industry, they can serve as a non-caloric stabilizer in low concentrations of 8%-10% by weight of aqueous dispersions [97]. Their high tensile strength, comparable to Kevlar fibre in stiffness, makes them an excellent reinforcing material for natural or synthetic matrix polymers [98]. When used as a filler phase in polymer matrices, they produce a biobased nanocomposite with excellent thermal and mechanical properties. Nanocellulose has been successfully applied to increase the fracture energy of concrete material [99]; however, to date it has not been widely used for asphalt cement modification. One study shows that including a small amount of nanocellulose in asphalt cement (1% by weight of asphalt cement) could decrease its thermal susceptibility, increasing the shear modulus at high temperature and increasing asphalt cement toughness at low temperature [100].

The studies mentioned above suggest that both nanoclay and nanocellulose, although not widely used as asphalt cement additives, have the potential to enhance the low temperature properties and performance of asphalt cement. Comprehensive research focusing on the rheological properties of asphalt cement modified using these materials at low temperatures and after different aging periods will be essential to properly investigate the effectiveness of this approach. The mechanical performance of asphalt mixes containing nanoclay and nanocellulose at low temperatures and under freeze-thaw conditioning is another area that requires more exploration.

5.3 Objectives and Scope

The objective of this paper is to investigate and compare the effects of the application of bentonite nanoclay, halloysite nanoclay and CNC on asphalt rheology and asphalt mix

performance. For this purpose, asphalt samples were mixed with hydrophilic bentonite nanoclay, halloysite nanoclay and CNC using a high shear mixer. Scanning electron microscopy (SEM) was used to investigate the dispersion of nanomaterial in the base asphalt after mixing. Dynamic mechanical analyses (DMA) were performed on the modified/unmodified asphalt binders using the dynamic shear rheometer (DSR), and the outputs were evaluated at 20°C and reduced frequencies. Viscosity measurements were taken to verify the mixing and compaction temperatures of the nanomodified asphalt mix specimens. Hamburg wheel tracking tests were conducted on the HMA samples prepared from the unmodified and modified asphalt binders to evaluate and compare the resistance to rutting and susceptibility to moisture. Indirect Tensile (IDT) Creep and Strength Test were performed to evaluate the cracking potential of asphalt mixes at low temperatures. In the end, a comparison between the impact of different nanomaterial on asphalt performance and the additional cost of nanomaterial was prepared.

5.4 Materials and Modified Asphalt Preparation

5.4.1 Asphalt Binder

Performance Grade (PG) 58-31 was used as the neat (or control) binder for this research. It appears as a black, viscous liquid with a melting/freezing point greater than 31°C, a boiling range above 228°C, and a flash point greater than 243°C. It has a relative density of 1.02 to 1.04 at 15°C and 1 atmosphere, and a viscosity of 0.100 to 0.800 pascal-seconds at 135°C.

5.4.2 Halloysite Nanoclay

Halloysite nanoclay (kaolin) has a molecular weight of 294.19 g/mol, density of 2.53 g/cm³, pore volume of 1.26-1.34 ml/g, specific gravity of 2.53, and surface area of 64 m²/g. It has a tube-like morphology with diameters ranging between 30 and 70 nm and lengths of 1-3 μm, and it appears as a white to tan nanopowder [101]. It demonstrates strong hydrogen interaction due to its inner hydroxyl groups, but it exhibits low electrical and thermal conductivity. Its application as reinforcement in nanocomposites has yielded improvements in thermal and mechanical properties, likely due to its characteristic tube-like morphology and high aspect ratio [102]. Considered as a pacesetter in green nanotechnology, halloysite provide several cross-industry applications including cosmetics, electronics, pharmaceuticals and polymer. With respect to cytotoxicity and cytocompatibility, the material is natural, non-toxic, biocompatible and chemically stable [103].

5.4.3 Nanoclay, Hydrophilic Bentonite

Bentonite (aluminum phyllosilicate clay) consists mainly of montmorillonite (smectite). It is highly absorbent and composed of two tetrahedral silicon oxide layers sandwiching an octahedral aluminum oxide layer, has a chemical formula of $H_2Al_2O_6Si$, and has a molecular weight of 180.1 g/mol. It exists in powder form with a particle size of $\leq 25\mu m$ [104]. Although clay platelets have negatively charged surfaces, the replacement of aluminum atoms in the octahedral layer with other cations (which sit on top of the tetrahedral silicon layer) tends to balance the charge in the octahedral layer, which creates a charging defect. This process generates organically treated clays, which can subsequently be dispersed in polymer matrices [89].

5.4.4 Cellulose Nanocrystals

Cellulose nanocrystals (CNC) are a derivative of cellulose, the most important and naturally abundant organic biopolymer in the biosphere. Constituting between 40% and 90% of plants and their associated derivatives, CNC is composed of carbon, hydrogen, and oxygen bioengineered as a linear homopolysaccharide chain with cellobiose as the recurrent building block. The cellulose molecules are held together by many hydrogen bonds that maintain a strong lateral association between the chain-like linear cellulose molecules [36]. However, when these crystalline regions (i.e. strong, highly oriented) are interrupted with amorphous regions (i.e. weak, poorly oriented), the nanosized cellulose-based crystals (or CNCs) can be isolated by acid hydrolysis [37].

5.4.5 Preparation of the Nanomodified Asphalt

Nanomaterials were added to the neat binder at concentrations of 3% and 6% for nanoclays (bentonite and halloysite) and 0.5% and 1% for CNC by weight of the neat asphalt binder (500 grams of binder per mix). The neat binder was preheated and poured into a cylindrical container and placed on a hot plate. Maintaining the temperature between 140°C and 150°C, the nanomaterial was added to the binder in small amounts and mixed using a high shear mixer at a shear rate of 5500-6000 revolutions per minute for 4.5 hours. To ensure that the mixing time, temperature and shear rate had no ageing effect on the neat binder, a 500 gram specimen of the neat binder was also subjected to the same mixing conditions and analyzed using DMA.

5.4.6 Qualitative Evaluation and Results of the Modified Asphalt Binder Sample

Qualitative evaluation of the dispersion of the nanomaterials in the neat asphalt binder was performed using a Field Emission Scanning Electron Microscope (FESEM). The nanomodified

asphalt samples were first sputter-coated with 2–20 nm gold films using Denton Vacuum gold coating equipment to improve conductivity by increasing the number of secondary electrons that could be detected on the surface of the specimen in the SEM [70]. Figure 5-1 shows the dispersion of nanoclay and CNC in the binder. The dispersion seems to be consistent after 4.5 hours of mixing at a rate of 5500-6000 rpm. However, there are some agglomerations of nanomaterial in some spots that may be improved by surface modification [79].

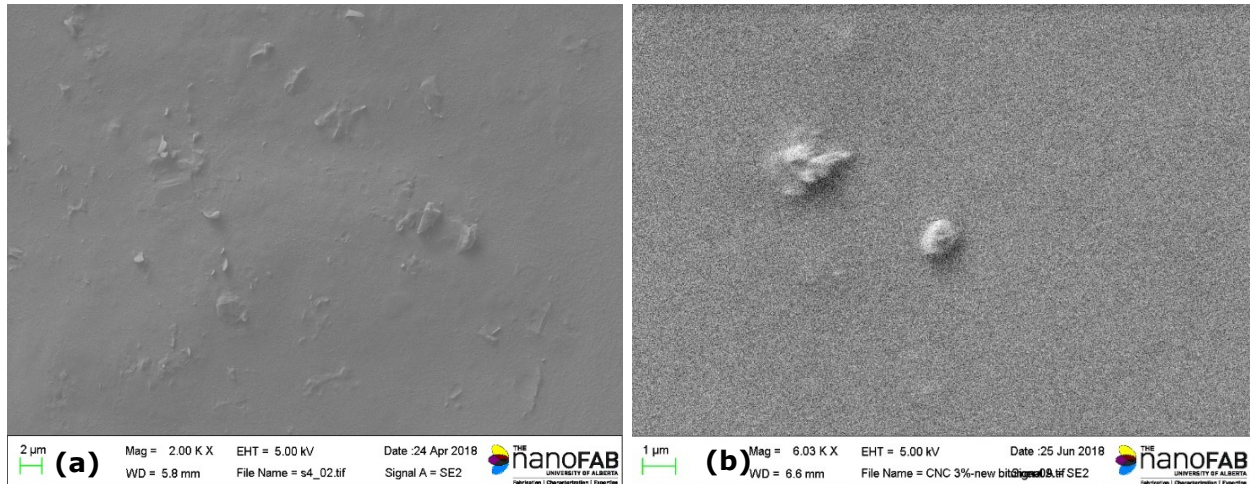


Figure 5-1: Scanning electron microscope images of modified binders: (a) 3% halloysite; (b) 1% CNC

5.5 Laboratory Testing, Results and Discussion

5.5.1 Dynamic Mechanical Analysis

Rheological tests were performed to investigate the performance of modified binders at different temperatures and loading frequencies. A sample of 20-30 g of the binder was taken in a small aluminum tray and oven heated at 140°C until sufficiently fluid for pouring into an 8-mm diameter silicone mold. Using a Smartpave 102 Dynamic Shear Rheometer (DSR), rheological measurements were carried out with an 8-mm diameter parallel plate, a gap of 2 mm and an angular frequency range between 0.3 and 300 rad/s, frequency sweep tests were performed on the samples at loop temperatures of 40°C, 30°C, 20°C, 10°C and 4°C.

A minimum of four tests were conducted for each of the modified samples, as well as the base asphalt binder, and the average of the results were compared to the values from the base asphalt binder. Master curves of the rutting parameter ($G^*/\sin \delta$) were plotted at 20°C and a broader frequency range using the time-temperature superposition principle, and the Williams-Landel-Ferry (WLF) equation was performed by the Rheoplus software.

As Figure 5-2 shows, there was an increase in the rutting parameter for all the nanomodified asphalt cement, and the increase is more significant at lower frequencies (or higher temperatures) as shown in Figures 5-2a, 5-2b and 5-2c. This is an indication that HMA produced with nanomodified binders should be less susceptible to rutting than that produced with neat binder.

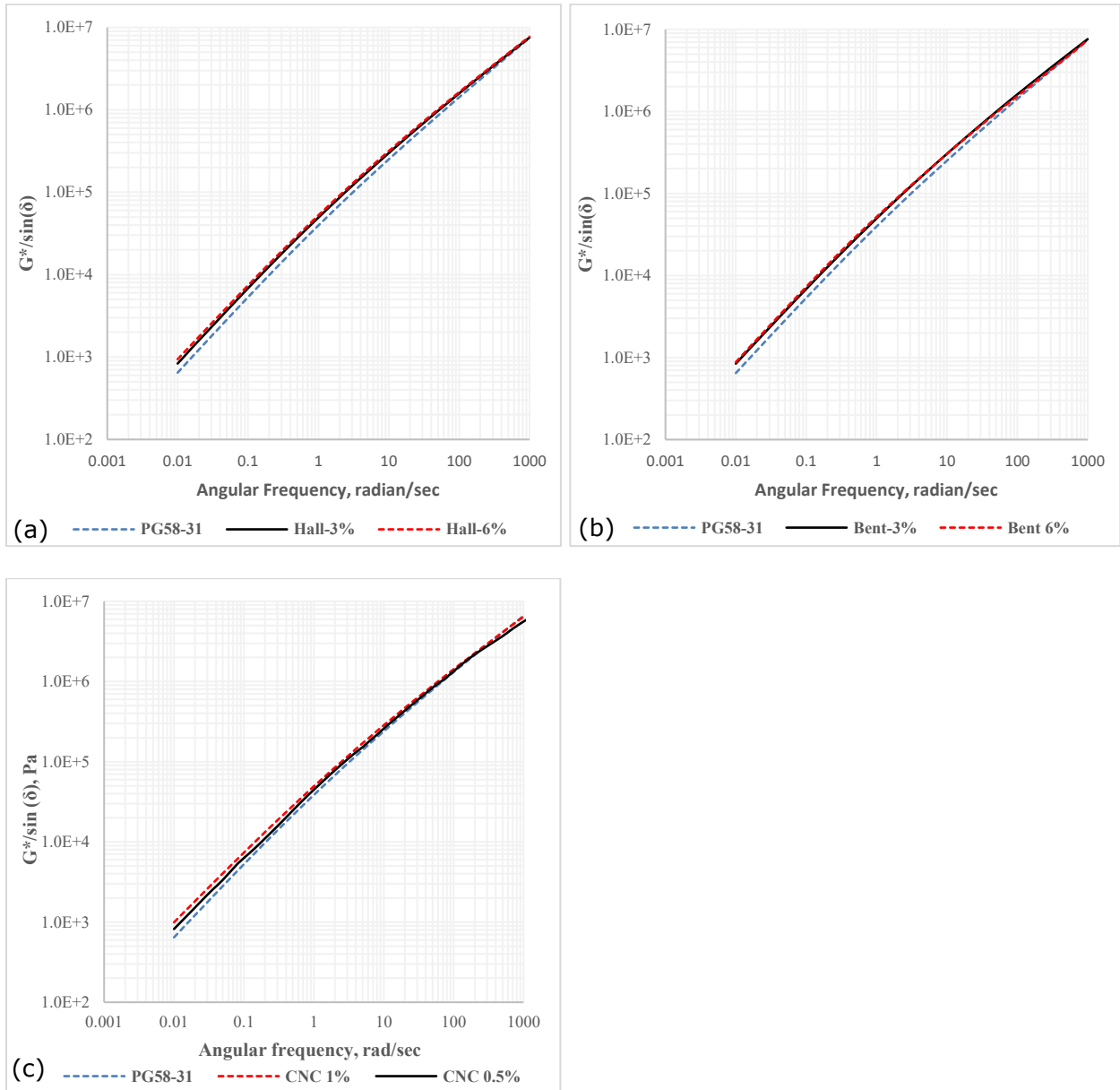


Figure 5-2: Rutting parameter vs angular frequency: (a) Halloysite (3% & 6%); (b) Bentonite (3% & 6%); (c) CNC (0.5% & 1%)

5.5.2 Rotational Viscometer Testing

For both modified and unmodified asphalt samples, a Fungilab EVO Expert Rotational Viscometer (RV) was used to determine the mixing and compaction temperatures by measuring the torque required to maintain a constant rotational speed of 20 revolutions per minute (RPM) of a cylindrical spindle submerged in an asphalt binder sample at constant temperature. This torque is converted to viscosity and displayed automatically by the equipment [105]. Based on these results, the mixing and compaction temperatures were 145°C and 135°C for HMA made with PG 58-31, 150°C and 140°C for HMA made with 3% nanoclay-and 1% CNC-modified binders, 155°C and 145°C for HMA made with 6% nanoclay-modified binders, 145°C and 135°C for HMA made with 0.5% CNC- modified binders (Figure 5-2).

Figure 5-3 illustrates that the addition of 3% and 6% of the nanoclays (halloysite and bentonite) increased the mixing and compaction temperatures by 5°C and 10°C, respectively. 1% of CNC had an effect similar to that of the 3% nanoclays, but the effect on temperature by the addition of 0.5% CNC was not significant. Increase in the mixing and compaction temperatures is an indication of an increase in stiffness of the asphalt binder.

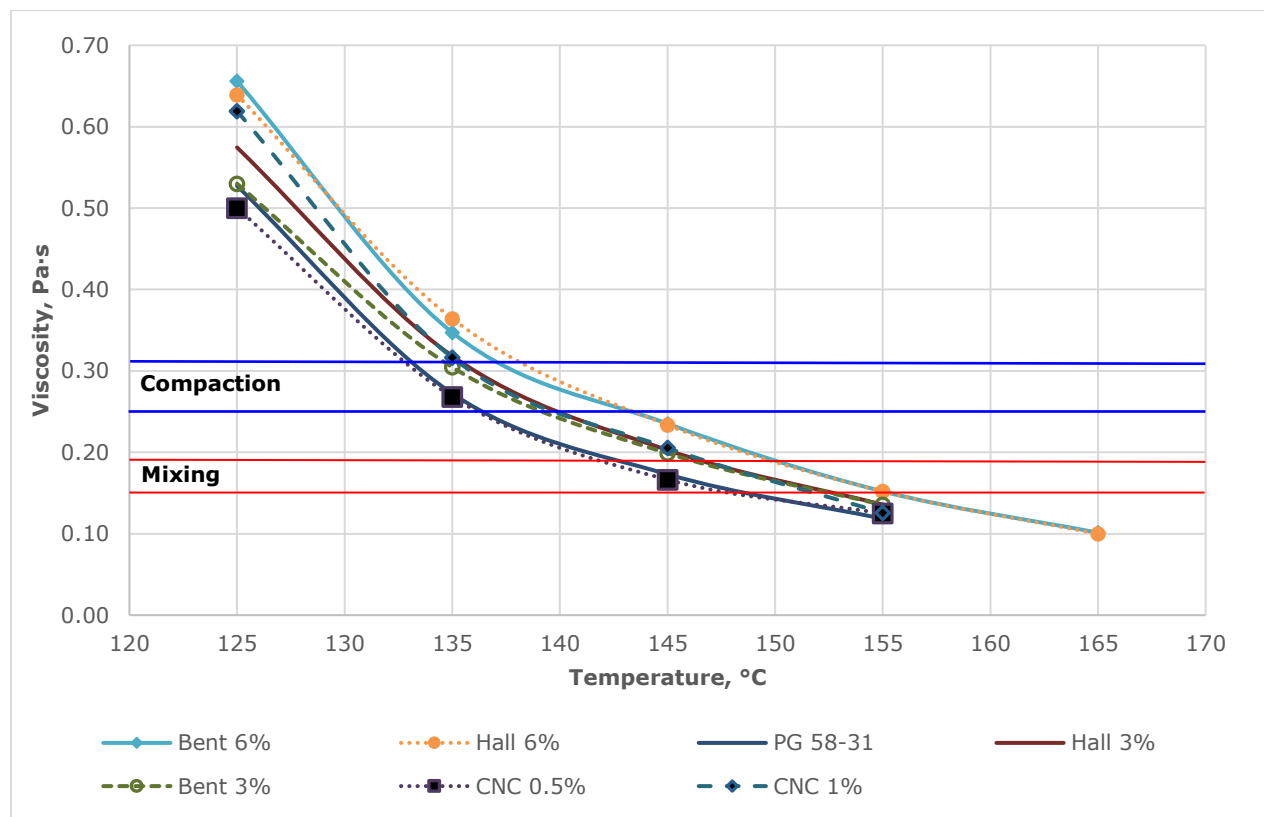


Figure 5-3: Viscosity-temperature curves for neat and modified binders

5.5.3 Mix Design

The Superpave mix design procedure for a 10 mm–High Traffic (HT) HMA layer design was used for this research. The asphalt mix properties and aggregate gradation summarized in Table 5-1 and Figure 5-4 in concordance with the Standard Specification for Highway Construction [71]. This mix design was used for preparing all modified and unmodified asphalt samples.

Table 5-1: Asphalt Mix Properties

Properties	Actual	Specifications
Number of gyrations	100	100
A.C. % of Total Mix	5.5	-
G_{mm} (kg/m ³)	2431	-
G_{mb} (kg/m ³)	2337	-
Air voids (%)	3.9	3.6 – 4.4
VMA (%)	14.9	13 min
VFA (%)	73.8	70 – 80
% G_{mm} @ N_{max}	96.8	98.0 max
Dust/AC	1.0	-

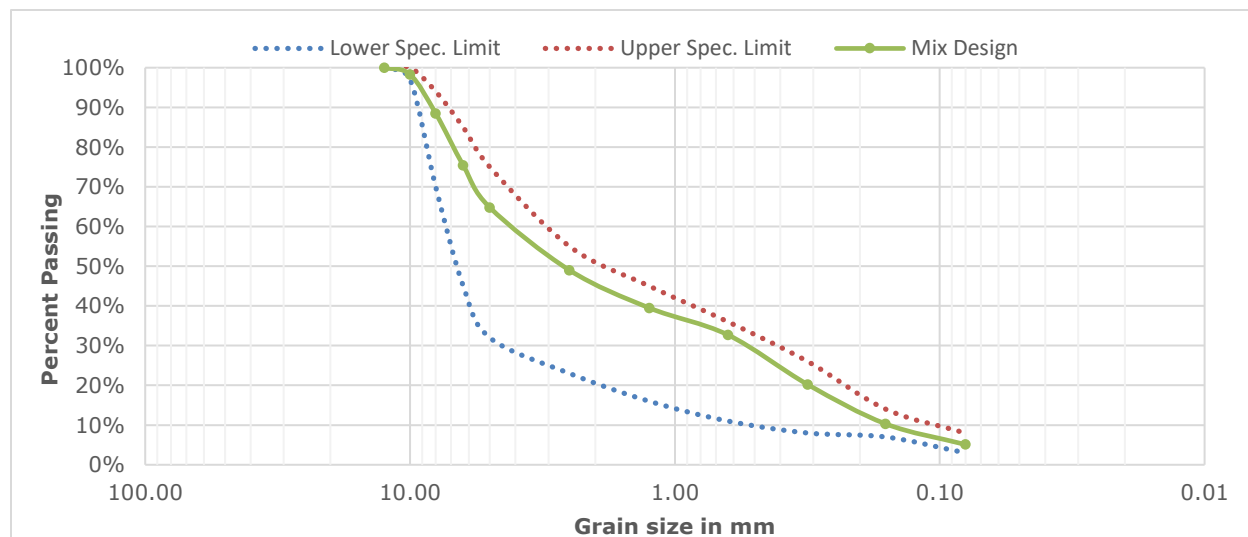


Figure 5-4: Mix design aggregate gradation curve

5.5.4 Rutting and Moisture Susceptibility Testing

HMA samples were evaluated for rutting potential and moisture susceptibility using a Hamburg Wheel Tracking Device (HWT), which tracks a $705 \pm 4.5N$, 47-mm wide steel wheel across a submerged HMA sample (cylindrical or slab) at a frequency of 52 ± 2 passes per minute

and a maximum speed of 0.305 m/s at midpoint. Each specimen in a pair of 150 mm diameter HMA core was compacted to approximately 6% air voids using a Superpave gyratory compactor for each binder type, then saw-cut along a secant line such that, when joined together in the high-density polyethylene molds, a maximum gap of 7.5 mm was achieved between the molds. Testing was performed at 45°C for 20,000 passes, or until a 12mm rut depth was achieved (whichever was earlier). The depth of rutting was plotted against the number of passes to provide valuable information about the asphalt concrete mixes' susceptibility to plastic deformation and moisture damage [106]. Moisture damage begins to take effect at the stripping inflection point (SIP) and accelerates the deformation. An HMA with SIP occurring at several load cycles less than 10,000 passes may be susceptible to moisture damage [48].

5.5.5 Indirect Tensile Creep and Strength Test

Breen and Stephens suggested that the Indirect Tensile (IDT) test is applicable to asphalt concrete since its ultimate compressive strength is greater than three times its ultimate tensile strength at low temperatures [56], and these tests have become the most promising method for predicting the low-temperature performance of asphalt concrete mixtures [57] [58]. Based on a recommendation of 4%-8% air voids [59], a total of 9 specimens (i.e. 3 replicates for each of the test temperatures of -20°C, -10°C and 0°C) were prepared at approximately 6% air voids for each of the binder types (PG 58-31, 3% bentonite, 6% bentonite, 3% halloysite, 6% halloysite, 0.5% CNC and 1% CNC). Having cut the faces of the specimens in accordance with AASHTO T322-07, the samples were conditioned in the environmental chamber of the IPC Global Universal Testing Machine (UTM-100) [60]. Linear variable differential transducers (LVDTs) mounted on brass gauge points with a gauge length of 25 mm on each face of the specimens measured horizontal and vertical strain deformations when loaded with a target creep load of 1 kN for 100 seconds, after which the strength test was conducted at a loading rate of 12.5 mm/min. The creep compliance $[D(t)]$, tensile strength and fracture energy were calculated for each asphalt mix as explained below.

Creep Compliance

Creep compliance was calculated as a function of horizontal and vertical deformation, gauge length over which the deformation is measured, dimensions of the test specimen, and magnitude of the static load. It is given by the formula:

$$D(t) = \frac{\Delta X_{tm,t} \times D_{avg} \times b_{avg}}{P_{avg} \times GL} \times C_{cimpl} \quad (5-1)$$

where:

$D(t)$ = creep compliance at time t (kPa)⁻¹

GL = gauge length (m)

D_{avg} = average diameter of all specimens (m)

b_{avg} = average thickness of all specimens (m)

P_{avg} = average creep load (kN)

$X_{tm,t}$ = trimmed mean of the normalized, horizontal deformations of all specimen faces at time t (m)

The parameter C_{cpl} is a correction factor and is given by

$$C_{cpl} = \text{correction factor} = 0.6354 \times \left(\frac{X}{Y}\right)^{-1} - 0.332 \quad (5-2)$$

where:

$\frac{X}{Y}$ = absolute value of the ratio of the normalized, trimmed mean of horizontal deformation to the normalized, trimmed mean of vertical deformation at a time corresponding to half the total creep test time (typically 50 seconds) for all specimen faces.

Tensile Strength

Based on the recommendation of the NCHRP Report 530, the tensile strength, $S_{t,n}$, was calculated as a function of the maximum load and then corrected to its true tensile strength [58]. The tensile strength is given by the formula below:

$$S_{t,n} = \frac{2 \times P_{f,n}}{\pi \times b_n \times D_n} \quad (5-3)$$

Tensile strength = $(0.78 \times S_{t,n}) + 38$ (for psi)

Tensile strength = $(0.78 \times S_{t,n}) + 0.262$ (for MPa)

where:

$S_{t,n}$ = "uncorrected" tensile strength of specimen, (MPa)

$P_{f,n}$ = maximum load observed for specimen, (MN)

b_n = thickness of specimen, (m)

D_n = diameter of specimen, (m)

Fracture Energy

An object's resistance to crack growth, or toughness, is dependent on the energy absorbed as the crack advances. This energy, called the fracture energy, is associated with plastic flow and concentrated at the crack tip, a plastic zone where the material's yield stress is present [61]. The fracture energy provides an indication of the propagation of cracks within asphalt

pavement at low service temperatures. In this study, it was determined by calculating the area under the curve of the IDT strength test using the trapezoidal method and dividing by the crack cross-section (ASTM D8225-19).

5.5.6 Wheel Tracking Tests

Rutting Test

Figure 5-5a displays the result of the wheel tracking test. As expressed, the increase in rutting resistance varies as the concentration of the respective nanomaterial in the neat binder. The neat binder had a rut depth of 11.6 mm at 20,000 passes. For nanoclays at 20,000 passes, the 6% samples of bentonite and halloysite had a respective 72% and 75% increase in rutting resistance (or rut depth reduction) when compared with the neat binder, while the 3% samples of bentonite and halloysite had a 32% and 33% increase in rutting resistance, respectively. The CNC, though used in smaller concentrations than the nanoclays, had a 29% and 44% increase in rutting resistance at 0.5% and 1% concentrations, respectively.

There exists some correlation between the rutting results from the dynamic shear rheometer (DSR) and those from the HWTD. The maximum velocity of the steel wheel at the centre of the sample in the HWTD is 0.305 m/s or 1.098 km/hour. The angular frequency of 10 rad/s in the DSR test corresponds to a speed of 88 km/h (55 mph) [107]; therefore, by linear interpolation, the frequency corresponding to 1.098 km/h is 0.124 rad/s. Hence, the rutting parameter at the angular frequency of 10^{-1} (approximately 0.124) rad/s on the DSR simulates a vehicle moving at 1.098 km/h on the HWTD. Comparing the rutting parameter improvement at 10^{-1} rad/s with that of the HWTD, there appears to be similarity except for the 6% nanoclays (bentonite and halloysite), which show a greater than 80% difference (Figure 5-5b).

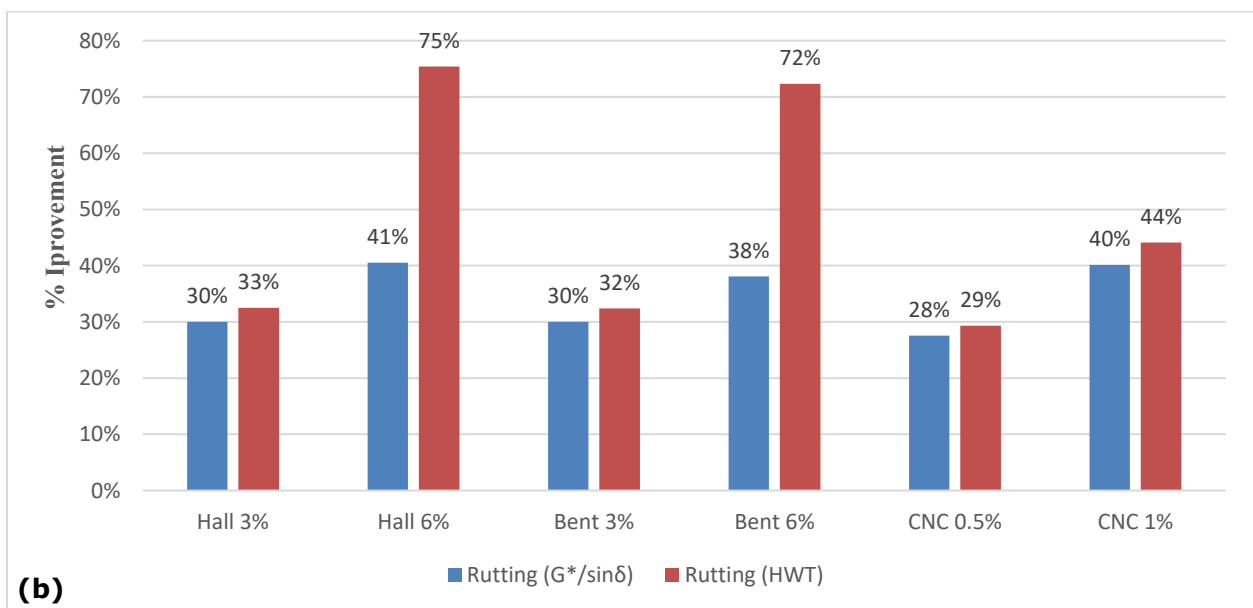
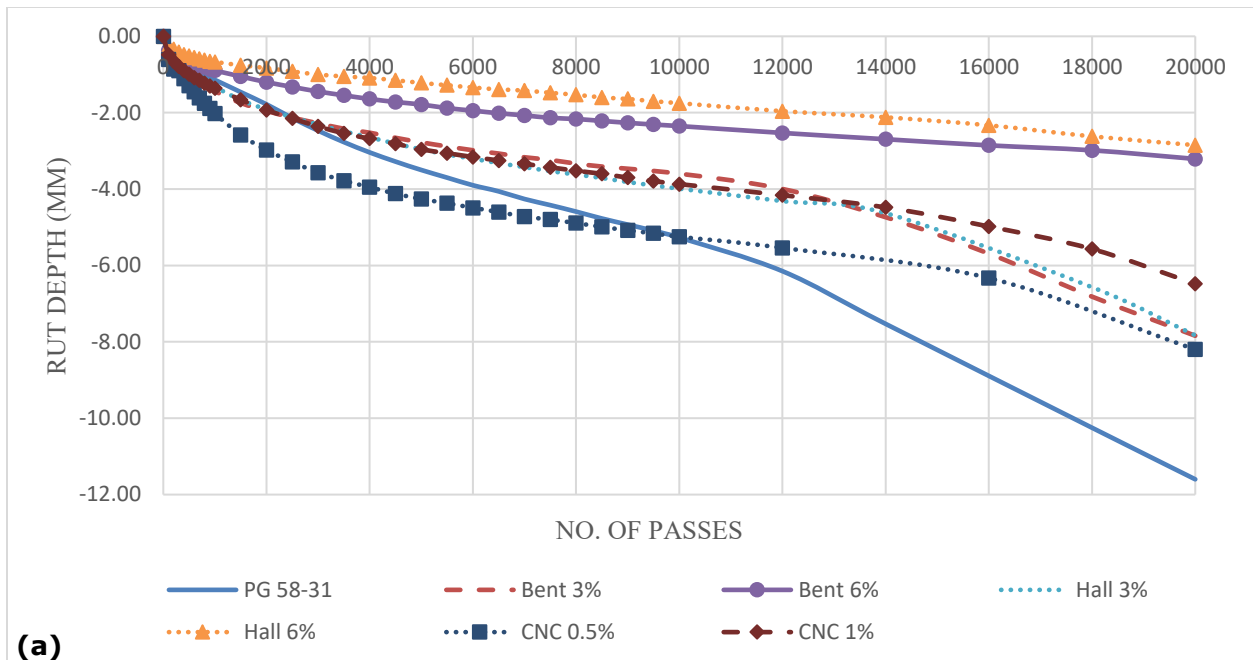


Figure 5-5: (a) HWT Results (b) Rutting improvement comparison of rheology test and wheel tracking test

Moisture Susceptibility

It is clear from Figure 5-6 that the neat binder is sensitive to moisture damage (i.e. SIP is less than 10,000). However, at least 55% improvement in the HMAs' resistance to moisture damage can be achieved with nano material modification.

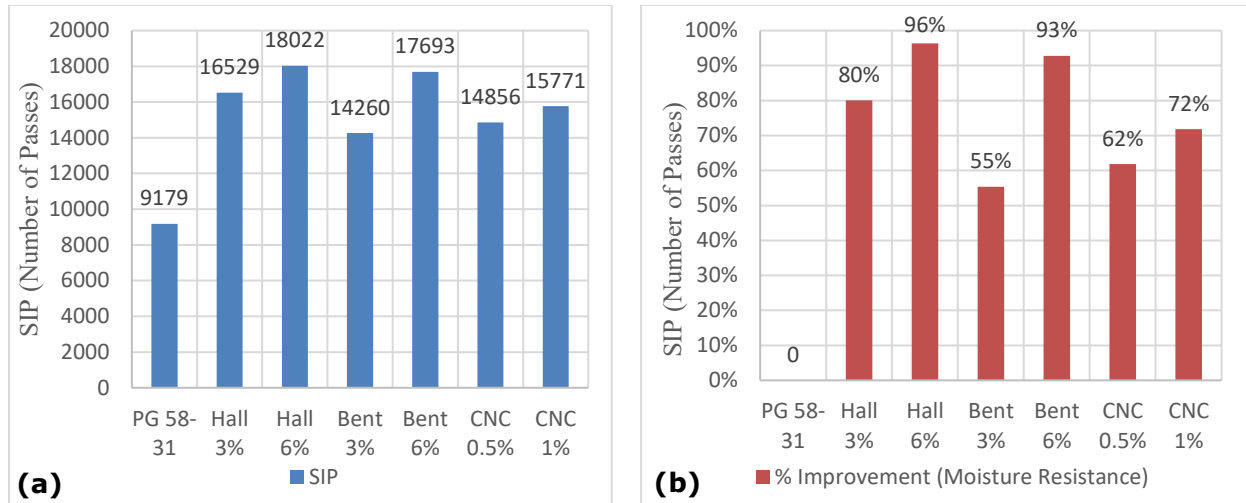


Figure 5-6: Moisture sensitivity: (a) Stripping inflection point; (b) Improvement in moisture resistance

Indirect Tensile Creep and Strength Tests

Based on the results shown in the Table 5-2, 6% bentonite and halloysite added to the base binder slightly reduced the tensile strength of the mix, by approximately 1% and 3% respectively, but increased the fracture energy, by 20% and 2% respectively. 3% nanoclay had little or no effect on the creep compliance when 3% nanoclay was used in the base binder; however, the addition of 6% nanoclay caused a 12% (halloysite) to 69% (bentonite) reduction in the creep compliance when compared to the control mix. The CNC, on the other hand, displayed an increase in tensile strength and fracture energy as concentration increased, but showed a reduction in creep compliance as concentration increased.

TABLE 5-2: Indirect Tensile Strength and Creep Test Results

Parameters	PG 58-31	3% Bent-modified	6% Bent-modified	3% Hall-modified	6% Hall-modified	0.5% CNC-modified	1% CNC-modified
Creep compliance [D(t)], 1/GPa (-20°C)	0.0032	0.0032	0.0010	0.0035	0.0028	0.0054	0.0046
Tensile strength (St,n), MPa (-20°C)	4.40	3.78	4.09	4.38	3.42	4.06	4.40
Fracture Energy, kJ/m ² (-20°C)	4.767	5.880	5.076	4.190	3.821	3.986	5.307
Tensile strength (St,n), MPa (-10°C)	3.72	3.73	3.67	4.15	3.62	3.61	3.80

Fracture Energy, kJ/m ² (-10°C)	4.057	4.994	4.873	4.574	4.166	4.783	4.951
---	-------	-------	-------	-------	-------	-------	-------

5.6 Cost Performance Analysis of Nanomodified Asphalt

The novelty of the technology and the complexity of the equipment and relatively high costs of currently available nanomaterials. The cost of the nanomaterials, at least, is one factor that can be reasonably expected to decrease over time, as a result of improvements in manufacturing technologies. Furthermore, it is expected that superior long-term performance of modified asphalt materials will result in a high performance to price ratio and thus a low life cycle cost relative to other materials [66]. Table 5-3 shows binders modified with 6% halloysite offer a substantial reduction in rut depth but come at a cost that is twice that of bentonite binders with the same concentration and rut-depth reduction values. Comparing the binders made with CNC and nanoclays, the 1% CNC binder provides a greater rut-depth reduction (44%) than the 3% nanoclay binders at approximately 3% and 5% of the cost of the bentonite and halloysite, respectively. Considering the cost of CNC material, its rate of application and effectiveness in decreasing permanent deformation and increasing fracture energy of asphalt mixes, it is concluded that CNC material has a good potential to be used as asphalt binder modifier.

TABLE 5-3: Added Cost Versus Performance Analysis Per Ton of HMA

Material	Mass of Asphalt /ton of mix (kg)	Added Quantity of Nanomaterial (%)	Added Quantity of Nanomaterial (kg)	Cost/kg of nano-material (CAD/kg)	Total Added Material Cost (CAD/ton)	Rutting Improvement (%)	Fracture Energy Improvement (%)
Bentonite	55	3	1.65	6.55 ¹	10.81	32	23
	55	6	3.3		21.62	72	20
Halloysite	55	3	1.65	6.55 ¹	10.81	33	13
	55	6	3.3		21.62	75	3
CNC	55	0.5	0.275	30.00 ²	8.25	29	18
	55	1	0.55		16.50	44	22

Note:

¹ Equivalent of US\$4.96 [13], [65]

² Early commercial stage cost estimates. A reduction in cost is expected with more continuous/automated manufacturing and chemical recovery

5.7 Conclusion

The conclusions obtained from this study can be summarized as follows:

- SEM results show that the use of the high shear mixer for the dispersion of untreated nano materials in the asphalt binder is adequate.
- $G^*/\sin \delta$ master curves for modified binders using both nano-clays and CNC show an improvement in rutting resistance at lower frequencies (higher temperatures) and no significant difference at higher frequencies (lower temperatures).
- The addition of nanoclay or CNC to an asphalt binder results in significant improvements to the rutting resistance, moisture sensitivity and toughness of the modified HMA mixes. However, the addition of nano material results in higher mixing and compaction temperatures (except for 0.5% CNC) that leads to an increase in energy consumption during modified HMA production and compaction.
- IDT test results show that the addition of nanoclays and CNC will not have any adverse effect on low-temperature properties of modified asphalt mixes.
- Comparison between two different nanoclays show that the addition of bentonite and halloysite affects modified HMA rutting resistance similarly; however, bentonite modified mixes are more flexible at lower temperatures.
- Using nanoclay (bentonite and halloysite) as an asphalt modifier offers significant improvements to the rheological properties of the asphalt with a consequent improvement in the asphalt mix performance (i.e. rutting resistance) particularly at high service temperatures (improvements are remarkable at high temperatures with 6% by weight of the binder). In the same vein, CNC offers up to 60% of the rutting resistance provided by the nanoclays with approximately 17% of the quantity and 76% of the cost. However, the expected reduction in the cost of the CNC provides both CNC and nanoclay as potential asphalt modifiers.

This research was limited to high and low temperatures performance tests. It will be continued with other performance tests such as IDEAL-CT to investigate the effect of nano material on cracking at intermediate temperatures and dynamic modulus test to investigate the stiffness of modified asphalt mixes using nano material at different temperatures and loading frequencies.

6 Laboratory Investigation of Permanent Deformation of Modified Asphalt mixes using Nanocellulose

6.1 Abstract

Rutting is one of the major distresses associated with flexible pavements. In North America, low performance grade (or softer) asphalt binders are usually used to prevent thermal cracking. However, these pavements undergo severe plastic deformation during the summer months. Rising in global temperatures and increase in vehicle axle loads may require engineered asphalt cement modification.

In recent years, nanomaterials, i.e. materials with at least one dimension less than 100 nm, have been introduced as potential modifiers of asphalt binders. Previous studies suggest that these materials, which have varying morphology depending on their origins (e.g. cellulose nanocrystals – rectangular rod-like), have the capacity to increase shear modulus at high temperatures, increase asphalt cement toughness at low temperatures and decrease thermal susceptibility.

This study focused on the permanent deformation of hot mix asphalt (HMA) produced with PG 58-31 asphalt binder modified using different contents of cellulose nanocrystals (0.5%, 1% and 3% by weight). Qualitative techniques were used to evaluate the dispersion of the cellulose nanocrystals in the asphalt binder. In addition, the rheological characteristics of both the modified and unmodified binders were evaluated. Finally, the mechanical performance of HMA containing nano-modified binders, including its permanent deformation and moisture susceptibility at high temperature, was evaluated and compared with that of the neat asphalt binder.

6.2 Introduction

Canada has a total of 1.13 million km of paved (40%) and unpaved (60%) roads making it the 7th largest road network in the world [108]. 90% of the paved roads in Canada's network is surfaced with asphalt and provide the dominant mode of transportation of moving goods between Canada and the U.S. [109], Exposure to extremely low air temperatures and seasonal freeze-thaw cycles have resulted in distress of these flexible pavements, decreased performance of the asphalt layer and, consequently, pavement life [110]. Considering the average annual expenditure of \$3.54 since 2006 [108], prevention of premature failure has become a primary strategy for road owners [111].

The Strategic Highway Research Program (SHRP) identified plastic deformation, or rutting, as one of the three major distresses associated with flexible pavements in North America. This distress appears as a surface depression in the wheel path which may be accompanied by uplift of the pavement along the sides of the rut. Ruts decrease performance and they pose safety risks to road users in several ways: (1) cause vehicle hydroplaning when filled with water; and (2) tend to pull a vehicle towards the rut path as it is steered across the rut [112].

Asphalt binder modification has been found to be promising for increasing the performance of asphalt pavements at extreme temperature ranges. Previous research suggests that the addition of cellulose nanocrystals to asphalt binder can increase its shear modulus at high temperatures, increase asphalt cement toughness at low temperatures, and decrease its thermal susceptibility [113].

6.2.1 Objectives and Scope

The objective of this research is to investigate and compare the effects on the properties of PG 58-31 with the addition of cellulose nanocrystals (CNC) in 3 distinct amounts by weight of the binder (i.e. 0.5%, 1% and 3%). The effects of the binder modifications on the asphalt mixes produced are also investigated and compared. The Superpave asphalt mixture design and analysis system was used to evaluate the following properties: (1) asphalt cement rheology at high service temperatures using the dynamic shear rheometer (DSR); (2) asphalt mix performance at high service temperatures using the Hamburg wheel tracker (HWT) permanent rutting test at 45°C; and (3) moisture sensitivity of asphalt mixes using the inflection points of asphalt mixes after conducting HWT tests.

6.3 Materials and Modification Method

6.3.1 Asphalt Binder

PG 58-31 was used as the control binder for this research. It appears as a black, viscous liquid with a melting/freezing point of more than 31°C, a boiling range above 228°C, and a flash point greater than 243°C. It has a relative density of 1.02 to 1.04 at 15°C and 1 atmosphere, and a viscosity of 0.100 to 0.800 Pascal-seconds at 135°C [114].

6.3.2 Cellulose Nanocrystals (CNC)

Cellulose nanocrystals (CNC) are a derivative of cellulose, the most important and naturally abundant organic biopolymer in the biosphere. CNC constitutes between 40% and 90% of plants and their associated derivatives, and is composed of carbon, hydrogen, and oxygen bioengineered as a linear homopolysaccharide chain with cellobiose as the recurring building

block. The cellulose molecules, which make up the cellobiose block, are held together by many hydrogen bonds that maintain a strong lateral association between the chain-like linear cellulose molecules. However, the interruption of these crystalline regions (i.e. strong, highly oriented) with amorphous regions (i.e. weak, poorly oriented) makes it possible for nanosized cellulose-based crystals (or CNCs) to be isolated by acid hydrolysis [36]

6.3.3 Preparation of the Nanomodified Asphalt

The neat binder was first preheated to 140°C. 500 grams was poured into a cylindrical container and placed on a hot plate. While maintaining the temperature between 140°C and 150°C, the CNC (at 0.5%, 1% and 3% by weight of 500 grams of neat asphalt binder for each mixture) was incrementally added to the binder in small quantities and mixed using a high shear mixer at a shear rate of 5500-6000 revolutions per minute for 4.5 hours. To ensure that the mixing time, temperature and shear rate had no ageing effect on the neat binder, a 500-gram specimen of the neat binder was also subjected to the same mixing conditions and analyzed using dynamic mechanical analysis (DMA).

6.3.4 Qualitative Evaluation of the Modified Asphalt Binder Sample

The dispersion of the CNC in the asphalt binder was qualitatively evaluated using the Zeiss Sigma Field Emission Scanning Electron Microscope (FESEM) at nanoFAB (University of Alberta). CNC-modified asphalt samples were first sputter-coated with 2–20 nm gold films using the Denton Gold Sputter Unit to improve conductivity of the specimen in the FESEM [70]. The dispersion of the CNC in the binder appeared to be consistent after 4.5 hours of mixing at a rate of 5500-6000 rpm (Figure 6-1). However, some agglomerations observed may be improved [115].

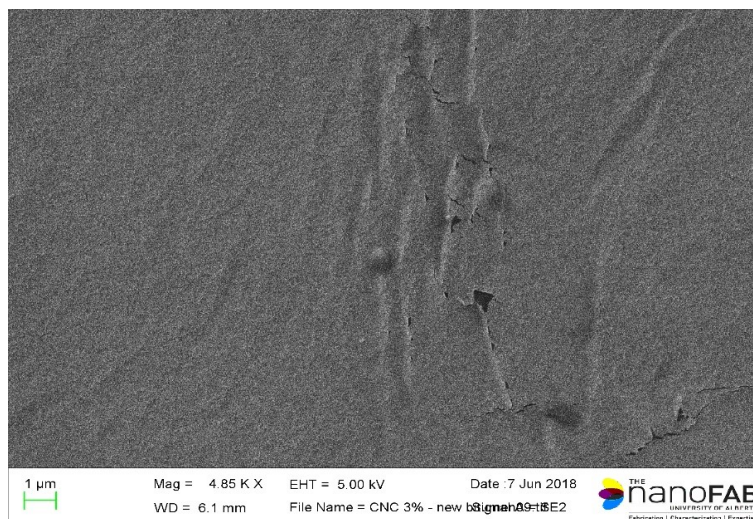


Figure 6-1: FESEM image of CNC-modified binder

6.4 Laboratory Testing

6.4.1 Rheological Testing (Asphalt Binder)

Using the dynamic shear rheometer, with an 8-mm diameter parallel plate, a gap of 2 mm and an angular frequency range between 0.3 and 300 rad/s, frequency sweep tests were performed at loop temperatures of 40°C, 30°C, 20°C, 10°C and 4°C (AASHTO T315-10). A minimum of four tests were conducted for each of the samples (modified and unmodified) and the average of the results were compared. The complex modulus (G^*) and the phase angle (δ) were determined by the Rheoplus software and the master curves of the rutting parameter ($G^*/\sin \delta$) were plotted at 20°C.

As shown in Fig. 2, there was an increase in the rutting parameter for all CNC-modified asphalt binders particularly at lower frequencies (or higher temperatures). This is an indication that HMA produced CNC-modified binders is less susceptible to rutting than HMA produced with the neat asphalt binder.

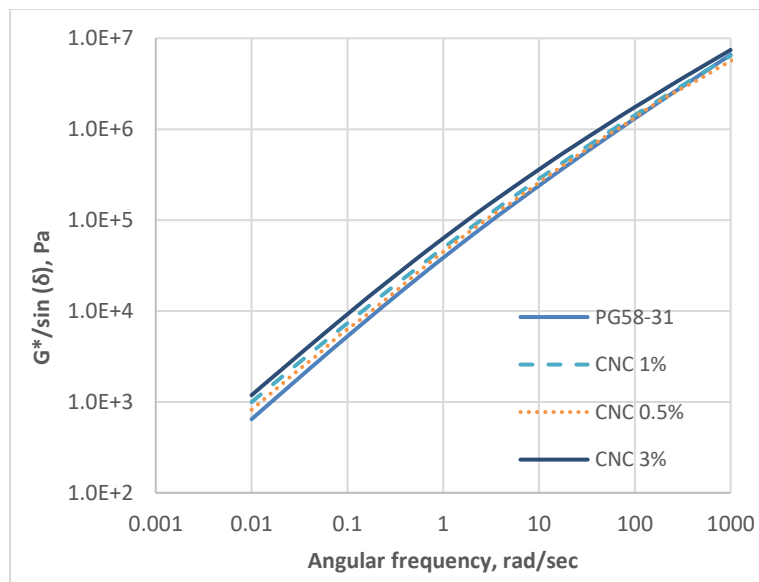


Figure 6-2: Comparison of rutting parameter vs angular frequency for the neat and CNC-modified asphalt binders

6.4.2 HWT Testing

Asphalt mix samples, produced using neat and modified binders, were evaluated for rutting potential and moisture susceptibility using a Hamburg Wheel Tracking Device (HWT). The device moved a steel wheel ($705 \pm 4.5\text{N}$, 47-mm wide) an approximate distance of 230 mm across a pair of submerged cylindrical HMA samples at a frequency of 52 ± 2 passes per minute and a maximum speed of 0.305 m/s at midpoint. Before testing using the HWT, each

specimen – composed of a pair of 150-mm diameter cores – was compacted to approximately 6% air voids using a Superpave gyratory compactor, then saw-cut along a secant line such that, when joined together in the high-density polyethylene molds, a maximum gap of 7.5 mm was achieved between the molds. Testing was performed in accordance with AASHTO T 324-16 at 45°C for 20,000 passes, or until a rut depth of 12mm was achieved (whichever occurred earlier). The rutting depth was plotted against the number of passes to provide valuable information about the susceptibility of the asphalt concrete mixes to plastic deformation and moisture damage. It is expected that moisture damage begins to take effect at the stripping inflection point (SIP) and accelerates the deformation. HMA samples with SIP less than 10,000 passes may be susceptible to moisture damage [116].

Figure 6-3 shows that the increase in rutting resistance varies as the concentration of the respective nanomaterial in the neat binder. The HMA with neat binder showed a rut depth of 11.6 mm at 20,000 passes. At 20,000 passes, HMA with CNC added to the binder showed a 29%, 44% and 60% increase in rutting resistance at 0.5%, 1% and 3% (by weight of the asphalt), respectively.

It is clear from Figure 6-4a that the HMA with neat binder is sensitive to moisture damage (i.e. SIP less than 10,000). With the CNC modification of the PG 58-31 performance grade asphalt binder, a minimum of a 54% improvement in the HMAs' resistance to moisture damage can be achieved (Fig. 6-4b).

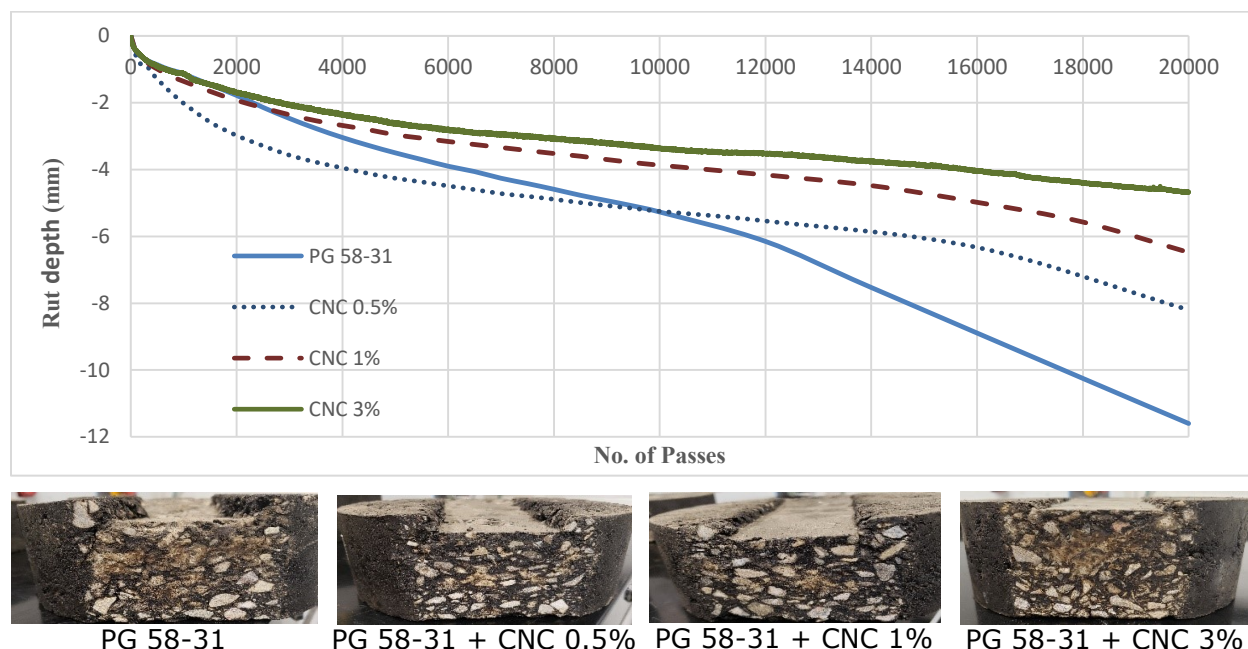


Figure 6-3: Results of HWT for HMA samples made with neat and CNC-modified asphalt binders

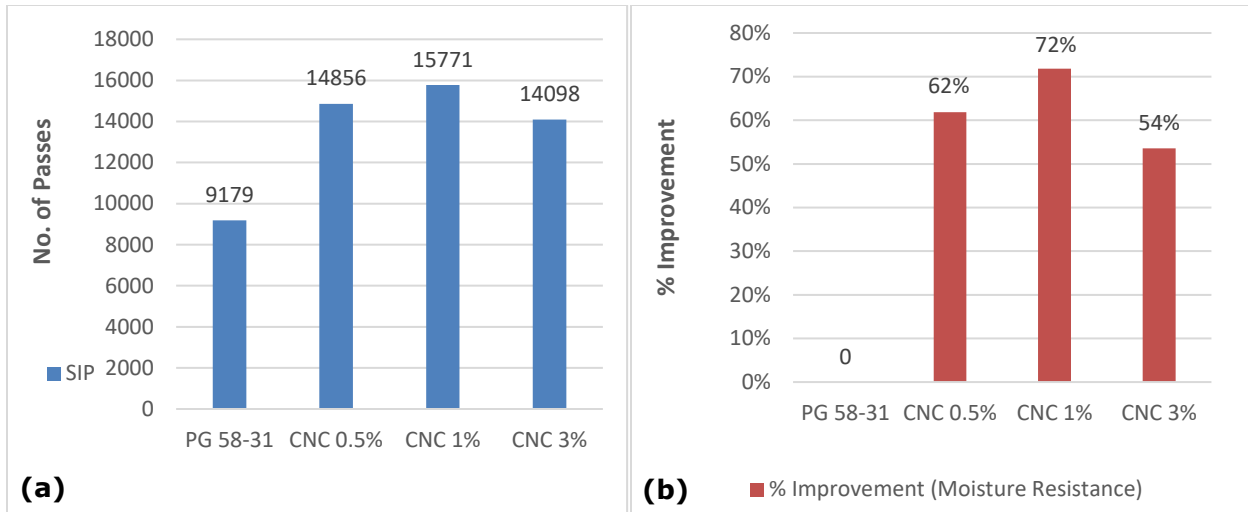


Fig. 6-4: (a) SIP for neat and CNC-modified asphalt binders (b) Improvement in moisture resistance

6.4.3 3.3 Comparison of Rheology Test and HWD Test Results

Rutting in asphalt pavements increases with increasing traffic volume and decreasing traffic speed. The maximum velocity of the steel wheel at the center of the sample in the HWTD is 0.305 m/s or 1.098 km/hour. The angular frequency of 10 rad/s in the DSR test corresponds to a speed of 88 km/h (55 mph) [107]; therefore, by linear interpolation, the frequency corresponding to 1.098 km/h is 0.124 rad/s. Hence, the rutting parameter at the angular frequency of 10^{-1} (approximately 0.124) rad/s on the DSR and the steel wheel on the HWTD simulates a slow-moving vehicle with a velocity of 1.098 km/h. The results of both the DSR and HWTD testing are shown in Fig. 6-5.

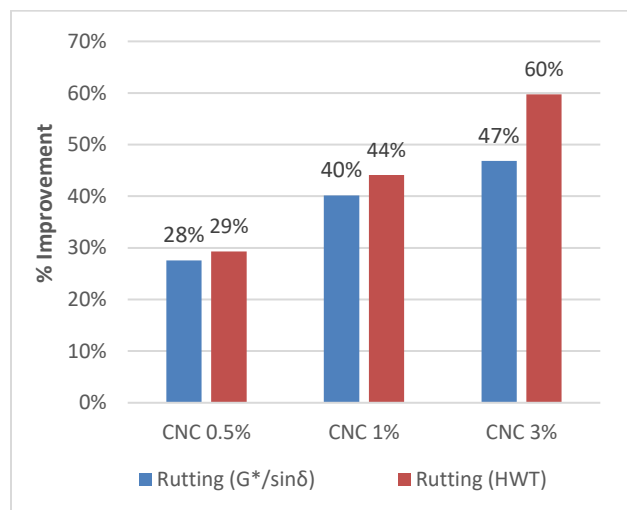


Fig. 6-5: Correlation between rutting improvement results for both DSR testing and HWT testing

6.5 Conclusions

The conclusions obtained from this study can be summarized as follows:

- SEM results revealed that using a high shear mixer was effective on dispersing CNC powder in asphalt binder, however, dispersion could be improved.
- The rheology test results showed that the addition of 0.5%, 1% and 3% concentrations CNC (per binder weight) to PG 58-31 performance grade asphalt binder improves the stiffness by 28%, 40% and 47%, respectively, of the binder.
- HWT results showed that there was 29%, 44% and 60% improvement in rutting characteristics of 0.5%, 1% and 3% concentrations CNC modified binders, respectively.
- HWT results showed also 62%, 72% and 54% improvement in moisture resistance of 0.5%, 1% and 3% concentrations CNC modified mixes, respectively
- Comparison between the rutting results of HWT and rutting criteria from rheology test showed that rheological measurements can conservatively predict the rutting potential of the asphalt mixs

7 Additional Testing

7.1 Asphalt Binder Performance Grading

7.1.1 High Temperature Performance Grading (Dynamic Shear Rheometer - DSR)

The high temperature PG grading of the unaged and RTFO-aged modified/unmodified asphalt binders were evaluated using the DSR and the results are displayed in Table 7-1. The failure temperatures of the unaged and the RTFO-aged specimens were then compared, and the lower failure temperature was considered the “continuous high PG grade” (meaning the temperature at which either or both specimens failed). The standard high PG grade becomes the highest standard temperature both specimens passed. These are also tabulated in Table 7-1.

Table 7-1: High Temperature PG Grade

No.	Binder Description	Supplier	High PG Grade (Unaged Binder)	High PG Grade (RTFO-Aged Binder)	Continuous High PG Grade	Standard High PG Grade
1	PG 58-31	Husky Lloydminster Refinery, AB, Canada	64.2	65.7	64.2	64
2	PG 58-31 + 3% Bentonite	Lab prepared	66.1	67.1	66.1	64
3	PG 58-31 + 6% Bentonite	Lab prepared	67.1	67.6	67.1	64
4	PG 58-31 + 3% Halloysite	Lab prepared	66.8	64.3	64.3	64
5	PG 58-31 + 6% Halloysite	Lab prepared	67.1	67	67	64
6	PG 58-31 + 0.5% CNC	Lab prepared	65.7	65.8	65.7	64
7	PG 58-31 + 1% CNC	Lab prepared	66.8	66.4	66.4	64

The asphalt binder received from Husky Energy was classified as PG 58-31, meaning that it is intended to be used where the average 7-day maximum pavement temperature is 58°C and the minimum pavement temperature of -31°C. However, upon validation, the high PG

grade of the unaged unmodified PG 58-31 was PG 64. Although the nanomodification experienced no grade bump (i.e. the standard high PG grade experienced less than 6°C increment in continuous high PG grade temperature), the 6% nanoclays and 1% CNC had higher increase in failure temperatures than their respective 3% nanoclays and 0.5% CNC. This indicates an increased load carrying capacity, as well as a higher resistance to rutting, of asphalt mixes produced with the nano-modified binders.

Interestingly, the unaged 3% halloysite high PG grade was 66.8 but did not perform as expected after the RTFO-ageing (64.3). Although the 3% bentonite performed better than the 3% halloysite in the continuous high PG grade, their respective 6% counterparts performed relatively similarly. The high continuous PG grade of the 1% CNC is similar to that of the 3% bentonite (Figure 7-1).

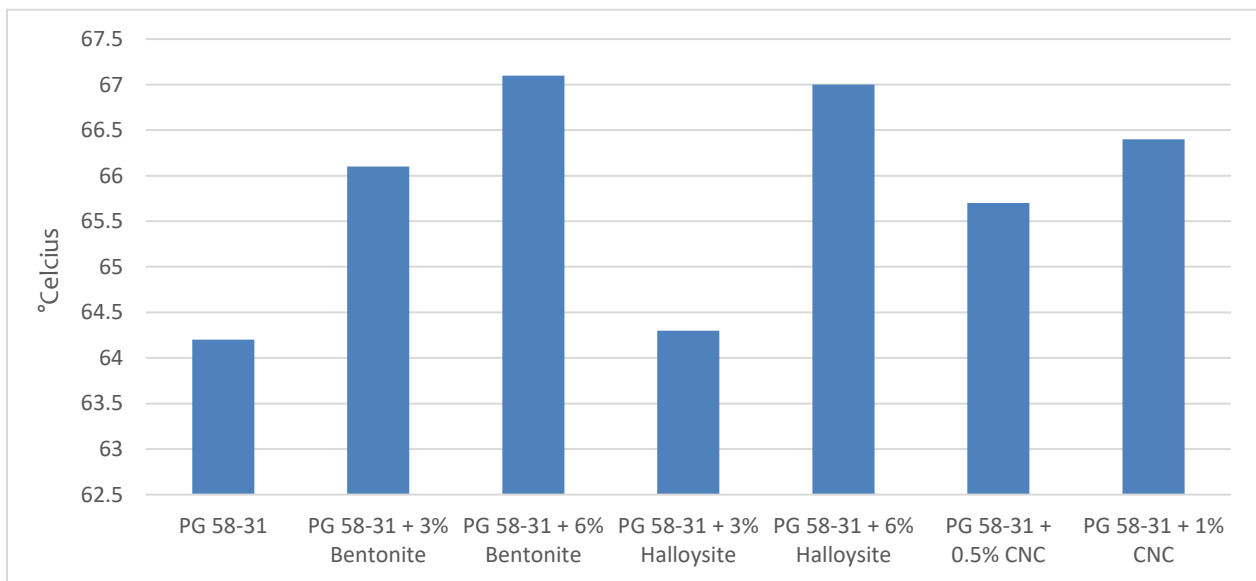


Figure 7-1: Continuous high PG grade

7.1.2 Low Temperature Performance Grading (Bending Beam Rheometer - BBR)

The bending beam rheometer (BBR) is used to determine the asphalt binder low temperature PG grade. The creep stiffness of the beam and the m-value are measured at 8, 15, 30, 60, 120 and 240 seconds and a stiffness master curve is plotted. Two replicates were tested for each asphalt binder type and the results are tabulated below (Table 7-2). The maximum temperature at which both the m-value and creep stiffness conditions were satisfied was considered the “continuous low PG grading” (or failure temperature). The highest standard temperature at which both creep stiffness and m-value were satisfied is considered the low temperature PG grade of the asphalt binder (Table 7-2).

Table 7-2: Low Temperature PG Grade

NO.	Binder Description	Supplier	m-value Low PG Grade	Stiffness Low PG Grade	Continuous Low PG Grade	Standard Low PG Grade
1	PG 58-31	Husky Lloydminster Refinery, AB, Canada	-32.91	-31.52	-31.52	28
2	PG 58-31 + 3% Bentonite	Lab prepared	-31.48	-31.05	-31.05	28
3	PG 58-31 + 6% Bentonite	Lab prepared	-30.97	-30.88	-30.88	28
4	PG 58-31 + 3% Halloysite	Lab prepared	-33.67	-31.85	-31.85	28
5	PG 58-31 + 6% Halloysite	Lab prepared	-31.72	-30.73	-30.73	28
6	PG 58-31 + 0.5% CNC	Lab prepared	-31.14	-31.23	-31.14	28
7	PG 58-31 + 1% CNC	Lab prepared	-29.96	-30.75	-29.96	28

For the low temperature PG grading of the unmodified asphalt binder, the continuous low PG grade was -31.52, which satisfies the description of the manufacturer. However, its standard low PG grade description is -28. Like the high temperature PG grade, there was no grade bump (i.e. the low PG grade remained at -28); however, the lower concentrations of nanoclays (3%) and CNC (0.5%) displayed a slightly better performance than their respective high concentrations of 6% and 1%, respectively. Moreover, 3% halloysite showed a slight improvement in the low temperature properties when compared with the unmodified asphalt binder (Figure 7-2). Again, the low temperature performance of the 1% CNC is similar to that of the 3% bentonite.

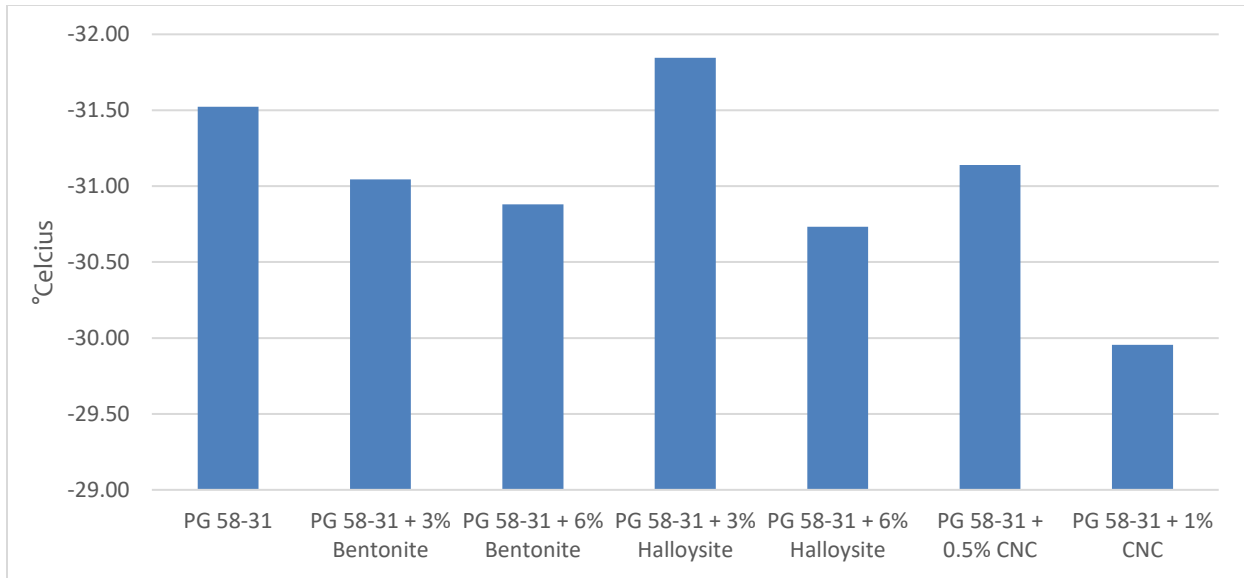


Figure 7-2: Continuous low PG grade

7.1.3 Intermediate Temperature Performance (Fatigue Resistance)

The performance of the modified/unmodified asphalt binders at intermediate service temperatures was evaluated using the DSR and the results are displayed below (Table 7-3).

Table 7-3: Fatigue Performance of Modified/Unmodified Asphalt Binders

NO.	Binder Description	Supplier	$G^* \sin \delta$ @ 16°C
1	PG 58-31	Husky Lloydminster Refinery, AB, Canada	4692.6
2	PG 58-31 + 3% Bentonite	Lab prepared	4253.3
3	PG 58-31 + 6% Bentonite	Lab prepared	4489.2
4	PG 58-31 + 3% Halloysite	Lab prepared	2342.9
5	PG 58-31 + 6% Halloysite	Lab prepared	4316.7
6	PG 58-31 + 0.5% CNC	Lab prepared	3506.6
7	PG 58-31 + 1% CNC	Lab prepared	4343.5

The 3% halloysite-modified binder offers the best fatigue resistance than all the modified/unmodified binders.

7.2 Indirect Tension Asphalt Cracking Test (IDEAL-CT) – Fatigue Resistance

Three replicates for each modified/unmodified binder type (total of 21 samples) were prepared in the laboratory and tested using the Universal Testing Machine (UTM) in accordance with ASTM D8225-19 and the results are shown below (Table 7-4 and Figure 7-3).

Table 7-4: Results for the IDEAL-CT

Binder Description	CT index
PG 58-31	294.36
PG 58-31 + 3% Bentonite	384.12
PG 58-31 + 6% Bentonite	527.06
PG 58-31 + 3% Halloysite	324.22
PG 58-31 + 6% Halloysite	381.42
PG 58-31 + 0.5% CNC	468.65
PG 58-31 + 1% CNC	344.92

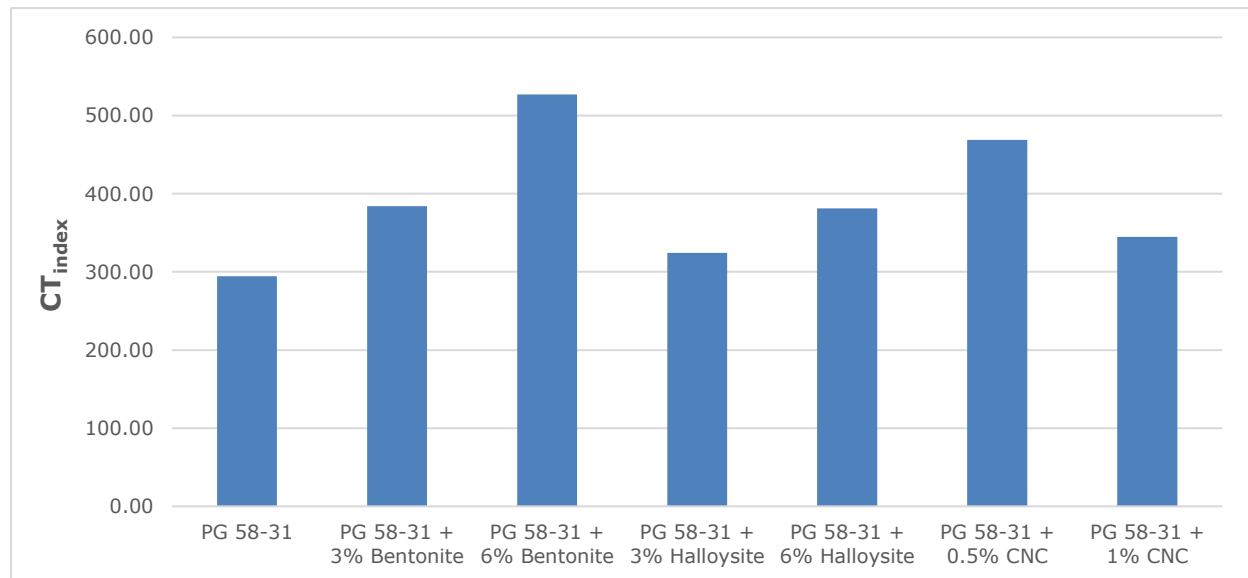


Figure 7-3: CT index of modified/unmodified asphalt mixes

As can be observed from the results, the samples prepared with the nano-modified asphalt binders displayed an increase in CT index with 6% bentonite exhibiting the highest value of 527 (almost twice that of the neat binder) and 0.5% CNC displaying approximately 468 in second place. The 2 concentrations of halloysite and 1% CNC displayed similar performance

as the 3% bentonite. It can be said that 6% bentonite provides the highest resistance to fatigue than all the nano-modified binders.

7.3 Moistures Sensitivity (Stripping)

The results of the moisture sensitivity evaluated using the Lottman procedure are tabulated in Table 7-5 below.

Table 7-5: Indirect Tensile Strength (ITS) Results

S/No.	Binder Description	Condition	No. of Specimens	Average Air Voids (%)	Tensile Strength (kPa)	Tensile Strength Ratio
1	PG 58-31	Dry	3	7%	643	0.83
		Wet	3	7%	533	
2	PG 58-31 + 3% Bentonite	Dry	3	6%	1060	0.72
		Wet	3	7%	762	
3	PG 58-31 + 6% Bentonite	Dry	3	6%	1031	0.69
		Wet	3	6%	707	
4	PG 58-31 + 3% Halloysite	Dry	3	6%	985	0.81
		Wet	3	6%	799	
5	PG 58-31 + 6% Halloysite	Dry	3	6%	1264	0.80
		Wet	3	6%	1007	
6	PG 58-31 + 0.5% CNC	Dry	3	7%	990	0.82
		Wet	3	6%	816	
7	PG 58-31 + 1% CNC	Dry	3	6%	974	0.82
		Wet	3	6%	799	

All the HMA specimens, except those produced with the bentonite-modified asphalt binder, made with the neat and modified binders displayed TSRs above 80%. These specimens can be considered to have an acceptable level of moisture sensitivity. The TSRs of the asphalt mixes produced with the bentonite-modified border the lower limit of the criteria and can still be considered acceptable.

8 Summary and Conclusions

8.1 Summary

The application of nanotechnology in pavement engineering is a novel technology with the potential to significantly enhance the rheological properties of the binder as well as the asphalt mixtures produced therewith. Hence, laboratory investigation is therefore, essential to provide valuable information with which to predict field performance more reliably.

The objective of this study is to investigate and compare the effects of the application of bentonite nanoclay, halloysite nanoclay and cellulose nanocrystals (CNC) on asphalt rheology and asphalt mix performance. For this purpose, nano-modified asphalt binders were prepared and subjected to the Superpave binder testing regime, and the asphalt mixes produced therewith were also tested.

8.2 Conclusions

The results of the laboratory analysis will contribute greatly to the existing information on nano-applications in flexible pavements. The conclusions obtained are summarized as follows:

1. A trial-and-error process was used in the laboratory to determine a mixing method that would provide a matrix with a well-dispersed nanomaterial. By carrying out a series of scanning electron microscopy (SEM) on the nano-modified asphalt specimens, it was determined that a mixing time of 5 hours, mixing speed of 5,500 revolutions per minute (rpm), and mixing temperature of $145\pm 5^{\circ}\text{C}$ produced a nano-modified asphalt binder with little or no agglomeration of the nano-particles. Hence, it can be concluded that use of a high shear mixer was effective for the dispersion of the nanomaterials in the asphalt binder.
2. Quality control/assurance was conducted on the mixing process to ensure that the neat binder did not undergo any significant structural or chemical change by subjecting the neat binder to the same mixing conditions: 5,500 rpm at a temperature of $145\pm 5^{\circ}\text{C}$ for 5 hours. No significant difference in rheology was observed thereafter.
3. Based on rheology test results, considering $G^*/\sin \delta$ as an indicator for asphalt cement rutting, and a low frequency of 0.1 rad/sec which correlates with the HWT, all nano-modified binders displayed an improvement in resistance to rutting (6% nanoclays and 1% CNC showed approximately 40% improvement; 3% nanoclays and 0.5% CNC showed about 30% improvement)

4. The results of the rutting tests performed using the Hamburg wheel tracking device (HWTd) can be correlated to DSR test results, since the maximum speed of the HWTd is equivalent to 0.1 rad/sec. Except for the higher concentrations of the nanoclays (6%) which displayed almost twice the improvement of the 3% concentrations, the HWTd corroborates all the rutting results of the DSR for lower concentrations of the nanoclays (i.e. 3%) and all concentrations of the CNC.
5. Based on viscosity test results conducted using a rotational viscometer, the addition of 1% CNC, 3% bentonite and 3% halloysite to neat asphalt binder caused a 5°C increment in the mixing and compaction temperatures of their respective binders, while the addition of 6% bentonite and 6% halloysite caused a 10°C increment in the mixing and compaction temperatures. The addition of 0.5% CNC to the binder had no significant effect on the mixing and compaction temperatures.
6. Indirect tensile creep and strength test results showed that the nano-modification increased the fracture energy as follows: (1) 3% and 6% bentonite (by weight of the binder) increased 23% and 20%, respectively; (2) 3% and 6% halloysite (by weight of the binder) increased 13% and 3%, respectively; and (3) 0.5% and 1% CNC (by weight of the binder) increased 18% and 22%, respectively. Fracture energy decreased for increasing concentrations of the nanoclays but increased for increasing concentrations of CNC. Moreover, increase in fracture energy is an indication of more resistance to crack propagation at low service temperatures.
7. The indirect tension asphalt cracking test illustrated the following increase in the CT index of modified asphalt mix specimens as follows: (1) 3% and 6% bentonite (by weight of the binder) increased 30% and 79%, respectively; (2) 3% and 6% halloysite (by weight of the binder) increased 10% and 30%, respectively; and (3) 0.5% and 1% CNC (by weight of the binder) increased 59% and 17%, respectively. This indicates an increase in the resistance to fatigue cracking.
8. The standard Superpave performance grade of the neat asphalt binder received from the manufacturer, determined by verification, was PG 64-28. Hence, the Superpave performance grade test results showed that the addition of bentonite (3% and 6%), halloysite (3% and 6%), and CNC (0.5% and 1%) in their respective proportions by weight to the base binder did not cause any change in the performance grade of their respective modified binders. The additions, however, increased the high temperature continuous grade of the respective modified binders. The overall performance test

results showed that the rheological performance of binder modified using 3% nanoclay (bentonite and halloysite) is similar to the binder modified using 1% nanocellulose.

9. Using nanoclay (bentonite and halloysite) as an asphalt modifier offers significant improvements to the rheological properties of the asphalt with a consequent improvement in the asphalt mix performance (i.e. rutting resistance) particularly at high service temperatures (improvements are remarkable at high temperatures with 6% by weight of the binder). In the same vein, CNC offers up to 60% of the rutting resistance provided by the nanoclays with approximately 17% of the quantity and 76% of the cost. However, the expected reduction in the cost of the CNC provides both CNC and nanoclay as potential asphalt modifiers.

References

1. T. Delft, "Annual Report about Flexible and Rigid Pavement," Delft, The Netherlands, 2012.
2. Shell Bitumen, *The shell bitumen industrial handbook.*, Surrey, UK: Thomas Telford, 1995.
3. OHMPA, *The ABCs of PGAC: The Use of Performance Graded Asphalt Cements in Ontario*, Ontario: Ontario Hot Mix Producers Association, 1999.
4. G. Airey, "Rheological characteristics of polymer modified and aged bitumens," University of Nottingham, Nottingham, 1997.
5. M. Porto, P. Caputo, V. Loise, S. Eskandarsefat, B. Teltayev and C. Oliviero Rossi, "Bitumen and bitumen modification: A review on latest advances.," *Applied Sciences*, vol. 9, no. 4, p. 742, 2019.
6. V. Papadimitropoulos, S. Karatzas and A. Chassiakos, "Applications of Nanomaterials in Pavement Engineering: A Review.," in *The Tenth International Conference on Construction in the 21st Century (CITC-10)*, Colombo, Sri Lanka, 2018.
7. R. M. Ho, A. Adedeji, D. W. Giles, D. A. Hajduk, C. W. Macosko and F. S. Bates, "Microstructure of triblock copolymers in asphalt oligomers," *Journal of Polymer Science Part B: Polymer Physics*, vol. 35, no. 17, pp. 2857-2877, 1997.
8. J. Zhu, B. Birgisson and N. Kringos, "Polymer modification of bitumen: Advances and challenges," 2017.
9. M. Vysotskaya and S. Shekhovtsova, "Nanotubes as a modifier polymer modified binder and asphalt concrete," in *International Conference on Structural, Mechanical and Materials Engineering ICSMME*, 2015.
10. Dhawo, I. Nur, W. Jiantao, L. Quan and I. Shaban, "The effects of nano silica particles on the physical properties and storage stability of polymer-modified bitumen," *Journal of Civil Engineering Research*, vol. 5, no. 4A, pp. 11-16, 2015.
11. P. Deepa, M. Laad, Sangita and R. Singh, "An overview of use of nanoadditives in enhancing the properties of pavement construction binder bitumen," *World Journal of Engineering*, 15 March 2019.

12. B. Golestani, B. Nam, N. F. Moghadas and S. Fallah, "Nanoclay application to asphalt concrete: Characterization of polymer and linear nanocomposite-modified asphalt binder and mixture," *Construction and Building Materials*, vol. 91, pp. 32-38, 2015.
13. Z. Hossain, M. Zaman, T. Hawa and M. C. Saha, "Evaluation of moisture susceptibility of nanoclay-modified asphalt binders through the surface science approach," *Journal of Materials in Civil Engineering*, vol. 27, no. 10, p. 04014261, 2014.
14. S. G. Jahromi and A. Khodaii, "Effects of nanoclay on rheological properties of bitumen binder," *Construction and building materials*, vol. 23, no. 8, pp. 2894-2904, 1 August 2009.
15. ASTM International, "ASTM E2456-06. Standard Terminology Relating to Nanotechnology," ASTM: West Conshohocken, PA, 2012.
16. Federal Highway Authority/National Highway Institute, "Superpave Fundamentals Reference Manual (NHI Course #131053)," 2000. [Online]. Available: /web/20191110115908/https://idot.illinois.gov/Assets/uploads/files/Transportation-System/Manuals-Guides-&-Handbooks/T2/P028.pdf.
17. J. G. Speight, "Petroleum Asphaltene-Part 1: Asphaltene, resins and the structure of petroleum," *Oil & gas science and technology*, vol. 59, no. 5, pp. 467-477, 2004.
18. L. W. Corbett, "Composition of asphalt based on generic fractionation, using solvent deasphalting, elution-adsorption chromatography, and densimetric characterization," *Analytical Chemistry*, vol. 41, no. 4, pp. 576-579, 1969.
19. Pavement Tools Consortium, "Pavement Interactive [PAV]," [Online]. Available: /web/20191111152314/https://www.pavementinteractive.org/reference-desk/testing/binder-tests/pressure-aging-vessel/. [Accessed 11 November 2019].
20. R. L. Terrel and J. L. Walter, "MODIFIED ASPHALT PAVEMENT MATERIALS-THE EUROPEAN EXPERIENCE (WITH DISCUSSION)," 1986. [Online]. Available: https://trid.trb.org/view/575987. [Accessed 18 October 2019].
21. Y. Becker, M. P. Mendez and Y. Rodríguez, "Polymer modified asphalt," *Vision tecnologica*, vol. 9, no. 1, pp. 39-50, 2001.
22. B. Boutevin, Y. Pietrasanta and J. J. Robin, "Bitumen-polymer blends for coatings applied to roads and public constructions. Progress in organic coatings,," vol. 17, no. 3, pp. 221-249..

23. Pareek, T. Gupta and R. K. Sharma, "Performance of polymer modified bitumen for flexible pavements," *International journal of structural and civil engineering research*, vol. 1, no. 1, pp. 77-86., 2012.
24. Rodrigues and R. Hanumanthgari, "Polymer modified bitumens and other modified binders," in *Shell Bitumen Handbook*, 6 ed., London, UK, ICE Publishing; ISBN 978-0-7277-5837-8, 2015, pp. 149-183.
25. G. D. Airey, "Rheological properties of styrene butadiene styrene polymer modified road bitumens," *Fuel*, vol. 82, no. 14, pp. 1709-1719, 2003.
26. J. F. Masson, P. Collins, G. Robertson, J. R. Woods and J. Margeson, "Thermodynamics, phase diagrams, and stability of bitumen– polymer blends," *Energy & Fuels*, vol. 17, no. 3, pp. 714-724., 2003.
27. V. S. Punith and A. Veeraragavan, "Behavior of asphalt concrete mixtures with reclaimed polyethylene as additive," *Journal of materials in civil engineering*, vol. 19, no. 6, pp. 500-507, 2007.
28. B. M. (. A. S. m. Das, *Advanced Soil Mechanics*, London and New York: Taylor & Frances, 2008.
29. E. Mostafa, "Examining the performance of hot mix asphalt using nano-materials," *International Organization of Scientific Research (IOSRJEN)*, vol. 6, no. 2, pp. 25-34, 2016.
30. B. Morgan, "Polymer-Clay Nanocomposites: Design and Application of Multi-Functional Materials," *Material Matters (Chemistry Driving Performance): Advanced Applications of Engineered Nanomaterials*, vol. 2, no. 1, pp. 20-23, 2007.
31. J. M. L. Crucho, J. M. C. das Neves, S. D. Capitão and L. G. de Picado-Santos, "Evaluation of the durability of asphalt concrete modified with nanomaterials using the TEAGE aging method," *Construction and Building Materials*, vol. 214, pp. 178-186, 2019.
32. J. Yang and S. Tighe, "A review of advances of nanotechnology in asphalt mixtures," *Procedia-Social and Behavioral Sciences*, vol. 96, pp. 1269-1276., 2013.
33. P. K. Ashish, D. Singh and S. Bohm, "Evaluation of rutting, fatigue and moisture damage performance of nanoclay modified asphalt binder," *Construction and Building Materials*, vol. 113, pp. 341-350, 2016.

34. S. Bagshaw, "Bitumen/clay nanocomposites: improving bitumen properties for waterproof roads," in *ARRB Conference, 27th, 2016*, Melbourne, Victoria, Australia., 2016.
35. V. Vergaro, E. Abdullayev, Y. M. Lvov, A. Zeitoun, R. Cingolani, R. Rinaldi and S. Leporatti, "Cytocompatibility and uptake of halloysite clay nanotubes," *Biomacromolecules*, vol. 11, no. 3, pp. 820-826, 2010.
36. T. D. Ngo, C. Danumah and B. Ahvazi, "Production of Cellulose Nanocrystals at InnoTech Alberta," in *Nanocellulose and Sustainability*, CRC Press, 2018, pp. 269-287.
37. Y. Habibi, L. A. Lucia and O. J. Rojas, "Cellulose nanocrystals: Chemistry, self-assembly, and applications," *Chemical Reviews*, vol. 110, no. 6, p. 3479–3500, 2010.
38. Zhou and Q. Wu, "Recent development in applications of cellulose nanocrystals for advanced polymer-based nanocomposites by novel fabrication strategies," in *Nanocrystals-synthesis, characterization and applications*, IntechOpen, 2012, pp. 103-120.
39. S. S. Nair, J. Y. Zhu, Y. Deng and A. Ragauskas, "High performance green barriers based on nanocellulose," *Sustainable Chemical Processes*, vol. 2, no. 1, p. 23, 2014.
40. D. Van Poel, "A general system describing the visco-elastic properties of bitumens and its relation to routine test data," *Journal of Applied Chemistry*, vol. 4, no. 5, pp. 221-236, 1954.
41. Chin, "Performance graded bitumen specifications," in *Road Engineering Association of Asia and Australasia (REAAA) Conference*, Incheon, Korea., 2009.
42. M. N. Nagabhushana, D. Tiwari and P. K. Jain, "Rutting in flexible pavement: an approach of evaluation with accelerated pavement testing facility," *Procedia-Social and Behavioral Sciences*, vol. 104, pp. 149-157, 2013.
43. J. Yu, X. Yu, Z. Gao, F. Guo, D. Wang and H. Yu, "Fatigue resistance characterization of warm asphalt rubber by multiple approaches," *Applied Sciences*, vol. 8, no. 9, p. 1495, 2018.
44. N. Tran, M. M. Robbins, D. H. Timm, J. R. Willis and C. Rodezno, "Refined Limiting Strain Criteria and Approximate Ranges of Maximum Thicknesses for Designing Long-Life Asphalt Pavements," (No. NCAT Report 15-05), 2015.
45. A. Molenaar, "Prediction of fatigue cracking in asphalt pavements: do we follow the right approach?," *Transportation research record*, vol. 2001, no. 1, pp. 155-162, 2007.

46. V. Dave and C. Hoplin, "Flexible pavement thermal cracking performance sensitivity to fracture energy variation of asphalt mixtures," *Road Materials and Pavement Design*, vol. 16, no. sup1, pp. 423-441, 2015.
47. J. M. Krishnan and C. L. Rao, "Mechanics of air voids reduction of asphalt concrete using mixture theory," *International Journal of Engineering Science*, vol. 38, no. 12, pp. 1331-1354, 2000.
48. T. Aschenbrener, "Evaluation of Hamburg Wheel-Tracking Device to Predict Moisture Damage in Hot Mix-Asphalt.," *Transportation Research Record*, vol. 1492, pp. 193-201, 1995.
49. R. P. Izzo and M. Tahmoressi, "Use of the Hamburg wheel-tracking device for evaluating moisture susceptibility of hot-mix asphalt," *Transportation Research Record*, vol. 1681, no. 1, pp. 76-85., 1999.
50. Parker Jr and F. A. Gharaybeh, "Evaluation of indirect tensile tests for assessing stripping of Alabama asphalt concrete mixtures," *Transportation Research Record*, vol. 1115, 1987.
51. D. G. Hazlett, "Evaluation of moisture susceptibility tests for asphalt concrete, 3-C-2-102 (No. 3C2102).," Materials and Test Division, Texas State Department of Highways and Public Transportation, Austin, Texas, 1985.
52. Advanced Asphalt Technologies, LLC., A Manual for Design of Hot Mix Asphalt with Commentary, vol. 673, Sterling, VA: Transportation Research Board, 2011.
53. Zhou, S. Im, L. Sun and T. Scullion, "Development of an IDEAL cracking test for asphalt mix design and QC/QA," *Road Materials and Pavement Design*, vol. 18, no. 4, pp. 405-427, 2017.
54. F. Zhou, D. Newcomb, C. Gurganus, S. Banihashemrad, E. S. Park, M. Sakhaeifar and R. L. Lytton, "Experimental design for field validation of laboratory tests to assess cracking resistance of asphalt mixtures.," College Station, Texas, 2016.
55. F. Zhou, "Development of an IDEAL Cracking Test for Asphalt Mix Design, Quality Control and Quality Assurance.," Transport Research Board, Washington D.C., USA, 2019.
56. J. Breen and J. Stephens, "Split Cylinder Test Applied to Bituminous Mixtures at Low Temperature," *Journal of Materials*, vol. 1, no. 1, pp. 66-76, 1966.

57. R. L. Lytton, J. Uzan, E. G. Fernando, R. Roque, D. Hiltunen and S. Stoffels, "Development and Validation of Performance Prediction Models and Specifications for Asphalt Binders and Paving Mixtures, Report SHRP-A-357," Strategic Highway Research Program, National Research Council, Washington D.C., 1993.
58. D. W. Christensen and F. B. Ramon, Evaluation of indirect tensile test (IDT) procedures for low-temperature performance of hot mix asphalt. Vol. 530, Washington D.C.: Transportation Research Board, 2004, p. 3.
59. D. N. Richardson and S. M. Lusher, "Determination of Creep Compliance and Tensile Strength of Hot-Mix Asphalt for Wearing Courses in Missouri," Missouri Department of Transportation Organizational Results, Jefferson City, 2008.
60. AASHTO, AASHTO T 322-07: Standard Method of Test for Determining the Creep Compliance and Strength of Hot Mix Asphalt (HMA) Using the Indirect Tensile Test Device, (American Association of State Highway and Transportation Officials), 2011.
61. D. Roylance, *Introduction to fracture mechanics.*, vol. 1, Cambridge, Massachusetts: Massachusetts Institute of Technology, 2001.
62. Y. Yue, M. Abdelsalam, D. Luo, A. Khater, J. Musanyufu and T. Chen, "Evaluation of the Properties of Asphalt Mixes Modified with Diatomite and Lignin Fiber: A Review. Materials," vol. 12, no. 3, p. 400, January 2019.
63. Yao, Z. You, L. Li, C. H. Lee, D. Wingard, Y. K. Yap and S. W. Goh, "Rheological properties and chemical bonding of asphalt modified with nanosilica.," *Journal of Materials in Civil Engineering*, vol. 25, no. 11, pp. 1619-1630, 2012.
64. M. Ajour, *Several projects, several types of surfaces.*, vol. 113, 1981, pp. 9-21.
65. L. M. Sherman, "Plastics Technology," 14 November 2004. [Online]. Available: [/web/20191214061102/https://www.ptonline.com/articles/chasing-nanocomposites](https://www.ptonline.com/articles/chasing-nanocomposites). [Accessed 13 December 2019].
66. W. Zhu, P. Bartos and A. Porro, "Application of nanotechnology in construction; Summary of a state-of-the-art report," *Materials and structures*, vol. 37, no. 9, pp. 649-658, November 2004.
67. Merck KGaA/Sigma-Aldrich, "Sigma-Aldrich," 2019. [Online]. Available: A snapshot was captured. Visit page: [/web/20191112095303/https://www.sigmaaldrich.com/catalog/product/aldrich/685445?lang=en&ion=US](https://www.sigmaaldrich.com/catalog/product/aldrich/685445?lang=en&ion=US). [Accessed 20 April 2019].

68. Marini J et al, "Elaboration and properties of novel biobased nanocomposites with halloysite nanotubes and thermoplastic polyurethane from dimerized fatty acids," *Polymer*, vol. 55, no. 20, pp. 5226-5234, 2014.
69. MilliporeSigma, "682659 ALDRICH: Nanoclay, hydrophilic bentonite - Specification Sheet (CAS Number: 1302-78-9; EC Number: 215-108-5; MDL Number: MFCD00132796)," 2018. [Online]. Available: [/web/20191112095652/https://www.sigmaaldrich.com/catalog/product/aldrich/682659?lang=en&ion=US](https://www.sigmaaldrich.com/catalog/product/aldrich/682659?lang=en&ion=US).
70. Electron Microscopy Sciences, 2019. [Online]. Available: [/web/20191107205246/https://www.emsdiasum.com/microscopy/technical/datasheet/sputter_coating.aspx](https://www.emsdiasum.com/microscopy/technical/datasheet/sputter_coating.aspx).
71. Alberta Transportation, Standard Specifications for Highway Construction, Edmonton, Alberta: Alberta Transportation, 2010.
72. T. Aschenbrener, "Evaluation of Hamburg Wheel-Tracking Device to Predict Moisture Damage in Hot Mix-Asphalt," *Transportation Research Record*, vol. 1492, pp. 193-201, 1995.
73. D. W. Christensen and R. F. Bonaquist, "Evaluation of indirect tensile test (IDT) procedures for low-temperature performance of hot mix asphalt," Transportation Research Board, 2004.
74. Petersen, R. Robertson, J. Branthaver, P. Harnsberger, J. Duvall, S. Kim, D. Anderson, D. Christiansen and H. Bahia, "Binder Characterization and Evaluation: Volume 1," Washington D.C., 1994.
75. R. N. Hunter, A. Self and J. Read, Shell Bitumen Handbook (6th Edition), 6 ed., London: ICE Publishing, 2015.
76. R. W. Kelsall, I. W. Hamley and M. Geoghegan, Nanoscale science and technology, Chichester: John Wiley & Sons, 2005.
77. L. Brinchi, F. Cotana, E. Fortunati and J. M. Kenny, "Production of nanocrystalline cellulose from lignocellulosic biomass: Technology and Applications," *Carbohydrate Polymers*, vol. 94, no. 1, p. 154-169, 2013.
78. Sinha, E. Martin, K.-T. Lim, D. Carrier, H. Han, V. Zharov and J.-W. Kim, "Cellulose nanocrystals as advanced 'Green' materials for biological and biomedical engineering, Biosyst. Eng.,," vol. 40, no. 4, p. 373-393., 2015.

79. Z. You, J. Mills-Beale, J. M. Foley, S. Roy, G. M. Odegard, Q. Dai and S. W. Goh, "Nanoclay-modified asphalt materials: Preparation and characterization," *Construction and Building Materials*, vol. 25, no. 2, pp. 1072-1078, 2011.
80. G. D. Airey, "Use of Black Diagrams to Identify Inconsistencies in Rheological Data," *Road Materials and Pavement Design*, vol. 3, no. 4, pp. 403-424, 2002.
81. P. Pfeiffer and R. N. J. Saal, "Asphaltic Bitumen as Colloidal System," *Physical Chemistry*, vol. 44, no. 1940, pp. 139-149, 1940.
82. D. Anderson, D. Christensen, H. Bahia, R. Dongre, M. Sharma, C. Antle and J. Button, "Binder Characterization and Evaluation, Volume 3: Physical Characterization," (American Association of State Highway and Transportation Officials), Washington DC, 1994.
83. D. N. Richardson and S. M. Lusher, "Determination of Creep Compliance and Tensile Strength of Hot-Mix Asphalt for Wearing Courses," Missouri Department of Transportation, Missouri, 2008.
84. S. Tang, "Evaluate the Fracture and Fatigue Resistances of Hot Mix Asphalt Containing High Percentage Reclaimed Asphalt Pavement (RAP) Materials at Low and Intermediate Temperatures," Ames, Iowa, 2014.
85. Y. Yue, M. Abdelsalam, D. Luo, A. Khater, J. Musanyufu and T. Chen, "Evaluation of the Properties of Asphalt Mixes Modified with Diatomite and Lignin Fiber: A Review. Materials," vol. 12, no. 3, p. 400, January 2019.
86. Teizer, M. Venugopal, W. Teizer and J. Felkl, "Nanotechnology and Its Impact on Construction: Bridging the Gap between Researchers and Industry Professionals," *Journal of Construction Engineering and Management*, vol. 138, no. 5, pp. 594-604, 1 May 2012.
87. H. R. Nafchi, M. Abdouss, S. K. Najafi, R. M. Gargari and M. Mazhar, "Effects of nano-clay particles and oxidized polypropylene polymers on improvement of the thermal properties of wood plastic composite," *Maderas. Ciencia y Tecnología*, vol. 17, no. 1, pp. 45-54, 2015.
88. Leszczynska, J. Njuguna, K. Pielichowski and J. Banerjee, "Polymer/montmorillonite nanocomposites with improved thermal properties. Part I. Factors influencing thermal stability and mechanisms of thermal stability improvement," *Thermochimica Acta*, vol. 453, no. 2, pp. 75-96, 2007.

89. B. Morgan, "Polymer-Clay Nanocomposites: Design and Application of Multi-Functional Materials," *Material Matters: Chemistry Driving Performance*, vol. 2, no. 1, p. 21, 2007.
90. Maiti, M. Bhattacharya and A. K. Bhowmick, "Elastomer Nanocomposites," *Rubber Chemistry and Technology*, vol. 81, no. 3, pp. 384-469., July 2008.
91. F. van de Ven, A. A. Molenaar and J. B. J. Noordergt'aaf, "401-012 NANOTECHNOLOGY FOR BINDERS OF ASPHALT MIXTURES.," in *4th EE Congress*, Copenhagen, 2008.
92. S. G. Jahromi and A. Khodaii, "Effects of nanoclay on rheological properties of bitumen binder," *Construction and building materials*, vol. 23, no. 8, pp. 2894-2904, 1 August 2009.
93. Zare-Shahabadi, A. Shokuhfar and S. Ebrahimi-Nejad, "Preparation and rheological characterization of asphalt binders reinforced with layered silicate nanoparticles," *Construction and Building Materials*, vol. 24, no. 7, pp. 1239-1244, 2010.
94. G. Polacco, P. Kříž, S. Filippi, J. Stastna, D. Biondi and L. Zanzotto, "Rheological properties of asphalt/SBS/clay blends," *European Polymer Journal*, vol. 44, no. 11, pp. 3512-3521, 2008.
95. M. Ajour, "Several projects, several types of surfaces.," *Bulletin of LCPA*, vol. 113, pp. 9-21, 1981.
96. G. Polacco, S. Filippi, F. Merusi and G. Stastna, "A review of the fundamentals of polymer-modified asphalts: Asphalt/polymer interactions and principles of compatibility.," *Advances in Colloid and Interface Science*, vol. 224, pp. 72-112, 2015.
97. C. Li, Q. Wu, K. Song, S. Lee, Y. Qing and Y. Wu, "Cellulose nanoparticles: structure–morphology–rheology relationships," *ACS Sustainable Chemistry & Engineering*, vol. 3, no. 5, pp. 821-832., 2015.
98. R. Moon, A. Martini, J. Nairn, J. Simonsen and J. Youngblood, "Cellulose nanomaterials review: Structure, properties and nanocomposites," *Chemical Society Reviews*, vol. 40, no. 7, p. 3941–3994, 2011.
99. S. Peters, T. Rushing, E. Landis and T. Cummins, "Nanocellulose and Microcellulose Fibers for Concrete," *Transportation Research Record*, vol. 2142, pp. 25-28, 2010.
100. S. Desseaux, S. Dos Santos, T. Geiger, P. Tingaut, T. Zimmermann, M. Partl and L. Poulikakos, "Improved mechanical properties of bitumen modified with acetylated cellulose fibers," *Composites Part B: Engineering*, vol. 140, pp. 139-144, 2017.

101. MilliporeSigma, "Sigma-Aldrich," 2019. [Online]. Available: [/web/20191112101342/https://www.sigmaaldrich.com/catalog/product/aldrich/685445?lang=en&ion=US](https://www.sigmaaldrich.com/catalog/product/aldrich/685445?lang=en&ion=US). [Accessed 20 April 2019].
102. Marini J et al, "Elaboration and properties of novel biobased nanocomposites with halloysite nanotubes and thermoplastic polyurethane from dimerized fatty acids," *Polymer*, vol. 55, no. 20, pp. 5226-5234, 2014.
103. V. Vergaro, E. Abdullayev, Y. M. Lvov, A. Zeitoun, R. Cingolani, R. Rinaldi and S. Leporatti, "Cytocompatibility and uptake of halloysite clay nanotubes," *Biomacromolecules*, vol. 11, no. 3, pp. 820-826, 2010.
104. MilliporeSigma, "682659 ALDRICH: Nanoclay, hydrophilic bentonite - Specification Sheet (CAS Number: 1302-78-9; EC Number: 215-108-5; MDL Number: MFCD00132796)," MilliporeSigma, 2019. [Online]. Available: <https://www.sigmaaldrich.com/catalog/product/aldrich/682659?lang=en®ion=CA>. [Accessed 31 May 2019].
105. AASHTO, AASHTO T 316-13: Standard Method of Test for Viscosity Determination of Asphalt Binder Using Rotational Viscometer, (American Association of State Highway and Transportation Officials), 2017.
106. AASHTO, AASHTO T 324-16: Standard Method of Test for Hamburg Wheel-Track Testing of Compacted Hot Mix Asphalt (HMA), (American Association of State Highway and Transportation Officials), 2016.
107. R. A. Tarefder, P. M. M. Hasan and S. P. T. Center, "Evaluating Rutting/Stripping Potentials of Asphalt Mixes Using Hamburg Wheel Tracking Device," 2018.
108. Transport Canada, "Transportation in Canada 2016 Comprehensive Report," Minister of Public Works and Government Services, Canada, 2017.
109. Transport Canada, "Transportation in Canada 2011 Comprehensive Review," Minister of Public Works and Government Services, Canada, 2012.
110. M. El-Hakim and S. Tighe, "Impact of Freeze-Thaw Cycles on Mechanical Properties of Asphalt Mixes," *Transportation Research Record: Journal of the Transportation Research Board*, vol. 2444, pp. 20-27, 2014.
111. Yee, B. Aida, S. Hesp, K. Tam and P. Marks, "Analysis of Premature Low-Temperature Cracking in Three Ontario, Canada, Pavements," *Transportation Research Record: Journal of the Transportation Research Board*, vol. 1962, no. 1, pp. 44-51, 2006.

112. Pavement Tools Consortium, "Pavement Interactive [Rut]," Pavement Tools Consortium, [Online]. Available: /web/20191118042109/https://www.pavementinteractive.org/reference-desk/pavement-management/pavement-distresses/rutting/. [Accessed 17 November 2019].
113. S. Desseaux, S. Dos Santos, T. Geiger, P. Tingaut, T. Zimmermann, M. Partl and L. Poulikakos, "Improved mechanical properties of bitumen modified with acetylated cellulose fibers," *Composites Part B: Engineering*, vol. 140, no. 1, pp. 139-144, 1 May 2018.
114. Husky Energy, "SDS - Asphalt Cements – Non-Modified," Calgary, 2016.
115. Z. You, J. Mills-Beale, J. M. Foley, S. Roy, G. M. Odegard, Q. Dai and S. W. Goh, "Nanoclay-modified asphalt materials: Preparation and characterization," *Construction and Building Materials*, vol. 25, no. 2, pp. 1072-1078, 2011.
116. T. Aschenbrener, "Evaluation of Hamburg Wheel-Tracking Device to Predict Moisture Damage in Hot Mix-Asphalt," *Transportation Research Record*, vol. 1492, pp. 193-201, 1995.